UNIVERSIDAD D CORDOBA

Tesis Doctoral

Determination of hydrological and erosion patterns in agricultural catchments

Antonio Jesús Espejo Pérez

Junio de 2014

TITULO: *Determinación de patrones hidrológicos y erosivos en cuencas agrarias. Determination of hydrological and erosion patterns in agricultural catchments*

AUTOR: *Antonio Jesús Espejo Pérez*

© Edita: Servicio de Publicaciones de la Universidad de Córdoba. 2014
Campus de Rabanales
Ctra. Nacional IV, Km. 396 A
14071 Córdoba

www.uco.es/publicaciones
publicaciones@uco.es

Universidad de Córdoba

Departamento de Agronomía

Programa de Doctorado

Dinámica de Flujos Biogeoquímicos y su Aplicación

Línea de Investigación

Análisis de Procesos Hidrológicos e Hidráulicos y sus Aplicaciones Ambientales.

Tesis Doctoral

Determination of hydrological and erosion patterns in agricultural catchments

Determinación de patrones hidrológicos y erosivos en cuencas agrarias

Autor

D. Antonio Jesús Espejo Pérez

Dirigida por

Dr. D. Juan Vicente Giráldez Cervera

Dr. D. Karl Vanderlinden

Córdoba, Junio de 2014

Universidad de Córdoba

Departamento de Agronomía

Programa de Doctorado

Dinámica de Flujos Biogeoquímicos y su Aplicación

Línea de Investigación

Análisis de Procesos Hidrológicos e Hidráulicos y sus Aplicaciones Ambientales.

Tesis Doctoral

Determination of hydrological and erosion patterns in agricultural catchments

Determinación de patrones hidrológicos y erosivos en cuencas agrarias

Tesis doctoral presentada por D. Antonio Jesús Espejo Pérez, en satisfacción de los requisitos necesarios para optar al grado de Doctor Ingeniero Agrónomo con mención internacional, dirigida por los Drs. D. Juan Vicente Giráldez Cervera, de la Universidad de Córdoba, y D. Karl Vanderlinden, del Instituto de Investigación y Formación Agraria y Pesquera de la Junta de Andalucía.

Los directores El Doctorando

Juan V. Giráldez Cervera Karl Vanderlinden Antonio J. Espejo Pérez

Córdoba, Junio de 2014

Título de la tesis: Determinación de patrones hidrológicos y erosivos en cuencas agrarias.

Doctorando: Antonio Jesús Espejo Pérez.

Informe razonado de los directores de la tesis

D. Juan Vicente Giráldez Cervera y D. Karl Vanderlinden, directores de la tesis, informan que el doctorando ha desarrollado los objetivos previstos compartiendo su formación con la investigación, completándola con tres estancias en dos centros extranjeros, la Universidad de Buenos Aires, Argentina (de Agosto a Septiembre de 2011, y de Enero a Febrero de 2014), y el Research Institute For Hydrogeological Protection, perteneciente al National Research Council de Italia (de Junio a Septiembre de 2013). La tesis se presenta separada en capítulos, los cuales se encuentran en fase de envío o ya publicados en revista indexadas.

Por todo ello, se autoriza la presentación de esta tesis doctoral.

Los directores

Juan V. Giráldez Cervera Karl Vanderlinden

Córdoba, 13 de Junio de 2014

"La tierra no es una herencia de nuestros padres.
Es un préstamo de nuestros hijos"

Autor desconocido

A Claudia …

A mis padres, mi familia y amigos, ..

Sin duda, a la agricultura, ya que su fruto me permitió estudiar

Contents

CHAPTER 3. Soil loss and runoff reduction in olive-tree dry-farming with cover crops

CHAPTER 4. A probabilistic water erosion model with variable cover factor for Mediterranean olive orchards

CHAPTER 5. A method to estimate soil water diffusivity from field moisture profiles and its application across an experimental catchment

List of Figures

List of Tables

List of Symbols

Symbol	Description
Chapter 2	
CT	convencional tillage
CC	cover crop
IR	inter row area
UC	under canopy of trees
Chapter 3	
RC	runoff cofficient
SC	fraction of surface cover
SL	soil loss
SL/RO	index of soil loss to runoff ratio
Chapter 4	
pdf	probability density function
Q	water loss
Q_s	sediment yield
R	rain depth
S	slope gradient
C	cover factor
Chapter 5	
SWC	Soil water content
a	parameter of the exponential fit
D	soil water diffusivity
Chapter 6	
SWBM	soil water balance model
I	tree canopy interception
Chapter 7	
MISDc	modello Idrologico Semi-Distribuito in Continuo
AWC	antecedent soil water content

Q_p	peak flow of catchment discharge
Q_e	accumulated runoff
RC	runoff coefficient

Chapter 8

Q	surface runoff
ΔS	water storage increment

Agradecimientos

En primer lugar el doctorando agradece a la **Secretaría General de Universidades, Investigación y Tecnología** (CICE-Junta de Andalucía) por la concesión y disfrute de la **beca predoctoral** en la convocatoria de selección de personal investigador en formación con cargo a los incentivos concedidos a los **proyectos de excelencia** incentivados mediante resolución de 29 de diciembre de 2009 (resolución de 24 de febrero de 2010, BOJA nº 44, de 5 de marzo de 2010).

Estos trabajos han sido realizados con financiación del **Ministerio de Ciencia e Innovación** y el programa FEDER (**AGL2009-12936-C03-03** y **AGL2012-40128-C03-03**), la CEIC de la Junta de Andalucía (**AGR-4782**), así como gracias al **Contrato de consultoría y asistencia técnica entre la Consejería de Agricultura y Pesca de la Junta de Andalucía y la Asociación Española Agricultura de Conservación / Suelos Vivos,** AEAC/SV**,** en el Desarrollo de un Programa de Seguimiento para la Evaluación de la Aplicación de las medidas de fomento de las Cubiertas Vegetales en Andalucía.

Asimismo, se agradece la colaboración de los propietarios de las fincas y a los investigadores que iniciaron los experimentos en las mismas, especialmente el Dpto. de Ingeniería Rural de la UCO. Se agradece muchísimo a *Manuel Morón*, a *Esther Rodríguez*, a *Jorge García Baquero* y a *Miguel A. Ayala* del IFAPA Las Torres-Tomejil, al laboratorio de Suelo y Agua del IFAPA Alameda del Obispo y al personal de la AEAC/SV, por su apoyo en las actividades de campo y laboratorio, sin cuya ayuda esto no hubiese sido posible.

El doctorando también agradece la financiación recibida del **ceiA3** para la realización de las estancias en centros extranjeros. Agradece enormemente el buen trato recibido en la Universidad de Buenos Aires, Argentina, por *Claudia M. Sainato* y por *John J. Márquez*, y en el CNR-IRPI de Perugia por *Luca Brocca* y sus compañeros.

Personalmente durante esta etapa de doctorando he aprendido mucho, pero sin duda, este documento y lo que ello conlleva es sólo un paso profesional y académico. Siempre intento no olvidar que lo realmente importante en mi vida son pequeñas cosas como un simple olor que me hace recordar la niñez o los buenos días de alguien, lo cual pienso

que debemos apreciarlo más. De esta manera, es tanta la gente y los acontecimientos que me han hecho llegar aquí, los momentos pasados, que a veces cuesta recordarlos, y otras me entristecen pensar en ellos porque ya no volveré a vivirlos de nuevo, o al menos con la intensidad, inocencia y emoción con la que me sorprendieron.

Agradezco todo lo que humana y académicamente me inculcaron todos los compañeros que he conocido durante la realización de esta tesis. Deseo agradecer enormemente al personal del Grupo PAIDI AGR 239 *Suelo y Agua*, en especial a mis directores. Gracias *Juan Vicente* por tu guía y comprensión, y por supuesto, a *Karl*, muchas muchas y muchas gracias. También quiero hacer mucha alusión a *Manolo* y a *Aura*, compañeros de fatigas en el campo, y a *Gonzalo*, porque este último día de lluvia te portaste como un campeón. Cómo no, *Tom*, te mereces una estrella por aguantarme tanto tiempo compartiendo despacho. *Mari Recio*, *Rafa* y *Andrea*, gracias por aguantarme también.

Gracias y muchas gracias a los buenos amigos que he hecho en el edificio Leonardo Da Vinci y a mis amigos del Master, donde destaco a *Pedro*. *Amanda*, gracias por hacerme sonreír tanto, hablamos luego!. Gracias *Miriam* por compartir los almuerzos. Sin duda, gracias a los chicos/as de mi departamento no oficial, Ingeniería Forestal, por los buenos momentos que me han hecho pasar, los que están y los que pasaron durante este tiempo por ahí: *José Ramón*, *Maite*, *Alma*, *Juan Ramón*, *Quique*, *Macarena*, *las Pilis*, *Roberto*, *Santiago*…Gracias a los integrantes del equipo de fútbol del pasillo, especialmente a *José A. Cobacho*.

Sin duda alguna, gracias a *Dios* por permitirme haber llegado hasta aquí, conocer y vivir rodeado de toda esta buena gente y tanta otra que no he mencionado.

Quiero dedicar este trabajo a la persona más importante en mi vida, *Claudia*.

A mi familia y amigos, a los que están y a los que se fueron. Tengo la oportunidad de brindaros este trabajo, gracias. Papa, mamá, hermanas, cuñados, titos y primos, aun no soy capaz de explicaros a lo que me dedico.

Sin duda, a todas las personas que cultivan con entusiasmo la tierra, espero os pueda servir.

Gracias.

Summary

The general objective of this dissertation was to identify spatial and temporal hydrological patterns using intensive soil erosion and water content measurements, and to assess soil and water conservation strategies in agricultural catchments. Two field experiments were carried on in some olive orchards of Andalusia. One experiment consisted of a network micro-plots installed at eight farms to measure runoff and sediment yield. The second experiment was based on the continuous recording of field soil moisture with a sensor network established on an experimental catchment, distinguishing under-canopy areas and inter-row areas.

The use of plant covers on the soil of olive tree plantation to reduce soil erosion and conserve runoff water has been evaluated comparing it with a conventional tillage system. The results indicated that the protection of the plant covers efficiently reduces soil loss, and to a lesser extent water loss. A simple probabilistic framework to explain runoff and sediment yield data has been proposed. The model is based on the Monte Carlo generation of the key variables: rain depth, fraction of soil surface covered by plant, and average slope. The main factors that control the spatio-temporal dynamics of soil water content within the olive tree planted catchment were investigated, using the information supplied by the soil moisture sensors network. The analysis of the soil moisture data allowed the evaluation of soil hydraulic properties, the different behaviour of soil under of outside of tree canopy, and the relationship of soil water storage and catchment runoff with the meteorological forcing functions such as rainfall and evaporation. Both, olive trees and soil moisture, control the runoff pattern within this catchment.

Resumen

El objetivo general de esta tesis fue identificar patrones hidrológicos usando medidas intensivas de pérdida de suelo y de humedad para evaluar de mejor manera diferentes estrategias de manejo y conservación de suelo y agua. Para dar respuesta a estos objetivos se realizaron dos experimentos, i) una extensa red de microparcelas de erosión distribuidas en lugares representativos del olivar de Andalucía, y ii) una cuenca de olivar equipada con un aforador de escorrentía en su parte más baja y una red de sensores de humedad distribuidos dentro de la cuenca y dispuestos en zonas entre calles y bajo copa de olivos.

Primero se analizó la eficacia de un sistema de cubierta vegetal entre calles de olivos para reducir la severidad de la erosión en comparación con el laboreo del suelo. Los resultados indicaron que este sistema reduce la pérdida de suelo y en menor grado la escorrentía. Se ha propuesto un modelo probabilístico sencillo para analizar estos datos e interpretar el comportamiento del sistema bajo diferentes condiciones. Para ello se ha recurrido a una simulación de Monte Carlo con la que se generaron valores de los factores esenciales del proceso de erosión hídrica: precipitación, fracción de superficie del suelo cubierta por la vegetación herbácea, y pendiente media del terreno. En los siguientes capítulos se exploró la dinámica espacio-temporal del agua en el suelo de la cuenca experimental, a partir de la información adquirida por la red de sensores de humedad. Los resultados permitieron evaluar algunas propiedades de transmisión del agua del suelo, la influencia de la copa del árbol sobre el comportamiento del suelo subyacente en comparación con el suelo alejado de la copa, y las relaciones entre la precipitación, la demanda evaporante de la atmósfera, el árbol, el suelo y la escorrentía producida en la cuenca.

Chapter 1

Introduction

1.1. Overview.

Soil degradation by water erosion in agricultural catchments is a major global problem in semiarid areas such as the Mediterranean (Montgomery, 2007) and a serious threat to farm sustainability. Water erosion contributes also to surface water pollution (Holland, 2004) and causes damage to public infrastructure (Boardman and Poesen, 2006, pp. 750-755). As a result, different EU policies have been put in place to assure soil protection (*e.g*. Soil Thematic Strategy, COM2006, European Commission, 2012). Soil and water conservation techniques are the research topic for many laboratories all over the world (Maetens et al. 2012). Despite this effort there is still a significant knowledge gaps in the field like an explanation for the observed different soil erosion rates (Graham and McDonnell, 2010; Taguas et al. 2009), and the influence of soil water content and vegetation (Moran et al. 2010).

A wide range of soil loss data has been obtained in Mediterranean areas (*e.g*. Taguas et al. 2009; Poesen et al. 2002). Despite the large dispersion in experimental soil erosion data, most of these studies demonstrate the importance of protecting the soil surface for reducing soil erosion to tolerable levels. Gómez et al. (2011) evaluated the effect of cover crops and conventional tillage on soil and runoff loss in vineyards and olive groves at six sites from Spain, France and Portugal. They concluded that cover crops are an effective tool in reducing soil loss, although runoff is less likely to be reduced. In addition, they suggest to identify vulnerable landscape positions where additional conservation measures can be implemented. These findings were in accordance with Maetens et al. (2012), who conducted a meta-analysis using data from 103 runoff-plots throughout Europe and the Mediterranean area.

Soil water content is a key for surface hydrological processes, as Rodríguez-Iturbe et al.

(1999, and later Ecohydrology papers) properly demonstrated. Williams and Albertson (2004) found that the carbon cycle could be characterized easily as a function of soil water content in semiarid zones. Soil water before rainfall influences the rainfall-runoff relationships (Alila et al. 2009). Despite its importance, only some exceptions (Robock et al. 2000) and recent efforts (Dorigo et al. 2013), historical series of soil water measurements are not generally available, in contrast to rainfall or other meteorological data (Palecki and Bell, 2013). In situ soil water measurements are necessary, but manual surveys are expensive (Robinson et al. 2008) and often prohibitive as a result of their destructive nature. Isolated soil water content surveys, or repeated surveys at different time intervals provide only limited information on rainfall pulse-related hydrological processes which occur at short time-scales and are typical for semiarid conditions, with short wet interruptions of long drying periods. A number of remotely sensed soil moisture products are currently available, but at a measurement scale that is too coarse to be of use for applications in agricultural catchments or fields. Low cost soil water sensors provide another means to monitor this property at the required time and space scales, and have provided already promesing results for agro-environmental applications (Mittelbach et al. 2011; Vereecken et al. 2008). However, measurement accuracy is often an issue and site-specific calibrations are usually required for each sensor model or soil type (Fares et al. 2013). In addition, an important effort in filtering and detecting invalid values in the measurement records is generally required (Dorigo et al. 2013).

Models are necessary to integrate information of processes over large space and time scales (Beven 2000). Several models have been developed for the description of the spatio-temporal evolution of soil water content (Famiglietti et al. 2008; Brocca et al. 2008), and for the soil erosion estimation (Cantón et al. 2011). The high number of parameters of many of these models, which are not always available, restricts their usefulness. Simplified models can be an option for the description of hydrological processes comprising just a few parameters (*e.g*. Majone et al. 2010; Sivakumar, 2008). However, in addition to evaluating their performance in reproducing observed soil water content series, such models have to be internally validated in order to assess their reliability and robustness, for which accurate field measurements across different spatial and temporal scales are needed.

This dissertation explores the characterization of the soil water dynamics and erosion in catchments using intensive field observations to identify relationships and spatio-temporal patterns. The study is concentrated in olive-planted. This crop is an important and traditional land use of Mediterranean area, and during the last twenty years its cultivated area has duplicated (European Commission, 2012). Olives are mainly planted on steep slopes and intensively tilled (Semple 1931, Cap. XIV). In this context, although the severity of erosion in this crop is still under debate (Gómez et al. 2008), it is necessary to develop better soil and water management practices to preserve olive productivity and environmental quality of the surrounding environment (Kairis et al. 2013).

1.2. Research objectives.

In order to implement better soil and water management practises in agricultural landscapes, it is necessary to identify and interpret the factors that control the hydrologic processes in a simple way. The general objective of this thesis was to identify spatial and temporal hydrological patterns using intensive soil erosion and water content measurements in olive cultivation.

To reach this general objective, the following research questions were put forward:

1) Is it possible to reduce soil and water loss to tolerable levels with a better soil management?

Soil erosion constitutes a major problem in the dry-farming agriculture of Mediterranean areas. In olive cultivation, the occurrence of intense rainfalls on unprotected and intensively tilled soil with steep slopes aggravates the problem. Therefore, the first objective was to evaluate different soil management systems that can be easily implemented by farmers, to reduce soil and water losses.

2) Can the erosive processes be expressed in a simple probabilistic form?

In Mediterranean environments soil erosion has received considerable attention as a result of its significant contribution to the decline of soil and surface water quality. There is general agreement that the effect of soil management practices play an

important role in the process, but a large heterogeneity exists in the observed effectiveness of soil and water management practices. Therefore, the second objective was to develop a method to analyse and describe probabilistically field observations in a simple way.

3) Is it possible to make field estimations of soil hydraulic properties using high frequency *data series of soil water content?*

Soil hydraulic properties are important indicators for assessing soil functioning and are essential for modeling matter and energy fluxes in the unsaturated zone. However, laboratory measurements of these properties are usually made on small soil cores, resulting in limited representativeness towards field-scale applications. In addition, laboratory methods are generally time-consuming and expensive. The third objective was to develop a method to estimate in a simple way hydraulic soil properties, exclusively from field water content measurements, using traditional laboratory methods, and use this method to evaluate the spatial variability of the soil-water diffusivity within an olive-cropped catchment and to assess the influence of the trees.

4) Can intensive soil water monitoring in combination with modelling be successfully used to characterize soil water dynamics in agricultural catchments?

Improving our understanding of soil water dynamics under different land uses is essential to soil and water conservation in agricultural and environmental systems. In situ measurements of moisture with sensor networks allows us to evaluate the soil water dynamics at discrete locations (Vereecken et al. 2008), and this information needs to be extrapolated in space and in time. Therefore, the fourth objective was to explore soil moisture dynamics within a catchment, using intensive measurements and modelling, and in doing so evaluate the measurement accuracy of a sensor network, the spatial variability of soil hydraulic properties, and the rainfall canopy interception.

5) Which factors influence the catchment response in term of runoff?

The hydrological response of hillslopes is extremely complex and for a better understanding it is necessary to use data from instrumented catchments for internal validation of simple rainfall-runoff models. By using runoff and soil water measurements, the fifth objective was to evaluate the reliability and robustness of a simple soil water balance model in terms of runoff and soil water content, with the

additional aim of analysing the influence of vegetation and the antecedent soil water content on the catchment response.

6) Is it possible to determine runoff flow patterns within catchments using intensive soil water observations?

In gauged catchments, surface flow within them can often not be measured, and nor can the influence of vegetation be inferred. To overcome these limitations the sixth objective was to investigate the possibility to characterize soil water movement within a small catchment using a simple water budget with high frequency readings from a soil water sensor network and meteorological information.

1.3. Structure of the thesis.

This thesis is divided in nine chapters. Chapter 1 presents the motivation of this work and the main research questions. Chapter 2 describes the field sites where soil erosion and water content were measured. Chapters 3 and 4 analyses the results of 2 yr field campaign with a micro-plot soil erosion network. A comparison of soil and water losses between two different soil managements is provided, and a simple probabilistic model is developed to represent water erosion. Chapters 5-8 focus on the characterization of the hydrology of a small catchment by using intensive soil water records collected with a capacitive sensor network, a gauging station at the catchment outlet and soil surveys. Chapter 5 proposes a method based on the Bruce and Klute equation to estimate effective soil water diffusivity from soil water profile data observed during pronounced desiccation periods. Chapter 6 uses soil water modelling to determine soil hydraulic properties and estimate rainfall canopy interception by olive trees. Chapter 7 evaluates the reliability and robustness of a simple rainfall-runoff model in simulating runoff and soil water content, to analyse the influence of vegetation and the antecedent soil water content on catchment response. Chapter 8 suggests a method to detect the spatial pattern of runoff flow within catchments by using a simple soil water balance with soil water records and meteorological information. Finally in chapter 9 the most relevant contribution of this thesis to improve soil and water conservation practises are summarized, and future research directions are proposed.

1.4. References.

Alila, Y., P.K. Kuras, M. Schnorbus, and R. Hudson. 2009. Forests and floods: a new paradigm sheds light on age-old controversies. Water Resour. Res. 45, W05205, doi:10.1029/2008wr007207.

Beven, K.J. 2000. Rainfall-runoff modelling, the primer. John Wiley, Chichester, UK.

Boardam, J., and J. Poesen. 2006. Soil erosion in Europe. Wiley. New York.

Brocca, L., F. Melone, and T. Moramarco. 2008. On the estimation of antecedent wetness condition in rainfall-runoff modelling. Hydrol. Proc. 22, 629-642.

Cantón, Y., A. Solé-Benet, J. de Vente, C. Boix-Fayos, A. Calvo-Cases, C. Asensio, and J. Puigdefábregas. 2011. A review of runoff generation and soil erosion across scales in semiarid south-eastern Spain. J. Arid Environ. 75, 1254-1261.

Dorigo, W.A., A. Xaver, M. Vreugdenhil, A. Gruber, A. Hegyiová, A.D. Sanchis-Dufau, and M. Drusch. 2013. Global automated quality control of in situ soil moisture data from the International Soil Moisture Network. Vadose Zone J. 12, doi:10.2136/vzj2012.0097.

European Commission. 2012. The soil thematic strategy. Available at: http://ec.europa.eu/environment/soil/index_en.htm, accessed on 12/05/2014.

European Commission, Directorate-General for Agriculture and Rural Development. 2012. Economic analysis of the olive sector. Available at: http://ec.europa.eu/geninfo/query/resultaction.jsp?query_source=AGRICULTURE&QueryText=olive+&swlang=en#queryText=Economic+analysis+of+the+olive+sector&tab=restricted, accessed on 12/02/2014.

Famiglietti, J.S., D. Ryu, A.A. Berg, M. Rodell, and T.J. Jackson. 2008. Field observations of soil moisture variability across scales. Water Resour. Res. 44, W01423.

Fares, A., M. Temimi, K. Morgan, and T.J. Kelleners. 2013. In-situ and remote soil moisture sensing technologies for vadose zone hydrology. Vadose Zone J., doi:10.2136/vzj2013.03.0058.

Gómez-Calero, J.A., C. Llewellyn, G. Basch, B. Sutton, J.S. Dyson, and C.A. Jones. 2011. The effects of cover crops and conventional tillage on soil and runoff loss in vineyards and olive groves in several Mediterranean countries. Soil Use and Manag. 27, 502-514.

Gómez, J.A., J.V. Giráldez, and T. Vanwalleghem. 2008. Comment on “Is soil erosion in olive groves as bad as often claimed?” by L. Fleskens and L. Stroosnijder. Geoderma 147, 93–95.

Graham, C.B., and J.J. McDonnell. 2010. Hillslope threshold response to rainfall: (2) Development and use of a macroscale model. J. Hydrol. 393, 77-93.

Holland, J.M. 2004. The environmental consequences of adopting conservation tillage in Europe: reviewing the evidence. Agric. Ecosyst. Environ. 103, 1-25.

Kairis, O., C. Karavitis, A. Kounalaki, L. Salvati, and C. Kosmas. 2013. The effect of land management practices on soil erosion and land desertification in an olive grove. Soil Use and Manag. 29, 597-606.

Maetens, W., J. Poesen, and M. Vanmaercke. 2012. How effective are soil conservation techniques in reducing plot runoff and soil loss in Europe and the Mediterranean?. Earth Sci. Reviews 115, 21-36.

Majone, B., A. Bertagnoli, and A. Bellin. 2010. A non-linear runoff generation model in small Alpine catchments. J. of Hydrol. 385, 300-312.

Mittelbach, H., F. Casini, I. Lehner, A.J. Teuling, and S.I. Seneviratne. 2011. Soil moisture monitoring for climate research: Evaluation of a low cost sensor in the framework of the Swiss Soil Moisture Experiment (SwissSMEX) campaign. J. Geophys. Res. 116, D05111, doi:10.1029/2010JD014907.

Montgomery, D.R. 2007. Soil erosion and agricultural sustainability. PNAS 104, 13268-13272.

Moran, M. S., E.P. Hamerlynck, R.L. Scott, J.J. Stone, C.D. Holifield Collins, T.O. Keefer, R. Bryant, L. DeYoung, G.S. Nearing, Z. Sugg, and D.C. Hymer. 2010. Hydrologic response to precipitation pulses under and between shrubs in the Chihuahuan Desert, Arizona. Water Resour. Res. 46, W10509, doi:10.1029/2009WR008842.

Palecki, M.A., and J.E. Bell. 2013. U.S. Climate reference network soil moisture observations with triple redundancy: measurement variability. Vadose Zone J. 13, doi:10.2136/vzj2012.0158.

Poesen, J., L. Vandekerckhove, J. Nachtergaele, D. Oostwoud Wijdenes, G. Verstraeten, and B. Van Wesemeal. 2002. Gully erosion in dryland environments. Chap. 8. In: L.J. Bull, and M.J. Kirkby, editors. Dryland rivers: Hydrology and Geomorphology of semi-arid climates. John Wiley & Sons. Chichester.

Robinson, D.A., C.S. Campbell, J.W. Hopmans, B.K. Hornbuckle, S.B. Jones, R. Knight, F. Ogden, J. Selker, and O. Wendroth. 2008. Soil moisture measurement for ecological and hydrological catchment-scale observatories: A review. Vadose Zone J. 7, 358-389.

Robock, A., K.Y. Vinnikov, G. Srinivasan, J.K. Entin, S.E. Hollinger, N.A. Speranskaya, S. Liu, and A. Namkhai. 2000. The Global Soil Moisture Data Bank. Bull. Am. Meteorol. Soc. 81, 1281-1299.

Rodríguez-Iturbe, I., A. Porporato, L. Rindolfi, V. Isham, and D.R. Cox,. 1999. Probabilistic modelling of water balance at a point: The role of climate, soil and vegetation. Proc. R. Soc. London, Ser. A. 4155, 3789-3805.

Semple, E.C. 1931. The Geography of the Mediterranean region. Its relation to ancient history. AMS Press. New York.

Sivakumar, B. 2008. The more things change, the more they stay the same: the state of hydrologic modelling. Hydrol. Proc. 22, 4333–4337.

Taguas E.V., J.L. Ayuso, A. Peña, Y. Yuan, and R. Pérez. 2009. Evaluating and modelling the hydrological and erosive behaviour of an olive orchard microcatchment under no-tillage with bare soil in Spain. Earth Surf. Process. Landforms 34, 738-751.

Vereecken, H., J.A. Huisman, H. Bogena, J. Vanderborght, J.A. Vrugt, and J.W. Hopmans. 2008. On the value of soil moisture measurements in vadose zone hydrology: A review. Water Resour. Res. 44, W00D06, doi:10.1029/2008WR006829.

Williams, C.A., and J.D. Albertson. 2004. Soil moisture controls on canopy-scale water and carbon fluxes in an African savanna. Water Resour. Res. 40, W09302, doi:10.1029/2004WR003208.

Chapter 2

Field sites

The experimental research was performed in representative agricultural landscapes of Andalusia, with olive tree cultivation on sloping terrain. Plot scale measurements of inter-rill soil erosion were collected with a micro-plot soil erosion network distributed across 8 representative private farms. At the catchment scale, soil water content was measured using a sensor network, and runoff was measured at the catchment outlet.

2.1. Micro-plot soil erosion network.

2.1.1. Farms description.

The micro-plot soil erosion network consisted of plots located in eight farms distributed across the region of Andalusia (Southern Spain), comparing cover crop (CC) and conventional tillage (CC). The farms were representative of the different olive-cropped, soil types, topographies, plant varieties, and management systems. The plots were located in the provinces of Córdoba (Castro del Río, plot C3; Nueva Carteya, C4 and Obejo C5), Huelva (Chucena, 2 plots, H1 and H2), Seville (La Campana, S2) and Jaén (Torredonjimeno, J1 and Torredelcampo, J2). Table 2.1 shows plot location, soil properties, including subgroup (Soil Survey Staff, 1999), olive tree variety, type of cover crop and average slope of the plots. Fig. 2.1 shows the location of the eight experimental farms.

Fig. 2.1. Location of the experimental farms indicated as small rhombi.

Table 2.1. Plot location with relevant soil properties of the farms. Cover type: native, spontaneous, vegetation (sp), sown (s), and slope.

farm	location			Soil properties				Soil Classification	Olive variety	cover	slope
	province	Geographical coordinates		sand	clay	OM †	pH				
		Latitude, N	Longitude, E	kg kg^{-1}							[ ]
C3	Córdoba	37º 63’ 7.2’’	-4º 48’ 67’’	.213	.329	.011	8.09	Calcic Haploxerept	Picual	sp	.167
C4		37º 62’ 1.8’’	-4º 46’ 5.9’’	.306	.225	.021	7.93	Calcic Haploxerept	Picual	sp	.185
C5		38º 14’ 5.9’’	-4º 78’ 7.2’’	.376	.052	.026	6.61	Ruptic Xerorthent	Mollar and other	sp	.180
J1	Jaén	37º 80’ 4.7’’	-4º 43’ 1.1’’	.164	.396	.019	7.93	Typic Calcixerept	Picual	s	.075
J2		37.83145	-3.958029	.270	.332	.010	7.98	Typic Haploxerept	Picual	s	.185
S2	Sevilla	37º 57’ 5.5’’	-5º 35’ 9.8’’	.426	.242	.015	8.29	Typic Xerochrept	Arbequina	sp	.060
H1	Huelva	37º 35’ 4.0’’	-6º 39’ 1.0’’	.354	.228	.014	7.92	Typic Xeropsamment	Arbequina	sp	.085
H2		37º35’ 3.7’’	-6º 39’ 3.1’’	.284	.298	.015	8.05	Typic Xerpsamment	Arbequina	sp	.095

† OM: organic matter content.

The management system and cover crop composition were chosen in accordance to the farmer's usual practice. Table 2.2 summarizes the agricultural operations for each farm.

Table 2.2. Timing of the main agricultural operations in the plots.

Farm	treatment	May	June	July	Aug.	Sep.	Oct.	Nov.	Dec.	Jan.	Feb.	Mar.	Apr.
C3	CC	T(fc)		T (v)						PC			
	CT	T (fc)		T (v)						PC		T(fc)	
C4	CC	PC		T (r)							PC		
	CT	T (v)		T (v)						T (dh)			T (fc)
C5	CC	PC										PC	
	CT	T (v)		T (v)							T (dh)		T (fc)
J1	CC	CW											
	CT			T (v)						T (dh)			T (fc)
J2	CC	CW											
	CT			T (v)						T (dh)			T (fc)
S2	CC												CW,
	CT										T (dh)		T (v)
H1	CC	CW										PC	
	CT	T (v)			T (r)							T (dh)	
H2	CC	CW										PC	
	CT	T (v)			T (r)							T (dh)	

† T, tillage; fc, field cultivator; v, vibrocultivator; dh, disc harrow; CW, chemical weeding; PC, physical clearing; R, roller; CC, cover crop, and CT, conventional tillage.

Typical species, according to the Valdés et al. (1987) classification, were field-marigold (*Calendula arvensis* L.), *Diplotaxis virgata* (Cav.) DC., and caterpillar-plant (*Scorpiurus muricatus* L.) in C3; mouse barley (*Hordeum leporinum* Link), bur medic (*Medicago polymorpha* L.), and annual sow thistle (*Sonchus oleraceus* L.) in C4; *Agrostis pourretii* Willd., Mediterranean needlegrass (*Stipa capensis* Thunb.), *Vulpia geniculata* (L.) Link, hare-foot plantain (*Plantago lagopus* L.), buck's-horn plantain (*Plantago coronopus* L.), European umbrella milkwort [*Tolpis barbata* L. (Gaertner)], Crete weed [*Hedypnois cretica* (L.) Dum.-Courset.], branched chamomile (*Chamaemelum mixtum* L.), ball clover (*Trifolium glomeratum* L.), cockspur thistle (*Centaurea melitensis* L.), nit grass [*Gastridium ventricosum* (Gouan) Schinz & Thell.], and *Bromus intermedius* Guss in C5; chopped pruning remains in plot J1; annual ryegrass (*Lollium rigidum* Gaudin) in J2; mouse barley, oval crowfoot [*Erodium malacoides* (L.) L'Hér.], field-marigold, ground-needles [*Erodium moschatum* (L.) L'Hér]., African wood-sorrel (*Oxalis pes-caprae* L.), *Diplotaxis virgata* (Cav.) DC.,

Argentine fleabane [*Conyza bonariensis* (L.) Cronq.], snail medic [*Medicago scutellata* (L.) Miller], and Cretan-hollyhock (*Lavatera cretica* L.) in H1 and H2, Argentine fleabane, *Diplotaxis virgata* (Cav.) DC, and oval crowfoot in S2.

2.1.2. Field data acquisition.

A randomized complete block design with three replications was adopted. The measured parameters were soil loss and runoff, and the factors were soil management system, with 2 levels (CT and CC), year (2 levels) and experimental field (8 levels). The experimental unit was a micro-plot of 1 m^2, delimited by galvanized steel sheets with an outlet routing the water and sediment to a plastic container. Fig. 2.2 shows a block of two microplots with CT and CC management.

Fig. 2.2. Picture of a microplot block with conventional tillage, CT, and cover crop, CC, soil management, located at the Obejo farm, C5.

After each rain spell the plots were visited and the runoff was collected (Espejo, 2004). The runoff volume was measured *in situ*, and three 1 L samples were taken, if available, for sediment analysis in the laboratory. The cover crop density was estimated following the method developed by Agrela et al. (2003), based on a visual inspection. Rainfall was also collected in situ using an automatic rain gauge (Hobo loggers, Onset Computer Corporation).

2.2. Soil water sensor network.

2.2.1. The Setenil catchment.

The experimental catchment is located in Setenil de las Bodegas (south-western Spain, province of Cádiz), 36º 52.2' N, 5º 7.8' W, 776 m-amsl. (Fig. 2.3). The climate is subhumid Mediterranean with an Atlantic influence and an annual average rainfall of 1100 mm concentrated mainly in the September-May period. The summer is dry and hot, with frequent spells of dry and hot east winds. The soil subgroup is an intergrade between Lithic and Typic Rhodoxeralf (Soil Survey Staff, 1999, pp. 269-270; García del Barrio et al. 1971).

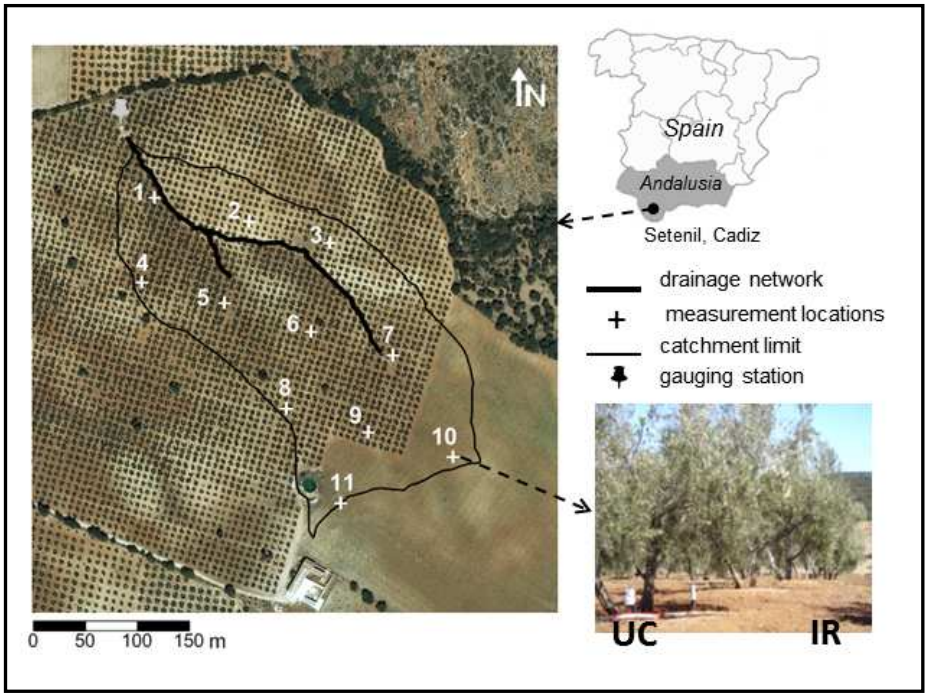

Fig. 2.3. Location of the experimental catchment, and position of the 11 measurement locations and the catchment outlet. At each location soil water content was monitored at the inter-row area, IR, and under the olive canopy, UC.

The catchment is cropped with olives of 18 years old, except for a small area in the south-eastern part of the catchment where trees were only 4 years old. In both zones, trees were planted on a 6 × 6-m grid. The soil is frequently tilled to remove weeds

(conventional tillage, CT). However, since 2012 the farmer has reduced the tillage intensity to minimum tillage, except for the area with young trees where the soil is still frequently tilled. Residues of pruning were spread on the soil surface during 2011. The soil was tilled in January, 2011, March, 2012, and in May, 2013. The landform is hilly with a mean slope near 10%, and a shallow hardened bedrock consisting of calcarenites that limits soil depth from 0.05 to 1.20 m (Fig. 2.4).

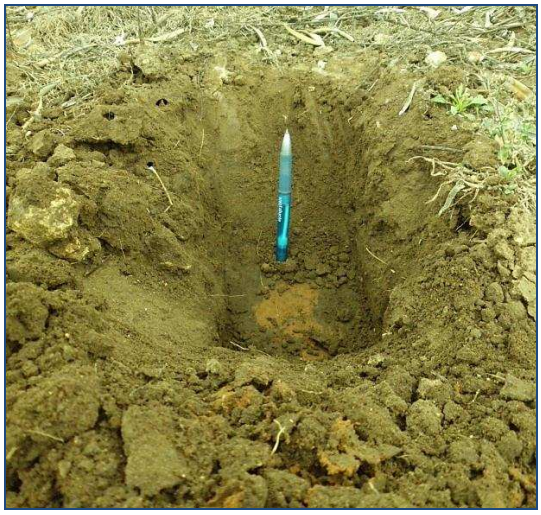

Fig. 2.4. Detail of drilling in the soil showing the presence of calcarenites.

A gully of nearly 2 m depth near the catchment outlet intersects the catchment from east to west. Plant tree establishment and periodic tillage created a sort of channelized surface relief with small mound surrounding the olive trees, Fig. 2.5. As a result, the water flow is concentrated through the central part of inter-row areas as a channel mode.

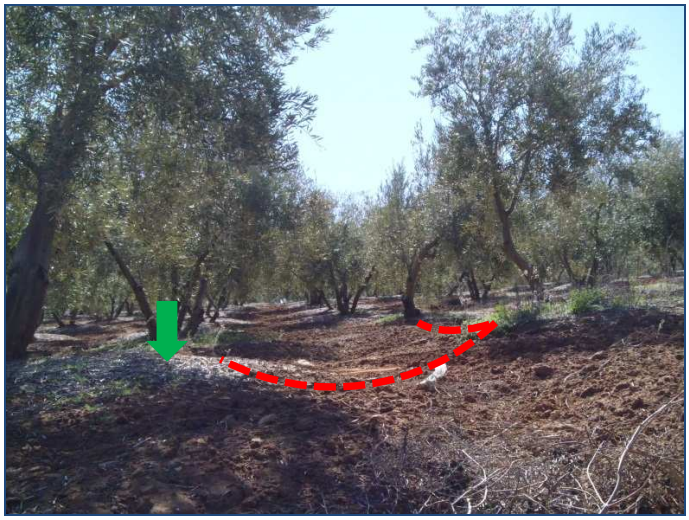

Fig. 2.5. Detail of the microdepression at inter row area, IR, and the small mounds surrounding the tree trunks. The green arrow shows the position of under canopy sample, UC, location.

2.2.2. Field data acquisition.

The sample grid consisted on 11 measuring locations. In each one the landscape was divided into inter row, IR, and under canopy, UC, area. UC location was placed at a distance of 0.75 m from the tree trunk towards south-east and IR in the north-east direction. Therefore UC locations were placed at downslope region from the tree trunk at north-west area of channel, and at upslope region at south-area, compared with the unique relative position of the IR locations. Undisturbed soil samples were collected at the 11 locations, 11 at IR + 11 at UC, across the catchment at 0.10 m interval depth until reach the maximum soil depth, limited by the bedrock, and soil and hydraulic properties were analysed.

2.2.2.1. Soil properties.

The average soil profile characteristics are summarised in Table 2.3, separately for IR and UC. No differences between properties were found between IR and UC, except for bulk density at location 6. According to textural analysis soil was classified as sandy loam, and the profile average clay and sand content was 19 and 69% for both locations, IR and UC. Appreciable differences in soil texture were observed along soil profile at locations 3, 5, 6 and 7, for IR, and at locations 5 and 10 for UC. These areas corresponded to the central part of the catchment, usually deeper. The spatial mean profile bulk density was 1.60 Mg m^{-3} for both locations. However spatial mean topsoil bulk density, 0-0.30 m, was higher at IR compared than UC, with average values of 1.74 Mg m^{-3} at IR, and 1.59 at UC respectively.

Table 2.3. Summary of the main soil profile properties separately for inter row, IR, and under canopy, UC, of olives. Results represent profile-averaged values, and in bracket the standard deviation.

	IR					UC					
	z_{max}	clay	sand	ρ_b	k_s†	z_{max}	clay	sand	ρ_b	k_s†	canopy‡
location	m	%	%	Mg m^{-3}	cm h^{-1}	m	%	%	Mg m^{-3}	cm h^{-1}	m^2
1	0.80	19.3 [3.33]	69.8 [3.22]	1.67 [0.07]	41.2	0.70	18.0 [2.53]	70.3 [2.42]	1.71 [0.12]	43.7	27.9
2	0.30	12.4 [1.20]	68.2 [2.69]	1.67 [0.05]	13.2	0.30	13.0 [0.64]	65.4 [3.04]	1.33 [-]	87.9	18.4
3	0.50	20.4 [4.60]	64.4 [6.29]	1.68 [0.20]	7.5	0.30	20.9 [2.67]	63.3 [2.52]	1.71 [0.19]	79.6	18.4
4	0.30	20.1 [0.07]	69.9 [0.71]	-	8.8	0.49	19.8 [1.72]	70.3 [1.22]	1.65 [0.12]	10.1	26.2
5	0.76	17.7 [3.54]	68.2 [6.90]	1.59 [0.12]	1.4	0.70	16.8 [3.08]	70.3 [5.93]	1.60 [0.11]	30.2	29.4
6	0.60	19.5 [4.64]	68.5 [4.81]	1.69* [0.06]	0.5	0.60	18.1 [1.87]	70.9 [2.81]	1.56 [0.10]	2.9	31.5
7	0.70	19.2 [3.00]	70.9 [4.49]	1.70 [0.05]	1.1	0.88	19.5 [2.73]	70.8 [3.59]	1.73 [0.12]	9.7	20.4
8	0.20	18.9 [1.63]	72.9 [1.84]	1.53 [0.14]	0.4	0.50	19.7 [1.06]	71.1 [1.48]	1.52 [0.23]	5.2	21.5
9	0.50	18.4 [3.20]	65.9 [3.68]	1.56 [0.13]	0.5	0.30	20.6 [2.15]	70.9 [2.55]	1.66 [0.27]	14.7	19.5
10	0.30	20.5 [1.57]	70.5 [1.50]	1.51 [0.21]	1.2	0.50	22.8 [4.93]	67.2 [5.95]	1.61 [0.09]	10.9	7.0
11	0.30	23.6 [0.96]	65.8 [0.80]	1.57 [0.21]	20.1	0.40	24.4 [1.48]	64.8 [1.33]	1.55 [0.16]	13.2	9.7
GM††	0.44	18.9	68.6	1.61	2.9	0.48	19.2	68.6	1.60	16.7	19.2

†, measured at 0-0.20 m interval.

‡, Projected area of trees was estimated assuming the tree as a conical surface.

††, geometric mean.

Values of clay, sand and bulk density at IR locations followed by * indicate significantly different for the Tukey test at $p< 0.05$ and, comparing IR and UC.

K_s was measured with a constant head permeameter (EijkelkampAgrisearch Equipment, Giesbeek, The Netherlands). The average value at 0-0.20 m were 2.9 cm h^{-1} at IR, and 16.7 at UC, respectively. The maximum soil depth was around 0.45 m at both locations, ranged from 0.30 m in upper areas at the north part of channel, to 0.88 m in lower levels. The average and standard deviation of canopy height and diameter was 2.9±0.6 and 3.7±0.9 m, respectively. These dimensions were highly variable between trees, and

also in time due to pruning operations. So the average projected canopy area assumed as a conical surface was 20±7.7 m^2.

The north-western part of catchment had more coarse particles concentration than the rest, and the average ranged from 0.70 at IR to 0.56% at UC. The topsoil organic matter content was low, with values below 1% for both sites. Generally these contents were slightly higher at UC. Information about the water retention curve measured at 0-0.20 m for these locations, and the fitting of van Genuchten equation can be found in Espejo et al. (2014).

2.2.2.2. Soil water sensor network.

Soil water content was measured at the 11 locations, at IR and at UC, respectively. The soil water sensor network consisted on 108 sensors: 10 5TE and 98 10HS devices (Decagon Devices, Pullman, WA). Both measure the soil water content via the dielectric constant of the soil using capacitance technology (Mittelbach et al. 2012; Rosenbaum et al. 2010). In addition to water content, the 5TE sensors also measures temperature and electrical conductivity. The 10HS sensors were installed horizontally and oriented against the slope direction at depths of 0.05, 0.15, 0.25, 0.35 and 0.45 m if soil depth was sufficient, at the IR and UC areas. The 5TE sensors were installed following the same procedure at 0.05 m adjacent to 10HS sensor to contrast their performance. Sensor readings were recorded every 5 minutes. Gravimetric soil moisture was periodically measured and used to calibrate the sensors at both locations, IR and UC. The results showed that default calibration overestimated the soil water content for both sensor models (Fig. 2.6). No differences in the sensors performance was observed between IR and UC, and therefore a common exponential fit similar to the one proposed by Mittelbach et al. (2011) was adopted for the 10HS sensors, while a linear fit was used for the 5TE sensors (R^2> 0.70, for both sensors).

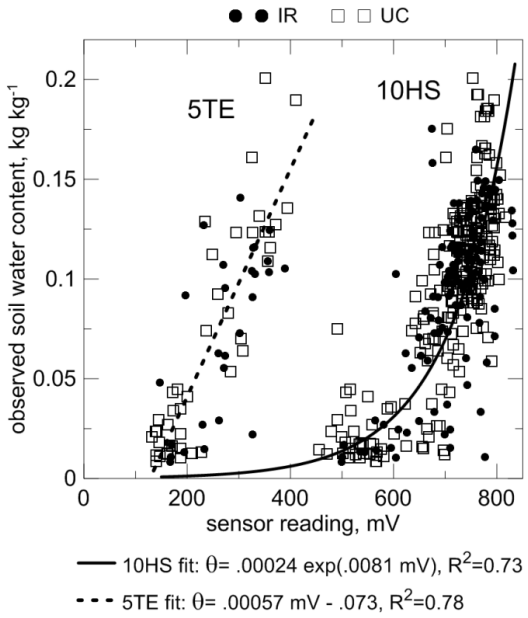

Fig. 2.6. Calibration function for the 10HS and 5TE sensors using gravimetric samples at inter row, IR, and at under canopy, UC, of trees.

2.2.2.3. Gauging station.

Runoff was measured at the outlet of the catchment with a gauging station, described by Taguas et al. (2009). Rainfall was also measured in situ at one-minute intervals with a rain gauge. Occasional data gaps were filled using data from nearby automated weather stations at hourly temporal resolution (CAP, 2013), located at distance of 6.6 km from the catchment. Previously data were compared and did not differ much from those measured in situ in the catchment.

2.3. References.

Agrela, F., J.A. Gil, J.V. Giráldez, R. Ordóñez, and P. González. 2003. Obtention of reference value in the measurement of the cover fraction in conservation agriculture. In: B. Cury, and L.B. Canalli, editors. Proceedings of 2nd World Congress on Conservation Agriculture. Brazilian Federation of Direct Drilling and Irrigation, Iguazú, Brazil, 44-47.

CAP, Consejería de Agricultura y Pesca de la Junta de Andalucía. 2013. Red de Alerta e Informacion Fitosanitaria (RAIF). Available at:

http://www.juntadeandalucia.es/agriculturaypesca/portal/servicios/estadisticas/servicio-de-informacion-agroclimatica/red-de-alerta-e-informacion/datos-de-las-estaciones-agroclimaticas.html, accessed on 06/05/2013.

Espejo, A.J., J.V. Giráldez, K. Vanderlinden, E.V. Taguas, and A. Pedrera. 2014. A method for estimating soil water diffusivity from moisture profiles and its application across an experimental catchment. J. Hydrol. 516, 161-168.

Espejo, A.J. 2004. Análisis de la erosión y escorrentía en microcuencas. Unpubl. Agr. Engng. Diploma Diss. Dpt. of Agronomy. University of Córdoba, Spain.

García del Barrio, I., L. Malvárez, and J.I. González. 1971. Mapas provinciales de suelos. Cádiz. Ministerio de Agricultura. Madrid. Spain.

Mittelbach, H., I. Lehner, and S.I. Seneviratne. 2012. Comparison of four soil moisture sensor types under field conditions in Switzerland. J. Hydrol. 430-431, 39-49.

Mittelbach, H., F. Casini, I. Lehner, A.J. Teuling, and S.I. Seneviratne. 2011. Soil moisture monitoring for climate research: Evaluation of a low cost sensor in the framework of the Swiss Soil Moisture Experiment (SwissSMEX) campaign. J. Geophys. Res. 116, D05111, doi:10.1029/2010JD014907.

Rosenbaum, U., J.A. Huisman, A. Weuthen, H. Vereecken, and H.R. Bogena. 2010. Quantification of sensor-to-sensor variability of the ECH2O EC-5, TE and 5TE sensors in dielectric liquids. Vadose Zone J. 9, 181-186.

Soil Survey Staff. 1999. Soil Taxonomy, 2nd ed. USDA Agr. Hbk. 436, Washington, D.C.

Taguas E.V., J.L. Ayuso, A. Peña, Y. Yuan, and R. Pérez. 2009. Evaluating and modelling the hydrological and erosive behaviour of an olive orchard microcatchment under no-tillage with bare soil in Spain. Earth Surf. Process. Landf. 34, 738-751.

Valdés, B., S. Talavera, and E. Fernández-Galiano. 1987. Flora vascular de Andalucía Occidental. Ketres, Barcelona, Spain.

Chapter 3

Soil loss and runoff reduction in olive-tree dry-farming with cover crops[1]

[1]Modified from: Espejo-Pérez, A.J., A. Rodríguez-Lizana, R. Ordóñez, and J.V. Giráldez. 2013. Soil loss and runoff reduction in olive-tree dry-farming with cover crops. Soil Sci. Soc. Am. J. 77, 2140–2148.

3.1. Abstract.

Soil erosion constitutes a major problem in the dry-farming agriculture of Mediterranean areas. The coincidence of fall showers falling over bare soils after a long, hot, dry summer, steep slopes, and intensive tillage, or the occurrence of large uncultivated patches like in tree-cropping, aggravate the problem. Among several soil conservation practices cover crops are being adopted by olive farmers as a promising method to reduce soil and water losses. This report summarizes the results of 2 yr from a network of micro-plots installed in olive orchards in the olive-growing area of Southern Spain to improve the technique of soil management and extend it to farmers. The cover crop diminished soil losses in all the experimental plots with an average of 76%. Water loss was also reduced, although to a lesser extent, in 6 of the 8 fields, with an average of 22%. Additionally, the results showed the great influence of the cover percentage in the decrease in soil loss and in the concentration of sediments in the runoff. However, it should be taken into account that plant cover consumes water, and that the advantages of the increase in runoff in the water balance with the cover could be eliminated if it is not managed appropriately. Therefore, more years of experimentation covering different climate conditions are necessary.

3.2. Introduction.

The olive is an important crop in Spain, both for its extension -over 1.5 Mha, *e.g.* 27% of the European Union total (FAOSTAT, 2012), and its production, 42% of the community total (CAP, 2012). Andalusia has 60% of the national surface, and contributes 76% to national production. Olive trees have traditionally occupied marginal and not very fertile, steep soils, which are hardly suitable for herbaceous crops (*e.g.* Semple, 1931, Chap. XIV). The Mediterranean climate does not favour the maintenance of a continuous vegetation cover, especially after the long, hot summer season, in which natural wildfires are not infrequent. During the fall there are frequent showers with a high rain intensity causing important soil losses.

In addition to natural factors, some unsuccessful management strategies in agriculture increase the soil erosion risk. For example, when farmers try to remove weeds that could compete with the olive tree for available nutrients, water included, not only reducing the scant vegetation, but dislodging soil aggregates and compacting surface and subsurface soil layers (*e.g.* García-Orenes et al. 2012). Montgomery (2007) estimated that the erosion/production ratio from conventionally tilled agriculture averages one to two orders of magnitude greater than the corresponding values for soil with native vegetation and long-term geological erosion. Zhang (2012) conducted long-range forecasts to estimate the relationship between soil management and rainfall changes in central Oklahoma, and found a positive relationship between soil loss and tillage intensity.

The consequences of soil erosion are widely known, and soil deterioration is one of the main problems in Europe. According to Oldeman et al. (1991), 12% of the cases of soil degradation on the continent are a direct consequence of water erosion. In certain areas, such as the Mediterranean region, the problem is still worse and it has been estimated that 25 Mha experiences severe erosion losses (De Ploey et al. 1991). Soil fertility is reduced due to the selectiveness of the erosion process (Sharpley, 1985), and the dispersion of sediments leads to water and soil pollution (Holland, 2004). The loss of the topsoil reduces its water holding capacity, which decreases the chances of good harvests in a region such as Andalusia, where 78% of its olive-cropped area is cultivated as dry-farming.

There are no reliable soil loss estimates at a regional scale, which is a more general problem (Wilkinson and McElroy, 2007). Some reasonable values in the range of data on erosion plots installed in Andalusian olive orchards ranged from 10 Mg ha^{-1} y^{-1} (Martinez et al. 2006), 6.9 Mg ha^{-1} yr^{-1} (Gómez et al. 2008), 0.3 to 1.0 Mg ha^{-1} yr^{-1} with a cover crop system at a basin scale (Taguas et al. 2010), and field mapping data of 74 Mg ha^{-1} yr^{-1} (Poesen et al. 2002). Even more uncertainty exists with its effect on runoff ratios, which is a critical variable in the soil loss ratio (Yu et al. 2000). Maetens et al. (2012) conducted a compilation of 103 plot-measuring stations throughout Europe and the Mediterranean area and observed that the exceedance probability of tolerable soil loss rates was 20% lower when soil water conservation techniques were applied. However, no notable effect on the frequency distribution of runoff coefficients was observed. They suggested that effectiveness in reducing soil loss and runoff ratios should be directly calculated by comparing measurements on a reference plot with conventional management.

There are several soil conservation strategies, (*e.g.* Morgan, 1986), but, possibly, the most effective ones in this region are those based on crop and vegetation management, which are better adapted to the environmental conditions, not needing any continuous or expensive maintenance care (Stocking, 1994). The use of a vegetative cover, either live or dead, is a convenient protection for the soil and the environment. There are many forms of vegetative cover, like winter cover crops for spring-cultivated soils, (Zhu et al. 1989), vegetation filters, (Daniels and Gilliam, 1996), grassed waterways, (Fiener and Auerswald, 2003), alley crops, hedgerows and other agroforestry types (Young, 1986). The protection from the cover reduces runoff and soil loss, (Hoffman et al. 1983), alleviates soil compaction through the *biodrilling* of the roots, (Williams and Weil, 2004), retains nutrients like phosphorus transported by runoff, (Hart et al. 2004), lowers the herbicide load entering streams either by enhancing water infiltration into the soil, (Klöppel et al. 1997) or by retention and degradation, (Gaston et al. 2003), and mitigates the pollution risk from animal pathogens (Tate et al. 2004).

Therefore, the use of plant covers in woody crops can be an effective system for soil conservation in olive cropping, which also reduces runoff. However, the relative complexity of their management may cause difficulties in their establishment, requiring

more selective and economic herbicides and more efficient weed removal machines. To solve many of the establishment problems, and to extend the practice to the region's farmers, several plots have been installed in private farms representing the main types of olive cropping systems. The purpose of this work is the evaluation of the reduction in the intensity of soil loss and runoff in those plots, comparing cover crops (CC) with conventional tillage (CT).

3.3. Material and methods.

Section 2.1 describes the soil erosion experiments. This report corresponds to the first 2 yr of the trial (1 June 2003-1 June 2005).

The analysis of variance (ANOVA) was used to establish the effects of the factors on the measured parameters (soil loss and runoff). Differences between individual means were tested using the LSD test. The analysis was performed using all the plot and event values to prevent the effects of a block trend on other plots. Variance homogeneity was studied with the Levene test prior to combining years, experiment fields and soil management systems. Before this, the problem of variance heterogeneity had been solved with a logarithmic transformation when necessary (Steel and Torrie, 1980).

3.4. Results and discussion.

The runoff and soil loss results are presented separately.

3.4.1. Runoff production.

Cover crops generally reduced the water yield of the plots, as indicated in Table 3.1. The rainfall interception on the cover canopy was more effective than the water retention on the depressions of the surface micro-relief. The raindrop impact on the bare soil surface was able to compact the top layers further reducing water infiltration into the soil. In six out of eight plots the average increment in water yield due to the absence of cover was above 34% with respect to the cover results.

Table 3.1. Cumulative rainfall and average water yield in the farms for the cover crop and conventional tillage treatments, during the period 1 June 2003 – 1 June 2005. The number of samplings and rainfall appear after the farm index.

Farm	number of events	Rainfall, mm	Runoff, mm†		Reduction ‡	Runoff coefficient	
			CC	CT		CC	CT
C3	13	689	37.7	46.3	0.186 **	0.05	0.07
C4	13	834	40.4	92.3	0.562 **	0.05	0.11
C5	12	1016	54.8	98.7	0.445 *	0.05	0.10
J1	12	673	52.7	45.9	-0.148 *	0.08	0.07
J2	12	628	74.8	107.2	0.302	0.12	0.17
S2	11	496	16.5	24.7	0.332 *	0.03	0.05
H1	9	770	55.8	69.5	0.197	0.07	0.09
H2	9	770	62.0	57.4	-0.080	0.08	0.07

* Significant at the 0.05 probability level.

** Significant at the 0.01 probability level.

† Average values of the plot repetitions; CC, cover crop; CT, conventional tillage.

‡ Positive values indicate cover crop reduction compared to tillage system and negative values the opposite case.

Only in two of the eight plots was the different cumulative runoff production between the two treatments significant at the 0.01 probability level, although CT usually gave higher values than the crop-covered soil.

Fig. 3.1 represents the runoff coefficients evaluated in all the samplings in the respective plots. A majority of cases fall under the 1:1 line indicating the higher water yield of conventional tillage with respect to the plant cover treatment. In some cases shallow soils formed on steep slopes, like those of farm C5, which corresponds to the Sierra Morena in the north of the Cordoba province. Under these adverse circumstances, farmers are shifting to organic agriculture by which sheep grazing between the trees remove weeds. The soil is often more compacted with CC than with CT, as was the case of the J1 farm. This farm has been intensively tilled over the last twenty years. The poor organic content and underdeveloped soil structure, together with the scarcity of seeds, hindered the establishment of a spontaneous cover crop. The results suggested that CC was not always a reliable water conservation practice. In some farms, an occasional shallow till may trigger a higher water recharge by the rain than under CC, which is more appreciated by the farmers starting with this management system after many years

of intensive tillage. Maetens et al. (2012) observed that, under Mediterranean conditions, zero and minimum tillage are not effective water conservation systems, even though they reduce soil loss. Thus, in a cover crop system, an occasional vertical tillage operation could help to loosen the soil, improving seed emergence and reducing runoff.

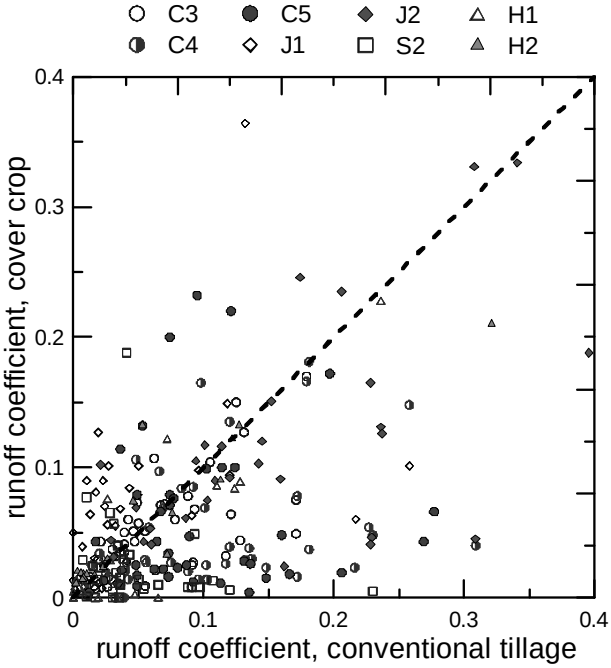

Fig. 3.1. Comparison of the respective runoff coefficients under conventional tillage and cover crop treatments for all the plots.

The influence of the surface cover on water yield is represented in Fig. 3.2, in which the estimated surface fraction is compared against the runoff coefficient for all the cases, and for the two treatments. The data taken on the CC treatment were confined to a smaller area of the plot, in contrast to the CT treatment, which was more widespread. This dispersion could be explained by the different soil erodibility conditions due to recent tillage operations, especially when the next rainfall occurred immediately. The maintenance of the vegetative cover ensured a more effective rainfall and runoff interception than periodic soil tillage. The advantage of CC is that a small surface density of plants may be efficient enough for water conservation purposes. An exponential upper envelope curve similar to the proposal of Gilley et al. (1986) could be drawn, but extended here to all the trials. There were two possible envelopes, the first one relating the runoff coefficient, *RC*, to the fraction of surface cover, *SC*, being

$$RC = 0.4e^{-1.5SC} \qquad \text{Eq. (3.1)}$$

This equation is valid for almost all the CT treatment sampling data, not including the plots with a dense vegetative cover like C5, S2 and H1, that had been under CC systems for a long period before the trial started, since their soils might be more compacted by agricultural machinery traffic during regular farm operations.

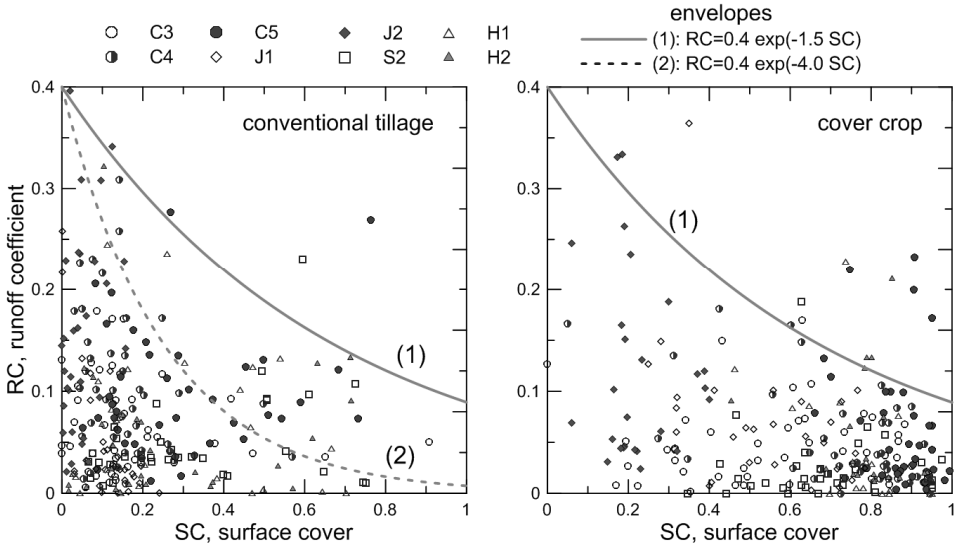

Fig. 3.2. Relationship between the fraction of surface covered by vegetation and runoff coefficients for the conventional tillage and cover crop treatments in all the plots, with upper envelope curve.

The second envelope is less restrictive and could be extended to the CC system

$$RC = 0.4e^{-4SC} \qquad \text{Eq. (3.2)}$$

Both coefficients in the exponent were close to the Gilley et al. (1986) numbers for sorghum [*Sorghum bicolor* (L.) Moench] and soybean [*Glycine max* (L.) Merr.] residues and to the proposal of Elwell and Stocking (1976, Fig. 4). Other authors like Freebairn and Wockner (1986b) found linear relationships between runoff coefficients and surface cover.

The average runoff coefficient value in the case of the CC system was 0.062 with a coefficient of variation of 0.997, while, in the case of CT, the corresponding values were 0.086 and 0.944. These results were much lower and coherent with the literature than those found by Zorn and Petan (2008) using plots of the same size on bare soil in a young olive grove in Slovenian Istria (0.32).

3.4.2. Soil loss.

The cumulative average soil loss data are shown in Table 3.2. The most important result was the great sediment yield reduction by the CC treatment in all cases, with values above 76% in seven out of eight farms. The average soil loss in the farms varied between 0.03 and 0.33 kg m^{-2} for the two year period in the cover crop treatment, and between 0.17 and 0.99 kg m^{-2} under conventional tillage, which was below the tolerable soil loss rate, (*e.g.* Morgan, 1986, section 7.1). These values were also lower than average ones reported for the period from 2000 to 2006 by Gómez et al. (2008), but similar to those measured in the same years of this report by those authors. In all the farm data, except in C3, the differences between the sediment yields under CT and CC treatments were significant. One explanation could be that the cover reduced soil loss on this farm but not significantly, possibly due to its partial removal after a tillage pass in March (Table 2.2), and so the coverage in CC was also eliminated.

Table 3.2. Cumulative average sediment yield in the farms for the cover crop and conventional tillage treatments, during the period 1 June 2003 – 1 June 2005. The samplings number appears after the farm index.

Farm	number of events	Sediment yield † kg m^{-2}		Reduction ‡
		CC	CT	
C3	13	0.118	0.168	0.298
C4	13	0.090	0.316	0.715 **
C5	12	0.116	0.423	0.726 *
J1	12	0.135	0.366	0.631 *
J2	12	0.329	0.993	0.669 *
S2	11	0.051	0.205	0.751 *
H1	9	0.067	0.616	0.891 *
H2	9	0.028	0.213	0.869 *

* Significant at the 0.05 probability level.

** Significant at the 0.01 probability level.

† Average values of the plot repetitions; CC, cover crop; CT, conventional tillage.

‡ Positive values indicate cover crop reduction compared to tillage system and negative values the opposite case.

The individual plot data for the different farms (Fig. 3.3) confirmed the soil conservation efficiency of the CC treatment. Almost all the data fall under the 1:1 line. Some data such as those of the J2 farm were very close in both treatments. From a soil conservation standpoint the establishment of cover crops was a very convenient agricultural practice, but it was more effective in soil conservation than in water retention in the plot.

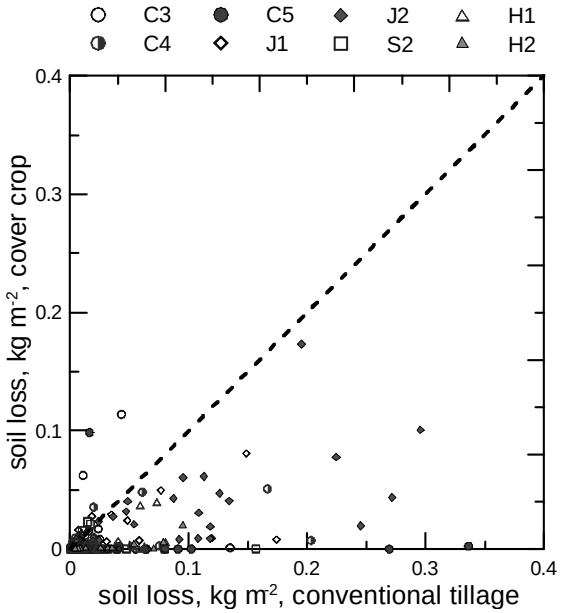

Fig. 3.3. Comparison of the individual soil loss samplings between conventional tillage and cover crop treatments for all the plots.

The lower reduction in soil loss on the C3 farm was also seen in Fig. 3.4, in which a comparison between the cumulative values of two farms is depicted. The areas with the steepest slope of the curve coincided with rain events following a tillage operation. The episodic nature of soil erosion is observed in the plots of Fig. 3.4 for two of the farms. The soil loss recorded in a few sampling intervals represented a large fraction of the total difference between treatments like 65% in the events receiving a cumulative rainfall of 212 mm in the case of the C3 farm, or 62% in the corresponding case of the

C4 farm. This pattern is very common in the Mediterranean region, as was observed by Taguas et al. (2010).

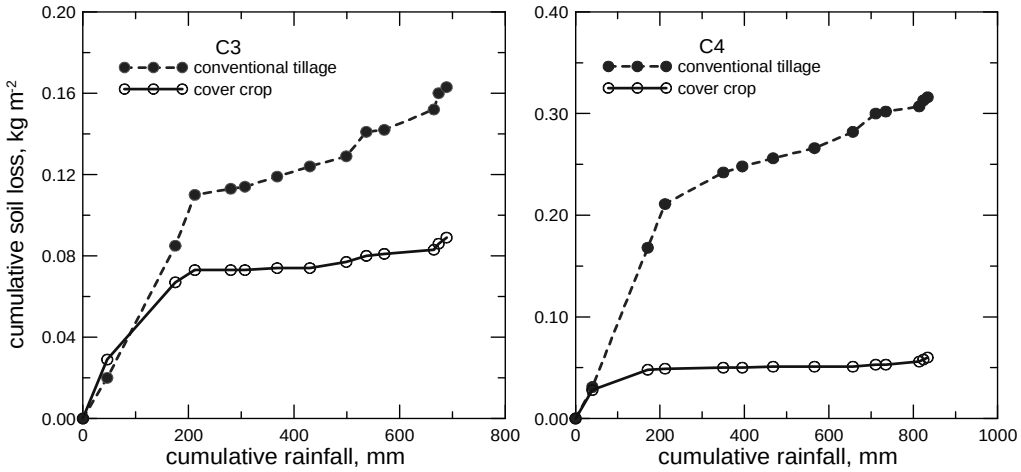

Fig. 3.4. Temporal evolution of the average cumulative soil loss in the plots of farm C3 and C4 during June 2003-June 2006 period.

The relation between soil loss and plant cover for all the cases is plotted in Fig. 3.5.

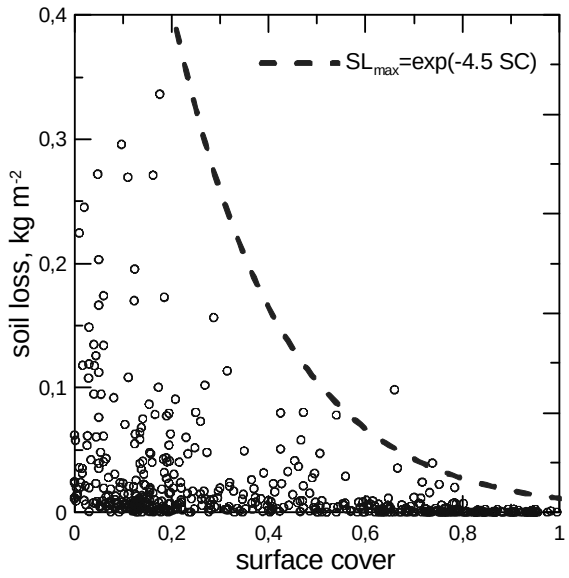

Fig. 3.5. Reduction of soil loss with fraction of surface covered by plants, including an upper envelope curve.

Soil loss reduction with the cover was more effective than runoff reduction, which can be observed by comparing Fig. 3.2. and 3.5. As in the runoff case, an exponential upper envelope has been delineated in the figure for the soil loss, SL,

$$SL = e^{-4.5SC} \qquad \text{Eq. (3.3)}$$

Other authors like Freebairn and Wockner (1986b), Gilley et al. (1986), and Khan et al. (1988) obtained similar results with other crops. Rogers and Schumm (1991) found a similar decreasing trend in soil loss with surface cover, although they suggested that other functions could fit their data better than the exponential. Proffitt et al. (1991) adopted the exponential function for the relationship between the rainfall detachability parameter and the shielding of the soil surface that can be taken as the complementary value of the surface cover. Rose and Freebairn (1985) presented data of sediment entrainment by overland flow that depended on surface cover. The last two parameters are components of the GUEST erosion model (Misra and Rose, 1996). As indicated by Freebairn et al. (1989), the Universal Soil Loss Equation model relates the soil cover-management factor to the surface cover exponentially.

Morgan (1986, section 8.4) stated that a mulch should cover between 70 and 75% of the soil surface to effectively protect the soil. Nevertheless, the results shown in Fig. 3.5 supported a more reduced surface fraction of about 50%, with a still safe range of between 20 and 50%. Rogers and Schumm (1991) suggested even a lower fraction, of between 15 and 43%.

Nunes et al. (2012) recently evaluated and compared the hydrological and erosion response of soils under different land uses and vegetation types in central Portugal. They observed that cereal cultivation and tree planting accelerated runoff and soil erosion compared to pasture and afforested lands. This was attributed to soil tillage which loosens the soil and reduces its erodibility. The maintenance of a 50% cover protection exponentially decreased the losses to tolerable levels.

Another useful index of cover crop performance is the soil loss to runoff ratio, *SL/RO*, as used by Meyer et al. (1970), or simply, the average sediment concentration in the

runoff flow. Fig. 3.6 presents the *SL/RO* data for all the samplings, plots, and farms. The average sediment concentration decreased as the surface cover grew, independently of the soil management system. An exponential upper envelope had been plotted with the Eq. (3.4),

$$\frac{SL}{RO} = 50e^{-2.5\,SC} \qquad \text{Eq. (3.4)}$$

There were some data points above the curve due to the cover's density and height in farm S2 plots. Also, one of the plots had a great deal of seed on the surface and an attack from ants, modifying the topsoil's natural conditions. The rest of the points were under the curve. Gilley et al. (1986) for their sorghum and soybean residue plots, and Freebairn and Wockner (1986a, 1986b) for their stubble mulch trial on Australian vertisols, reported similar results. The relationship of average sediment concentration and surface cover of Loch and Donnollan (1988) was closer to a straight line than to an exponential.

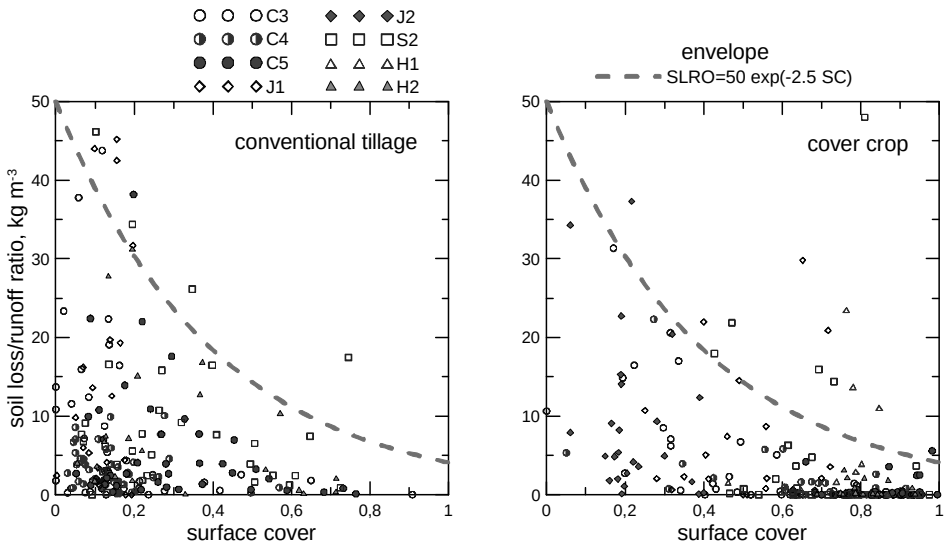

Fig. 3.6. Relationship of soil loss to runoff ratio with fraction of surface covered by plants, including an upper envelope curve.

These results were encouraging ones for the adoption of cover crop practice in the region. However, the establishment of cover crops takes a few years in order to try to

find the optimal plant species which is able to reproduce itself after the summer season and support the impact of agricultural practices like the olive fruit harvest that causes severe soil compaction. Given the reduced size of the plots, the fraction of surface cover obtained here may change at a larger scale. The spatial density of the cover is another aspect that should be explored since, in many farms, the alignment of trees follows the steepest direction on the slopes. In this case, the cover crops must be set up following the contour lines to increase the interception efficiency of water and sediments.

3.5. Conclusions.

Cover crops provide a suitable soil and water conservation practice for olive-cropping farms in Southern Europe. In our assays the vegetative cover was more effective in reducing the intensity of soil loss than in diminishing runoff. Decreases in erosion rates were obtained in all the plots, with values of between 30 and 87%, with a mean of 76%. With respect to water loss from runoff, a diminution was found in six of the eight farms but in two of them it increased, possibly because of a surface compaction of the land. The results were not usually significant in all the experimental fields, although the means did turn out to be lower. The mean decrease was 22% (all farms) with the eight fields, and 34% when excluding the plots in which the runoff was greater with tillage.

The annual soil loss distribution was not uniform with the rainfall events and some of these signified around 40% of the losses accumulated. These occurred in the fall rains, when the soil was unprotected. With regard to runoff, a more homogeneous distribution was noted as, unlike the soil loss, the maximum episodes did not give rise to such a high percentage of loss as those of the soil.

Soil cover is vital in the reduction of soil loss, doing so proportionally as the coverage percentage rises. It could be considered that a soil with a cover of over 20% is well protected against most events. However, covers of over 70% reduced erosion to practically zero values, with a mean of under 0.003 kg m^{-2} (IC95%= [0.85, 3.70]) regardless of the erosivity of the rain event, which demonstrates the effectiveness of vegetation in reducing the kinetic energy of raindrops. In fact, in 41% of the cases, when considering the whole of the plots, blocks and events, no soil loss occurred when

it was covered with vegetation. However, under our climate conditions, the maintenance of these soil coverage rates at a basin scale can be difficult if good management strategies are not established. Furthermore, the plant remains help improve the soil quality of many olive groves.

Similarly, the sediment concentration diminished as the degree of cover increased, so that the establishment of a vegetation cover not only achieved a lesser leakage of water from the system but also decreased the cloudiness of this water.

Anyway, although a vegetation cover seems, in principle, to be beneficial for runoff reduction, it should be borne in mind that it consumes water that could be of use to an olive grove, which is mostly grown under dry-farming, so that the water balance could be negatively affected if the system is not adequately managed. It would therefore be necessary to carry out research with different species in this respect. Likewise, it would be necessary to analyze what effect surface compaction could have on the olive-vegetation cover system-. Finally, in the light of the results obtained, it can be said that a vegetative cover in woody crops is a highly effective technique for reducing soil loss and an acceptable one for diminishing water losses from runoff.

3.6. References.

Consejería de Agricultura y Pesca. 2012. Anuario de Estadísticas Agrarias y Pesqueras, 2009. Available at http://www.juntadeandalucia.es/agriculturaypesca/portal/servicios/estadisticas/estadisticas/agrarias/resumen-anual.html, accessed on November 9, 2012.

Daniels, R.B., and J.W. Gilliam. 1996. Sediment and chemical load reduction by grass and riparian filters. Soil Sci. Soc. Am. J. 60, 246-251.

De Ploey, J.A., A. Imeson, and L.R. Oldeman. 1991. Soil erosion, soil degradation and climate change. In: F.M. Broker, A.J. Thomas, and M.J. Chadwick, editors. Land use change in Europe. Kluwer, London. pp. 275-292.

Elwell, H.A., and M.A. Stocking. 1976. Vegetal cover to estimate soil erosion hazard in Rhodesia. Geoderma 15, 61-70.

FAOSTAT. 2012. Agricultural statistics, available at http://faostat.fao.org. Retrieved on November 3, 2012.

Fiener, P., and K. Auerswald. 2003. Effectiveness of grassed waterways in reducing runoff and sediment delivery from agricultural watersheds. J. Environ. Qual. 32, 927-936.

Freebairn, D.M., and G.H. Wockner. 1986a. A study of soil erosion on vertisols of the Eastern Darling Downs, Queensland. I. Effects of surface conditions on soil movement within contour bay catchments. Aust. J. Soil Res. 24, 135-158.

Freebairn, D.M. and G.H. Wockner. 1986b. A study of soil erosion on vertisols of the Eastern Darling Downs, Queensland. II. The effect of soil, rainfall, and flow condition on suspended sediment losses. Aust. J. Soil Res. 24, 159-172.

Freebairn, D.M., G.H. Wockner, and D.M. Silburn. 1986. Effects of catchment management on runoff, water quality and yield potential from vertisols. Agric. Water Manag. 12, 1-19.

Freebairn, D.M., D.M. Silburn, and R.J. Loch. 1989. Evaluation of three soil erosion models for clay soils. Aust. J. Soil Res. 27, 199-211.

García-Orenes, F., A. Roldán, J. Mataix-Solera, A. Cerdá, M. Campoy, V. Arcenegui, and F. Caravaca. 2012. Soil structural stability and erosion rates influenced by agricultural management practices in a semi-arid Mediterranean agro-ecosystem. Soil Use Manag. 28, 571-579.

Gaston, L.A., D.J. Boquet, and M.A. Bosch. 2003. Fluometuron sorption and degradation in cores of silt loam soil from different tillage and cover crop systems. Soil Sci. Soc. Am. J. 67, 747-755.

Gilley, J.E., S.C. Finkner, and G.E. Varvel. 1986. Runoff and erosion as affected by sorghum and soybean residue. Trans. ASAE 29, 1605-1610.

Gómez, J.A., T.A. Sobrinho, J.V. Giráldez, and E. Fereres. 2008. Soil management effects on runoff, erosion and soil properties in an olive grove of Southern Spain. Soil Till. Res. 102, 5-13.

Hart, M.F., B.F. Quin, and M.L. Nguyen. 2004. Phosphorus runoff from agricultural land and direct fertilizer effects: A review. J. Environ. Qual. 33, 1954-1972.

Hoffman, L., R.E. Ries, and J.E. Gilley. 1983. Relationship of runoff and soil loss to ground cover of native and reclaimed grazing land. Agron. J. 75, 599-602.

Holland, J.M. 2003. The environmental consequences of adopting conservation tillage in Europe: reviewing the evidence. Agric. Ecosyst. Environ. 103, 1-25.

Khan, M.J., E.J. Monke, and G.R. Foster. 1988. Mulch cover and canopy effect on soil loss. Trans. ASAE 31, 706-714.

Klöppel, H., W. Kordel, and B. Stein. 1997. Herbicide transport by surface runoff and herbicide retention in a filter strip- Rainfall and runoff simulation studies. Chemosphere 35, 129-141.

Loch, R.J., and T.E. Donnollan. 1988. Effects of the amount of stubble mulch and overland flow on erosion of a cracking clay soil under simulated rain. Aust. J. Soil Res. 26, 661-972.

Maetens, W., J. Poesen, and M. Vanmaercke. 2012. How effective are soil conservation techniques in reducing plot runoff and soil loss in Europe and the Mediterranean?. Earth Sci. Reviews 115, 21-36.

Martínez, A., V.H. Durán, and J.R. Francia. 2006. Soil erosion and runoff response to plant-cover strips on semiarid slopes (SE Spain). Land. Degrad. Develop. 17, 1-11.

Meyer, L.D., W.H. Wischmeier, and G.R. Foster. 1970. Mulch rates required for erosion control on steep slopes. Soil Sci. Soc. Am. J. 34, 928-931.

Misra, R.K., and C.W. Rose. 1996. Applications and sensitivity analysis of process-based erosion model GUEST. Eur. J. Soil Sci. 47, 593-604.

Montgomery, D.R. 2007. Soil erosion and agricultural sustainability. PNAS 104, 13268-13272.

Morgan, R.P.C. 1986. Soil erosion and conservation. Longman. London. UK.

Nunes, A.N., A.C. de Almeida, and C.O.A. Coelho. 2012. Impacts of land use and cover type on runoff and soil erosion in a marginal area of Portugal. Appl. Geogr. 31, 687-699.

Oldeman, L.R., R.T.A. Hakkeling, and W.G. Sombroek. 1991. World map of the status of human-induced soil degradation. An explanatory note. Revised ed. UUEP and ISRIC. Wageningen. The Netherlands.

Poesen, J., L. Vandekerckhove, J. Nachtergaele, D. Oostwoud Wijdenes, G. Verstraeten, and B. Van Wesemeal. 2002. Gully erosion in dryland environments. Chap. 8. In: L.J. Bull, and M.J. Kirkby, editors. Dryland rivers: Hydrology and Geomorphology of semi-arid climates. John Wiley & Sons. Chichester.

Proffitt, A.R., C.W. Rose, and P.B. Hairsine. 1991. Rainfall detachment and deposition: experiments with low slopes and significant water depths. Soil Sci. Soc. Am. J. 55, 325-332.

Rogers, R.D., and S.A. Schumm. 1991. The effect of sparse vegetative cover on erosion and sediment yield. J. Hydrol. 123, 19-24.

Rose, C.W., and D.M. Freebairn. 1985. A new mathematical model of soil erosion and deposition processes with application to field data. In: S.A. El-Swaify, W.C. Moldenhauer, and A. Lo, editors. Soil erosion and conservation. Soil and Water Conservation Society. Ankeny. pp. 549-557.

Semple, E.C. 1931. The Geography of the Mediterranean region. Its relation to ancient history. AMS Press. New York.

Sharpley, A.N. 1985. The selective erosion of plant nutrients in runoff. Soil Sci. Soc. Am. J. 49, 1527-1534.

Steel, R.G., and J.H. Torrie. 1980. Principles and procedures of statistics: a biometrical approach. 2nd ed. McGraw-Hill, New York.

Stocking, M.A. 1994. Assessing vegetative cover and management effects. in Lal, R. ed. *Soil erosion research methods*. 2nd ed. Soil and Water Conservation Society. Ankeny, Chap. 9.

Taguas, E.V., A. Peña, J.L. Ayuso, R. Pérez, Y. Yuan, and J.V. Giráldez. 2010. Rainfall variability and hydrological and erosive response of an olive tree microcatchment under no-tillage with a spontaneous grass cover in Spain. Earth Surf. Proc. Landf. 35, 750-760.

Tate, K.W., M.D.G. Pereira, and E.R. Atwill. 2004. Efficacy of vegetated buffer strips for retaining *Cryptosporidium Parvum*. J. Environ. Qual. 33, 3342-3351.

Williams, S.M., and R.R. Weil. 2004. Crop cover root channels may alleviate soil compaction effects on soybean crop. Soil Sci. Soc. Am. J. 68, 1403-1409.

Wilkinson, B.H., and B.J. McElroy. 2007. The impact of humans on continental erosion and sedimentation. Geol. Soc. Am. Bull. 119, 140-156.

Young, R.A. 1986. The potential of agroforestry for soil conservation. Part I. Erosion control. ICRAF working paper 42. ICRAF. Nairobi.

Yu, B., S. Sombatpanit, C.W. Rose, C.A.A. Ciesiolka, and K.J. Coughlan. 2000. Characteristics and modelling of runoff hydrographs for different tillage treatments. Soil. Sci. Soc. Am. J. 64, 1763-70.

Zhang, J. 2012. Cropping and Tillage Systems Effects on Soil Erosion under Climate Change in Oklahoma. Soil Sci. Soc. Am. J. 76, 1789–1797.

Zhu, J.C., C.J. Gantzer, S.H. Anderson, E.E. Alberts, and P.R. Beuselinck. 1989. Runoff, soil, and dissolved nutrient losses from no-till soybean with winter cover crops. Soil Sci. Soc. Am. J. 53, 1210-1214.

Zorn, M., and S. Petan. 2008. Interrill soil erosion on flysch soil under different types of land use in Slovenian Istria. IOP Conf. Ser. Earth Environ. Sci. 4 012045. http://iopscience.iop.org/1755-1315/4/1/012045.

Chapter 4

A probabilistic water erosion model with variable cover factor for Mediterranean olive orchards

4.1. Abstract.

A simple probabilistic model to describe soil and water loss in olive planted areas in Mediterranean environments is presented. The model is based on the field observations obtained during three hydrological years (2003-2007) in a network of 1-m^2 microplots located in different sites of southern Spain. The soil was subjected to two different managements systems: conventional tillage, where the weeds were removed by disk harrows or cultivators, and establishment of cover crops with a protective layer of vegetation maintained on the surface until the beginnings of spring when this layer was chemically killed to avoid any competence for soil nutrients among the grass and the olive trees.

Since the essential processes are runoff generation, soil erosion, and sediment interception through the cover crop, the most relevant data were rain depth, fraction of vegetation covered area, and slope. Rain depth and slope were generated, respectively, with a Gamma and a Uniform probability distribution function, and the fraction of vegetation covered area with a sigmoid type function.

To validate the model simulations were generated with a Monte Carlo scheme to reproduce the observed results. The moments of the observed and simulated results were compared.

4.2. Introduction.

Dry-farming systems require appropriated soil management system to capture runoff water in soil, inducing infiltration and reducing evaporation. Olive tree crops were confined to the poor soils developed on steep lands from the antiquity. The combined effect of intense rains, reduced infiltration capacity, and high slopes with a rather sparse vegetation cover after the long dry summer period, enhance erosive processes. For these reasons the assessment of soil erosion in Mediterranean environments, has received great attention with significant contributions (*e.g.* Sheridan et al. 2013; Lesschen et al. 2009; Kirkby et al. 2002).

Soil and water losses in semiarid lands have been estimated with small erosion plots, or microplots with a reduced area around 1 m^2 (*e.g.* Moreno de las Heras et al. 2010; Michaelides et al. 2009; Parsons et al. 2006; Chaplot et al. 2005; Bagarello and Ferro, 2004; Joel et al. 2002; Cerdá, 1998). The problem of soil erosion plots is the difficult extension of the results to other areas of different size given the variability of the climatic, soil, topographic and agronomic factors involved (*e.g.* Maetens et al. 2012).

Conservation of soil and water is essential for the maintenance of the Mediterranean lands (*e.g.* McNeill, 1992), although there are not simple solutions. A usual conservation practice for the olive tree planted areas is the establishment of cover crops which is many cases are very successful (*e.g.* Espejo et al. 2013; Gómez et al. 2009). Nevertheless there is a great heterogeneity of results evaluating the effectiveness of management systems on soil and water conservation.

In order to explore the results of Espejo et al. (2013) a simple soil erosion model has been proposed to improve the understanding of these processes. The hypothesis of the work is that it is possible to describe the process in a simple way due to the water erosion process have a stochastic character and a description of it probabilistic structure is required.

4.3. Field measurements.

Runoff and sediment yield were measured during three years (2003-2006) on 48 1-m^2 erosion microplots in eight olive tree farms across Andalusia (chapter 2, section 2.1).

An exploratory analysis of runoff and sediment yield for the measurement period, separately for soil management and farm was performed using the L-moment frequency analysis method (Hosking and Wallis 1997; Vogel and Fennessey, 1993). In hydrological studies this method allows compensating for insufficiently long time series using data from other locations with similar statistical characteristics. Individually for each indicators, runoff and sediment yield, and soil management, the values of the first five L-moments were coincident for the different farms. The L-moment diagram which described the theoretical relationship between L-kurtosis and L-skewness plotting all farms was a three parameters lognormal distribution for both indicators and soil management. In this manner the results suggested that microplots data set could be studied together.

The rain depth data were fitted to a two-parameter gamma probability distribution function whose density functions is (*e.g.* Bury 1999, Chapter 13),

$$f(x;\lambda,\sigma)=\frac{1}{\sigma\cdot\Gamma(\lambda)}\cdot\left(\frac{x}{\sigma}\right)^{\lambda-1}e^{-x/\sigma}\quad x\geq 0\quad \sigma,\lambda>0 \qquad \text{Eq. (4.1)}$$

The parameters λ and σ are, respectively the shape and scale factors. The values of the parameters fitted with the maximum likelihood method were λ=0.049 and σ=0.398. According to the χ^2 test the hypothesis of the gamma fit to these data could not be rejected at the 0.05 probability level.

The runoff volume data measured in the plots for the two treatments were also fitted by the two-parameter Gamma probability function, Eq. (4.1). The fits were not as good as in the case of the rain depth. For the cover crop treatment, CC, the fit could not be rejected at the 0.01 probability level, with the parameter values λ=0.292 and σ=0.690. For the conventional tillage treatment the fit was worse, with the parameter values λ=0.216 and σ=0.650.

Sediment yield data were fitted to an Exponential distribution function (Bury 1999, Chapter 12),

$$f(x;\mu,\beta)=\frac{1}{\beta}\exp\left(-\frac{x-\mu}{\beta}\right) \quad x\geq\mu \quad \mu\geq 0 \quad \beta>0 \qquad \text{Eq. (4.2)}$$

This distribution function is a special case of the Gamma function, Eq. (4.1) when the shape parameter λ is $\lambda=1$. The fitted parameter values for the cover crop treatment, CC, were μ=0.0100 kg m^{-2} and β=0.0182 kg m^{-2}. The hypothesis of the exponential fit to the data could not be rejected, using the χ^2 test at the 0.05 probability level. For the conventional tillage treatment, CT, the values were μ=0.0333 kg m^{-2} and β=0.0662 kg m^{-2}. The hypothesis of the exponential probability distribution function fit to the data could not be rejected, using the χ^2 test at the 0.01 probability level.

Finally, after considering the data range (0,1) for the fraction of plot area covered by vegetation, *C*, a Beta probability distribution function was chosen. The probability density function is (Bury 1999, Chapter 14),

$$f\left(x;\xi,\zeta,c,d\right)=\frac{\Gamma\left(\xi+\zeta\right)}{\Gamma\left(\xi\right)\Gamma\left(\zeta\right)}\left(\frac{x-c}{d-c}\right)^{\xi-1}\left(\frac{d-x}{d-c}\right)^{\zeta-1}\frac{1}{d-c} \quad c<x<d \quad \xi,\zeta>0 \quad \text{Eq. (4.3)}$$

The value of the boundary values for both treatments were c=0 and d=1. The fitted parameters to the data of the cover crop treatment, CC, were ξ=3.31 and ς=1.76. The Beta function fit could not be rejected at the 0.05 probability level. For the conventional tillage treatment, CT, the parameter values were ξ=1.44 and ς=3.30. Again the Beta fit to these data with the χ^2 test could not be rejected at the 0.05 probability level.

4.4. A simple erosion model for microplots.

After examining the behaviour of the erosive processes in the microplots, a simple model was conceived based on the time evolution of the vegetation covered fraction, *C*,

the runoff volume induced by the rain, the vegetative cover and the soil, Q, and the sediment mass, Q_s, generated by the rain on the soil for the mean slope, S.

There are many simple models in the runoff and soil erosion literature which have contributed to understand the involved processes (Reaney et al. 2014; Sheridan et al. 2013; Langhans et al. 2013; Kirkby et al. 2002; Stompth et al. 2002; Yu et al. 2000; Julien and Frenette 1985).

The temporal dynamics of C was characterized adopting the model of West et al. (2001), who expressed the variation of the body mass of living organisms as the difference between the incoming energy flow rate and the own mass, which leads to

$$C = \kappa_1 \left(1 - e^{-\kappa_2 t}\right) + \delta_c \qquad \text{Eq. (4.4)}$$

where κ_1 and κ_2 are parameters of the model, t is the day of observation, and δ_C is a residual term, defined as $\delta_C = C_o - C_e$, with C_o, and C_e, as the observed and estimated values of C, respectively. Fig. 4.1 shows the fit of Eq. (4.4) to the measured data in both treatments. The residual term could be best represented by a Gaussian probability distribution function. Eq. (4.4) is valid for the time interval (1,180), which corresponds to the period September 1, to February 27, when usually farmers kill the plants of the surface cover in the CC treatment. For the conventional tillage treatment the time interval is larger (1, 276), since natural weeds decline by the first days of June. A Uniform probability distribution function was chosen to generate the time.

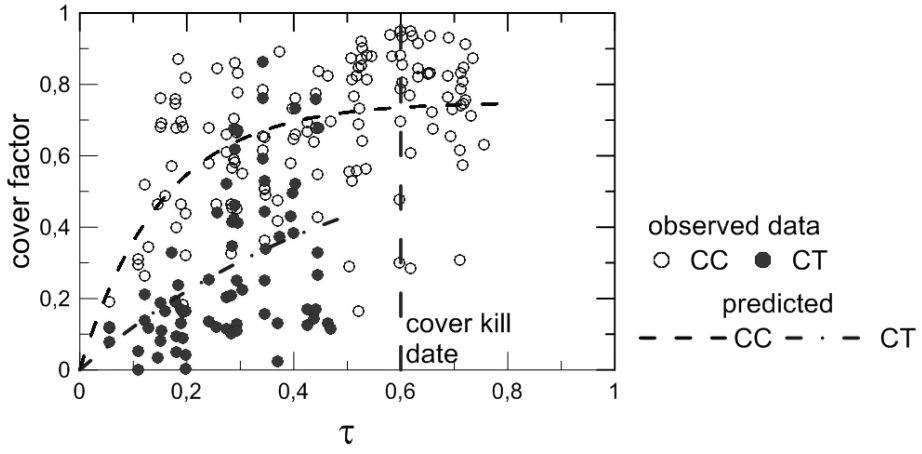

Fig. 4.1. Evolution of observed and simulated fraction of soil surface covered by vegetation, *C*, with normalized time, $\tau=t/T$, with the period being one year, for conventional tillage, CT, and cover crop, CC, treatments. Parameter values of Eq. (4.4), κ_1 and κ_2 were 0.72 and 1.83 for CT, and 0.75 and 6.53 for CC, respectively.

Runoff was characterized by a simple model, somewhat similar to the USDA SCS Curve Number method (*e.g.* Michel et al. 2005; Steenhuis et al. 1995) since it is assumed to be linearly related with the rain depth, R, including a correction factor for the vegetation covered fraction, C.

$$Q = \max\left\{\eta\left[R\left(1-C\right)\right]+\delta_Q, 0\right\} \qquad \text{Eq. (4.5)}$$

There is a dimensionless factor, η, and a residual term, δ_Q, with the same units as the rain depth and runoff volume, defined as $\delta_Q=Q_o-Q_e$, with Q_o and Q_e as the observed and estimated values of the runoff value, respectively. The residue δ_Q was fitted by a Gaussian probability distribution function (Table 4.1).

Table 4.1. Parameters of the Gaussian probability functions to the residuals of observed variables, fraction of soil surface plant covered area, δ_C, runoff volume, δ_Q, and sediment yield, δ_{Qs}, for the two treatments, conventional tillage, CT, and cover crops, CC.

residual	treatment	range	mean	s	probability level†
δ_C	CT	-0.331, 0.128	-0.00294	0.189	0.10
	CC	-0.562, 0.346	-0.00274	0.172	0.10
δ_Q, mm	CT	-16.1, 17.2	-0.0748	5.54	0.10
	CC	-8.08, 10.6	1.173	3.19	0.10
δ_{Qs}, kg m^{-2}	CT	-0.160, 0.261	-0.00386	0.0787	0.01
	CC	-0.0466, 0.0723	-0.00394	0.0219	0.10

† at which the proposed fit to the data could not be rejected

The sediment mass yield by water erosion in the microplot, Q_s, can be described by the simple expression proposed by Moore and Burch (1986) from the transport capacity concept characterized by the Yang total load Eq. (*e.g.* Yang, 1996, section 6.3.2.4).

$$Q_s = \gamma\left[(1-C)R\right]^{2/5} S^{13/10} + \delta_{Q_s} \qquad \text{Eq. (4.6)}$$

There is a coefficient, γ, and a residual term, δ_{Qs}, defined as in Eq. (4.4) and (4.5), by $\delta_{Qs} = Q_{so} - Q_{se}$, fitted, again, by a Gaussian probability distribution function. Fig. 4.2 shows the fit of Eq. (4.5) and (4.6) to the measured data.

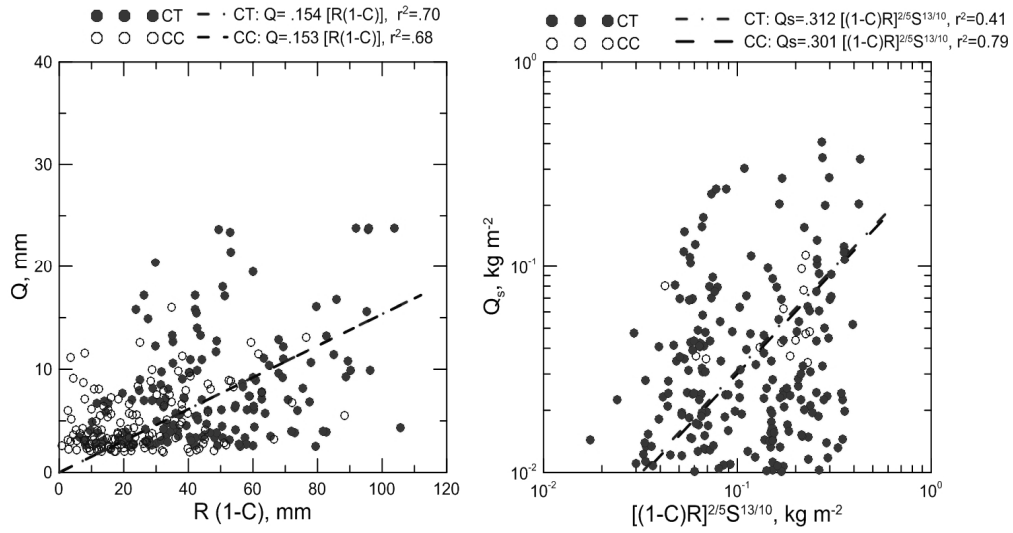

Fig. 4.2. a) Relationship between observed runoff, Q, and the product of rain depth, R, by the uncovered fraction of soil surface, $R(1-C)$, for conventional tillage, CT, and cover crop, CC, management. R is storm precipitation and C is cover factor. b) Relationship between observed sediment yield, Q_s, and $\left[(1-\boldsymbol{C})\boldsymbol{R}\right]^{0.4}\boldsymbol{S}^{1.3}$ for CT and CC. S is slope.

4.5. Monte Carlo simulation scheme: model validation and extension.

The model consisting of Eq. (4.4)-(4.6) was tested through a Monte Carlo simulation to generate sets of runoff volumes and sediment yields to compare with the observed results (*e.g.* Press et al. 2007, Chapter 7; Rubinstein 1981). The simulation starts with the generation of time, t, slope, S, and rain depth, R, using respectively Uniform, and a Gamma probability distribution functions, for the first two variables, and for the third one. Next the residues, δ_C, δ_Q, and δ_{Qs} were generated using the Gaussian probability distribution function with the parameters of Table 4.1. After applying Eq. (4.4) the

fraction of the soil surface covered by vegetation, *C*, was evaluated and, subsequently runoff volume, *Q*, with Eq. (4.5), and sediment yield, Q_s, with Eq. (4.6) were computed.

To validate the model 50,000 simulations were realized. The fit of the Beta probability function to measured data is shown in Fig. 4.3.

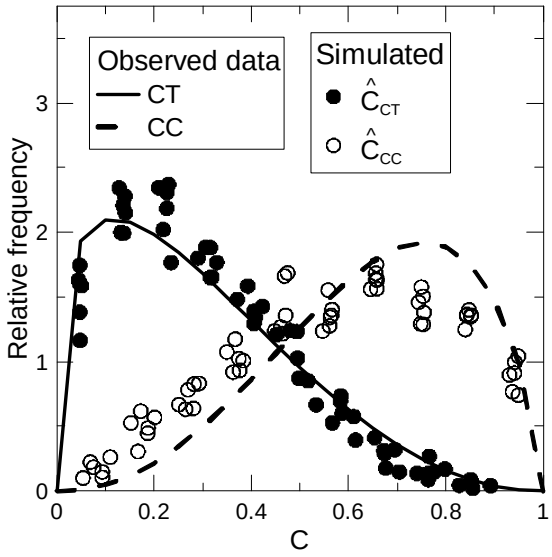

Fig. 4.3. Relative frequencies of simulated cover factor, *C*, obtained using Monte Carlo simulations, and truncated Beta pdf for observed C in conventional tillage, CT, and cover crop, CC, management. Parameters of the Beta function were 1.28 and 3.10 for CT, and 2.21 and 1.55 for CC, respectively.

The corresponding runoff volume and sediment yield data were analyzed and their basic statistical moments were determined. The comparison between these statistical moments is shown in Table 4.2. Fig. 4.4 indicates the close fit of simulated to measured data, represented by a simple line similar to the plots used by Settin et al. (2007)

Table 4.2. Comparison between the statistical moments of the measured and Monte Carlo simulated values of the runoff volume, Q, and sediment yield, Qs, separated by the treatment, conventional tillage, CT, and cover crop, CC

	moment	LT		CC	
		measured	simulated	measured	simulated
Q	mean, mm	5.82	5.59	2.12	2.67
	s, mm	3.98	3.91	2.67	2.82
	coefficient of skew	2.72	2.74	3.37	2.98
Q_s	mean, kg m^{-2}	0.0286	0.0370	0.00533	0.00724
	s, kg m^{-2}	0.0527	0.0523	0.0124	0.0153
	coefficient of skew	97.1	73.8	28.9	34.6

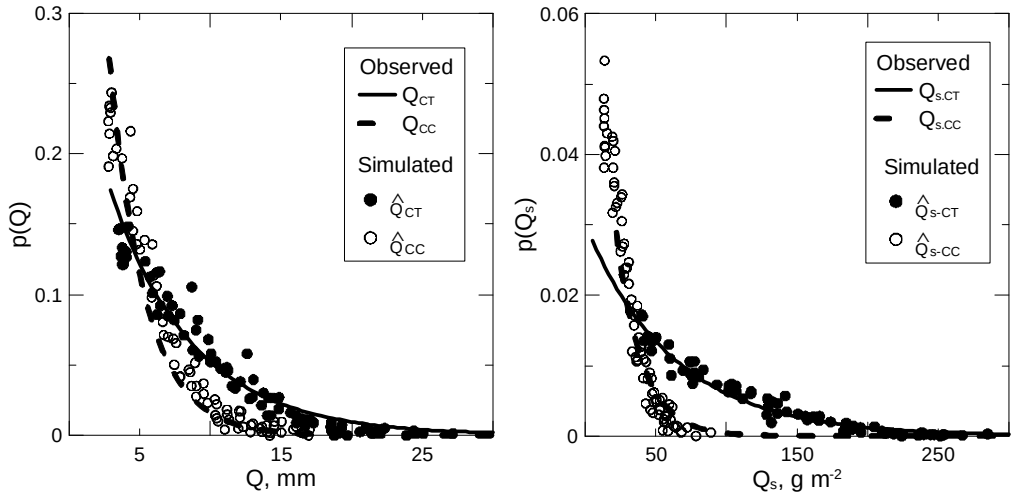

Fig. 4.4. Comparison between observed empirical probability density functions and simulated relative frequencies of (a) runoff, Q, and (b) sediment yield, Q_s.

4.6. General discussion and conclusions.

The key variables that controlled runoff and sediment yield in the microplots considered here were the fraction of soil surface covered by vegetation, C, the average slope, S, and the rainfall depth, R. The relationships between these variables and soil and water losses given by Eq. (4.5) and (4.6) explained approximately 60% of the sediment yield, Q_s, and 70% of runoff volume, Q. The smaller slope in the soil loss model, Eq. (4.6), for the cover crop, CC, as compared to conventional tillage treatment, CT, (0.19, and 0.52, respectively for CC, and CT management systems) shows the relevance of the agricultural practice n the processes, indicated by many authors as Yu et al. (2000). Soil

losses were greater under conventional tillage than under a cover crop, as expected. The reduction was more effective for sediment yield, what helps for the soil conservation purpose. Nevertheless in semiarid areas water as very important as a production factor, what encourages the design of conservation systems, (*e.g.* Rockström et al. 2012), like infiltration inducing trenches, or water harvesting such as half moon, or lunettes, which are being introduced slowly by farmers of the region.

The dispersion of simulated points (expressed as relative frequencies, Fig. 4.4) was larger for Q as compared to Q_s, and large in CT than in CC. It is interesting to note that the dispersion in the simulated data tended to be higher for lower losses, which can be an effect of tillage on porosity and natural infiltration capacity. These points also showed a higher probability of occurrence, but were small in number located around the observed probability distribution function.

In summary, the method presented to describe the production of runoff and sediment yield developing the probability density function for CC and CT treatments was successful. The use of multivariate techniques to correlate the water and soil loss with key variables, along with the stochastic generation of these key variables, allows easily describing a complex process such as erosion and evaluating the response of process in function of varying key factors. Thus we have taken an important step because we have achieved to interpret field observations and evaluate the influence of key variables, and their integration into a probabilistic model easy to use in other settings.

4.7. References.

Agrela, F., J.A. Gil, J.V. Giráldez, R. Ordóñez, and P. González. 2003. Obtention of reference value in the measurement of the cover fraction in conservation agriculture. In: Cury, B., and L.B. Canalli (Eds.). Proceedings II World Congress on Conservation Agriculture, Iguazú, Brazil. pp 44-7.

Bagarello, V., and V. Ferro. 2004. Plot-scale measurement of soil erosion at the experimental area of Sparacia (southern Italy). Hydrol. Proc. 18, 141-157.

Bury, K.A. 1999. Statistical distributions in Engineering. Cambridge Univ. Press. Cambridge. U.K.

Cerdá, A. 1999. Parent material and vegetation affect soil erosion in eastern Spain. Soil Sci. Soc. Am. J. 63, 362-368.

Chaplot, V.A.M., C. Rumpel, and C. Valentin. 2005. Water erosion impact on soil and carbon redistributions within uplands of Mekong River. Global Biogeochem. Cycl. vol. 19, GB4004, doi:10.1029/2005GB002493.

Espejo-Pérez, A.J., A. Rodríguez-Lizana, R. Ordóñez, and J.V. Giráldez. 2013. Soil loss and runoff reduction in olive-tree dry-farming with cover crops. Soil Sci. Soc. Am. J. 77, 2140–2148.

Gómez, J.A., T.A. Sobrinho, J.V. Giráldez, and E. Fereres. 2009. Soil management effects on runoff, erosion and soil properties in an olive grove of Southern Spain. Soil Till. Res. 102, 5-13.

Hosking, J.R.M., and J.R. Wallis. 1997. Regional frequency analysis. An approach based on L-Moments. Cambridge, University Press. Cambridge. U.K.

Joel, A., I. Messing, O. Seguel, and M. Casanova. 2002. Measurement of surface water runoff from plots of two different sizes. Hydrol. Proc. 16, 1467-1478.

Julien, P., and M. Frenette. 1985. Modelling of rainfall erosion. J. Hydr. Eng. ASCE 111, 1344-59.

Kirkby, M.J., and L.J. Bracken. 2009. Gully processes and gully dynamics. Earth Surf. Proc. Landf. 34, 1841-51.

Kirkby, M.J., L. Bull, and S. Reaney. 2002. The influence of land use, soils and topography on the delivery of hillslope runoff to channels in SE Spain. Earth Surf. Proc. Landf. 27, 1459-1473.

Langhans, C., G. Govers, and J. Diels. 2013. Development and parameterization of an infiltration model accounting for water depth and rainfall intensity. Hydrol Proc. 27, 3777-3790.

Lesschen, J.P., J.M. Schoorl, and L.H. Cammeraat. 2009, Modelling runoff and erosion for a semi-arid catchment using a multi-scale approach based on hydrological connectivity Geomorphol. 109, 174-183.

Maetens, W., J. Poesen, and M. Vanmaercke. 2012. How effective are soil conservation techniques in reducing plot runoff and soil loss in Europe and the Mediterranean?. Earth Sci. Rev. 115, 21-36.

McNeill, J.R. 1992. The mountains of the Mediterranean world. Cambridge Univ. Press, Cambridge, U.K.

Michaelides, K., D. Lister, J. Wainwright, and A.J. Parsons. 2009. Vegetation controls on small-scale runoff and erosion dynamics in a degrading dryland environment. Hydrol. Proc. 23, 1617-1630.

Michel, C., V. Andréassian, and C. Perrin. 2005. Soil Conservation Service Curve Number method: How to mend a wrong soil moisture accounting procedure? Water Resour. Res. 41, W02011, doi:10.1029/2004WR003191.

Molina, A., G. Govers, V. Vanacker, J. Poesen, E. Zeelmaekers, and F. Cisneros. 2007. Runoff generation in a degraded Andean ecosystem: Interaction of vegetation cover and land use. Catena 71, 357-370.

Moore, I.D., and G.J. Burch. 1986. Physical basic of the length-slope factor in the Universal Soil Loss Equation. Soil. Sci. Soc. Am. J. 50, 1294-98.

Moreno de las Heras, M., J.M. Nicolau, L. Merino-Martín, and B.P. Wilcox. 2010. Plot scale effects on runoff and erosion along a slope degradation gradient. Water Resour. Res. 46, W04503, doi:10.1029/2009WR007875.

Nunes, A.N., A.C. Almeida, and C.O.A. Coelho. 2012. Impacts of land use and cover type on runoff and soil erosion in a marginal area of Portugal. Appl. Geogr. 31, 687-99.

Parsons, A.J., R.E. Brazier, J. Wainwright, and D.M. Powell. 2006. Scale relationships in hillslope runoff and erosion. Earth Surf. Proc. Landf. 31, 1384-1393.

Press, W.H., S.A. Teukolsky, W.T. Vetterling, and B.P. Flannery. 2007. Numerical recipes: The art of scientific computing, 3rd ed. Cambridge Univ. Press, Cambridge, U.K.

Reaney, S.M., L.J. Bracken, and M.J. Kirkby. 2014. The importance of surface controls on overland flow connectivity in semi-arid environments: results from a numerical experimental approach. Hydrol. Proc. 28, 2116-2128.

Rockström, J., M. Falkenmark, M. Lannerstad, and L. Karlberg. 2012. The planetary water drama: Dual task of feeding humanity and curbing climate change. Geophys. Res. Lett. 39, L15401, doi:10.1029/2012GL051688.

Rubinstein, R.Y. 1981. Simulation and the Monte Carlo method. J. Wiley, New York, USA.

Settin, T., G. Botter, I. Rodriguez-Iturbe, and A. Rinaldo. 2007. Numerical studies on soil moisture distributions in heterogeneous catchments. Water Resour. Res. 43, W05425, doi:10.1029/2006WR005737.

Sheridan, G.J., P.J. Noske, P.N.J. Lane, O.D. Jones, and C.B. Sherwin. 2013. A simple two-parameter model for scaling hillslope surface runoff. Earth Surf. Proc. Landf., doi:10.1012/esp.3503.

Steenhuis, T.S., M. Winchell, J. Rossing, J.A. Zollweg, and M.F. Walter. 1995. SCS runoff equation revisited for variable source runoff areas. J. Irrig. Drain. Engng. ASCE 121, 234-238.

Stompth, T.J., N. de Ridder, T.S. Steenhuis, and N. van de Giessen. 2002. Scale effects of hortonian overland flow and rainfall-runoff dynamics: laboratory validation of a process-based model. Earth Surf. Proc. Landf. 24, 847-855.

Vogel, R.M., and N.M. Fennessey. 1993. L-moment diagram should replace product moment diagrams. Water Resour. Res. 29, 1745-52.

West, G.B., J.H. Brown, and B.J. Enquist. 2001. A general model for ontogenetic growth. Nature 413, 628-31.

Yang, C.T. 1996. Sediment transport. Theory and practice. McGrawth-Hill, New York, USA.

Yu, B., S. Sombatpanit, C.W. Rose, C.A.A. Ciesiolka, and K.J. Coughlan. 2000. Characteristics and modelling of runoff hydrographs for different tillage treatments. Soil. Sci. Soc. Am. J. 64, 1763-70.

Chapter 5

A method to estimate soil water diffusivity from field moisture profiles and its application across an experimental catchment[1]

[1]Modified from: Espejo, A.J., J.V. Giráldez, K. Vanderlinden, E.V. Taguas, and A. Pedrera. 2014. A method for estimating soil water diffusivity from moisture profiles and its application across an experimental catchment. J. Hydrol. 516, 161-168.

5.1. Abstract.

Despite the well-accepted value of soil hydraulic properties for describing and modeling matter and energy fluxes in the unsaturated zone, their accurate measurement across scales is still a daunting task. The increasing availability of continuous soil water content measurements at discrete points in space, as provided by sensor networks, offers still unexplored possibilities for evaluating soil physical properties across landscapes. In this study, we propose a new method, based on the Bruce and Klute equation, to estimate effective soil water diffusivity from soil water profile data observed during continuous desiccation periods. An analytical expression is proposed for the diffusion-soil water relationship, assuming an exponential relationship between soil water content and the Boltzmann variable. The method has been evaluated using soil water profile data observed at inter-row and under canopy locations across a rainfed olive orchard in SW Spain. The spatial variability of the effective soil water diffusivity across the orchard was estimated. Different soil conditions under the tree canopies as compared to inter-row areas resulted in significantly different effective diffusivity relationships, reflecting the effect of trees on soil physical properties and water dynamics across olive orchards. The proposed method offers a suitable alternative to traditional laboratory methods and can be easily extended to estimate soil hydraulic conductivity and water retention curves.

5.2. Introduction.

Soil hydraulic properties are important indicators for assessing soil functioning and are essential for modeling matter and energy fluxes in the unsaturated zone. However, laboratory measurements of these properties are generally time-consuming, expensive and labor-intensive. Since measurements are made on small soil cores, the results often lack representativeness for field-scale applications.

The increasing use of soil water content (SWC) sensor networks offers as yet unexplored possibilities for estimating effective soil physical properties across landscapes (Martinez et al. 2013). Such networks are generally established to provide detailed measurements of the soil water dynamics across a range of scales (Vereecken et al. 2008). Though still limited in its spatial resolution, SWC sensor networks deliver quasi-continuous information on the temporal dynamics of SWC at discrete points in space. In this work, we have extended a traditional laboratory method for estimating soil water diffusivity (Bruce and Klute, 1956) in order for it to be used with field-measured SWC data obtained during a continuous drying period, as an alternative to laboratory measurements of soil physical properties. To our knowledge, the method has so far not been used under such conditions.

Based on the diffusion theory Matano proposed in 1933 (Crank, 1956, section 11.62) a method for estimating the diffusivity coefficient, which was adopted later in soil science by Bruce and Klute (1956) for the evaluation of soil water diffusivity, $D(\theta)$, where θ is the volumetric water content, from horizontal absorption experiments, when the gradient of the gravitational component of soil water potential is negligible. In this case, space and time coordinates can be combined with the Boltzmann transform which converts the Richards' equation for horizontal water flow into an ordinary differential equation. The original method of Bruce and Klute (1956) required water content and horizontal distance measurements of the wetting front from the water inlet at fixed times. Whisler et al. (1968) broadened the method for water content measurements at fixed positions along the horizontal soil column. Selim et al. (1970) confirmed the validity of both methods for estimating the soil diffusivity, $D(\theta)$. The Bruce and Klute (1956) method for horizontal flow, was extended by Turner and Parlange (1975) to account for radial flow from a line source.

In order to account for the experimentally observed relationship between the water content, θ, and the Boltzmann variable, η, several approaches have been suggested. One of them is the use of explicit $D(\theta)$ functions such as those proposed by Gardner and Mayhugh (1958), Ahuja and Swartzendruber (1972), Miller and Bresler (1977), and Brutsaert (1979). Alternatively, Cassel et al., (1968) fitted continuous functions to the $\theta(\eta)$ data for evaluation of the Bruce and Klute (1956) equation. Clothier et al. (1983) adopted a more elegant approach choosing fit functions, for which an analytical diffusivity expression can be obtained. Such relationships have also been proposed by McBride and Horton (1985), Shao and Horton (1998) and Evangelides et al. (2005; 2010). Clothier and Wooding (1983) and Clothier et al. (1983) analyzed the shortcomings of the method to accurately determine the diffusivity for soil conditions near saturation, as a result of inaccuracies in the measured data and the improper values of the water retention curve slope in this moisture range.

Other solutions for the horizontal adsorption problem were presented by Shao and Horton (1996), Wang et al. (2004), Prevedello et al. (2008), and Barry et al. (2010). The Bruce and Klute (1956) method has also been extended to estimate unsaturated hydraulic conductivity, $K(\theta)$, and water retention curves, $\psi(\theta)$. Shao and Horton (1998) proposed an integral method for estimating soil hydraulic properties based on horizontal absorption experiments. Wang et al. (2002) and Ma et al. (2009; 2010) developed analytical methods to determine Brooks and Corey model parameters.

All these methods were applied to soil samples under laboratory conditions. Nevertheless, the use of soil moisture probes allows the extension of the method to estimate effective hydraulic properties in experimental plots or watersheds, overcoming scale and representativeness problems of laboratory results. Gardner (1970) proposed a field method to estimate $D(\theta)$ from successive tensiometer readings at a specific depth during drainage of a soil profile, more specifically using the rate of decrease of the matric component of soil water potential with time and the hydraulic gradient. Clothier and White (1981) lengthened the Bruce and Klute (1956) method for field measurements under infiltration.

The objectives of this work were (1) to develop a method for estimating the soil water diffusivity from field-measured moisture data during a desiccation period, and (2), to assess the influence of olive trees on soil hydraulic properties across an experimental catchment. An analytical solution has been provided for soil water diffusivity, assuming that the evolution of the soil water profile with time can be described by an exponential relationship.

5.3. Material and methods.

Data were collected in Setenil catchment. Section 2.2 describes the experimental catchment and the field data acquisition methodology. This report uses field observations collected during 2012.

5.3.1. Soil hydraulic measurements in laboratory.

Water retention was measured in 44 undisturbed samples collected at the 11 locations across the catchment, with 0.05-cm long and 0.04-cm diameter stainless steel rings. At each location, a sample was taken at 0.05 and 0.15 m depth at UC and IR areas. Water retention for 1 cm <|h|< 500 cm was measured using sand and sand-kaolin boxes. The dry end of the water retention curve, roughly for 3×10^3 cm < |h| < 3×10^6 cm, was measured using a dew point psychrometer (WP4-TE, Decagon Devices Inc., Pullman, WA). In order to evaluate the water retention curve slope, the van Genuchten (1980) equation was fitted to the data, with the residual and saturated water content, θ_r, and θ_s, respectively, and the parameters α, m and n

$$\theta = \theta_r + (\theta_s - \theta_r)\left[1+(\alpha\psi_m)^n\right]^{-m} \qquad \text{Eq. (5.1)}$$

Table 5.1 shows the fitted parameters and the goodness of the fit.

Table 5.1. Parameters of the van Genuchten (1980) water retention equation to the measured data, and corresponding coefficient of efficiency, for the inter-row (IR) areas and under the canopy (UC) at the eleven locations.

	θ_s	θ_r	α	n	m	C_{eff}	θ_s	θ_r	α	n	m	C_{eff}
	$m^3 m^{-3}$	$m^3 m^{-3}$	m^{-1}	[ ]	[ ]		$m^3 m^{-3}$	$m^3 m^{-3}$	m^{-1}	[ ]	[ ]	
location	IR						UC					
1	.334	.016	3.38	2.15	.118	.988	.393	.025	3.54	2.38	.204	.993
2	.323	.018	3.37	1.91	.114	.994	.445	.011	2.84	2.20	.114	.993
3	.384	.015	3.11	1.94	.108	.994	.413	.010	3.20	2.06	.121	.993
4	.352	.020	3.38	1.93	.118	.986	.425	.035	4.03	2.66	.179	.992
5	.395	.034	4.13	3.14	.120	.987	.491	.033	5.30	3.23	.149	.992
6	.350	.015	3.37	2.15	.114	.983	.568	.035	4.80	3.79	.126	.990
7	.311	.026	3.47	1.78	.110	.973	.366	.028	3.86	2.65	.127	.991
8	.428	.019	3.36	2.36	.104	.988	.495	.035	5.35	3.10	.123	.987
9	.277	.021	3.43	1.79	.141	.985	.539	.035	5.30	3.61	.115	.988
10	.352	.011	3.15	2.00	.113	.992	.425	.031	5.11	2.00	.177	.990
11	.373	.010	2.96	1.77	.118	.991	.460	.011	3.29	1.90	.117	.994
mean	.350	.020	3.37	2.08	.120	.990	.453	.030	4.24	2.69	.140	.990
s	.041	.007	0.297	0.395	.010	.006	.061	.011	.958	.660	.031	.002

θ_s, saturated water content; θ_r, residual soil water content; α, n, m, parameters; C_{eff}, Nash-Sutcliffe coefficient; s, standard deviation.

5.3.2. Estimation of the diffusivity using the Boltzmann coordinate.

A simple way to estimate the water transmission properties of the soil is the evaluation of the water diffusivity, $D(\theta)=k(\partial\psi/\partial\theta)$, the product of the hydraulic conductivity, k, and the water retention curve slope, $\psi(\theta)$. The Richards equation for horizontal absorption, or, more generally, for water flow where the gradient of the gravitational component of soil water can be neglected, with the space coordinate x, and the time t, is

$$\frac{\partial\theta}{\partial t}=\frac{\theta}{\partial x}\left(D\frac{\partial\theta}{\partial x}\right) \qquad \text{Eq. (5.2)}$$

subject to the initial and boundary conditions with the initial water content, θ_i, and the surface water content, θ_o

$$\begin{aligned} &\theta=\theta_i \quad t=0 \quad x>0 \\ &\theta=\theta_i \quad t>0 \quad x\to\infty \\ &\theta=\theta_0 \quad t>0 \quad x=0 \end{aligned} \qquad \text{Eq. (5.3)}$$

The introduction of the Boltzmann coordinate, $\eta=xt^{-1/2}$, leads to a new form of Eq. (5.2), from which the diffusivity can be expressed as

$$D(\theta)=-\frac{1}{2}\left(\frac{d\eta}{d\theta}\right)_\theta \int_{\theta_i}^{\theta}\eta(\theta')d\theta'=-\frac{1}{2}\left(\frac{d\eta}{d\theta}\right)_\theta S\left(\theta_i,\theta\right) \qquad \text{Eq. (5.4)}$$

The integral of Eq. (5.4) represents the sorptivity, S, of Philip (*e.g.* Ahuja and Swartzendruber 1972).

The soil depth must be great enough to keep the water content at the bottom of the soil profile at the initial value. From the observed relationship between the water content, depth and time, coupled in the Boltzmann coordinate, Eq. (5.4) allows the estimation of the soil water diffusivity.

The soil water profiles in Fig. 5.2 show a quasi-parallel shape, similar to the profiles given by Warrick (2003), Figs. 5.3-5.7. Unfortunately machine traffic and soil tillage

did not allow sensors to be installed at or near the soil surface. Introducing the Boltzmann variable, the water profiles collapsed into the familiar shape of the horizontal absorption described by Warrick (2003) Figs. 4-11, as shown in Fig. 5.3 for measurements from location 2.

The Bruce and Klute method for estimating soil water diffusivity can be adopted here by solving Eq. (5.4) with numerical techniques. However there are several simple analytical functions that can be chosen, as indicated by Philip (1960), McBride and Horton (1985) or Evangelides et al. (2010). For the profiles shown in Fig. 5.3, a simple exponential equation expressing soil moisture, θ, as a function of the Boltzmann coordinate, η, with a reference moisture value, θ_w, and a parameter, a, yielded good results:

$$\theta = \theta_w \left(1 - e^{-a\eta}\right) \qquad \text{Eq. (5.5)}$$

Inserting Eq. (5.5) into the integral of Eq. (5.4), the sorptivity, S, as a function of a reference moisture content, θ_d, different from $\theta_w$is

$$S\left(\theta_d, \theta\right) = -\frac{1}{a}\left[\left(\theta_w - \theta_d\right) ln\left(1 - \frac{\theta_d}{\theta_w}\right) + \left(\theta - \theta_w\right) ln\left(1 - \frac{\theta}{\theta_w}\right) + \theta_d - \theta\right] \qquad \text{Eq. (5.6)}$$

Therefore, the final expression for the diffusivity as a function of S, is

$$D\left(\theta\right) = -\frac{S}{2a(\theta_w - \theta)} \qquad \text{Eq. (5.7)}$$

Eq. (5.5) was fitted to the recorded data using the constrained optimization procedure of Levenberg-Maquardt (Press et al. 1992, section 15.5). The Nash and Sutcliffe (1970) index was selected to assess the efficiency of the fit.

Using the slope of the water retention curve (Eq. 5.1), the hydraulic conductivity of the soil, $k(\theta)$ can be estimated as

$$k(\theta) = D(\theta)\left(\frac{d\psi_m}{d\theta}\right)^{-1} \qquad \text{Eq. (5.8)}$$

5.4. Results and discussion.

5.4.1. Exploration of soil water profiles.

The hydrologic year 2011-12 was extremely dry, with a total rainfall of 357 mm, well below both the average annual rainfall of the area, and the 2012-13 annual rainfall of 1108 mm. Fig. 5.1 shows the evolution of the topsoil (0-0.3 m) water content at location 2, both under the olive canopy (UC) and at the nearby inter-row area (IR), from January to September 2012. Pronounced drying periods could be observed, induced by a high evaporative demand, during which water content decreased exponentially at both IR and UC locations. At UC locations, the drying process was initially faster than at IR locations. The dry period from DOY 120 to 252 corresponded to the summer season, from June to September. At all measurement locations lower soil water contents were found at UC as compared to IR areas. The evolution of the moisture profiles from May 8 to 18, 2012, at location 2 is shown in Fig. 5.2. A similar pattern was observed at the other locations.

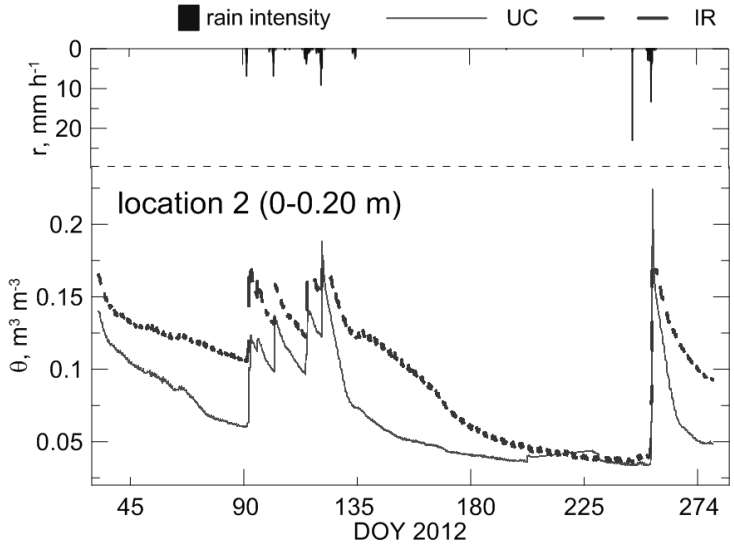

Fig. 5.1. Temporal evolution of topsoil (0-0.3 m) water content at location 2 from January to September 2012.

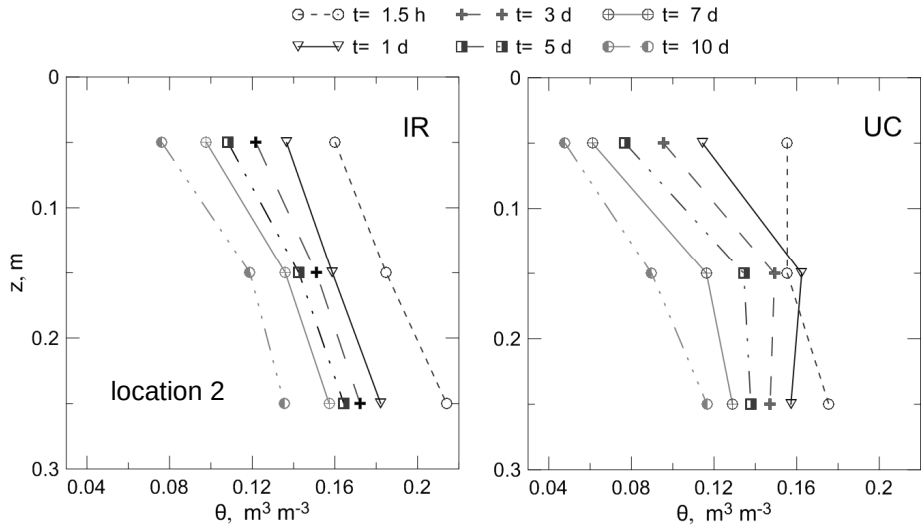

Fig. 5.2. Evolution of measured soil water profiles at location 2 from May 8 to 18, 2012, under the tree canopy (UC) and at the adjacent inter-row (IR) area.

Table 5.2 shows the fitted parameters of Eq. (5.5) and the corresponding coefficient of efficiency for the eleven measurement locations, at IR and UC areas. The results show that the proposed exponential equation represented the $\eta(\theta)$ relationships adequately.

Table 5.2. Parameters of the fitted exponential function proposed and corresponding coefficient of efficiency, for the inter-row (IR) areas and under the canopy (UC) at the eleven locations.

	θ_w $m^3 m^{-3}$	a $cm^{-1}min^{1/2}$	C_{eff}	n	θ_w $m^3 m^{-3}$	a $cm^{-1}min^{1/2}$	C_{eff}	n
location	IR				UC			
1	.292	20.8	.854	436	.212	2.96	.966	766
2	.232	6.52	.940	314	.232	3.93	.849	346
3	.223	7.05	.849	259	.358	2.04	.869	341
4	.283	12.3	.989	1217	.241	8.71	.923	947
5	.215	11.7	.960	405	.229	5.76	.928	989
6	.264	17.1	.908	781	.239	16.0	.962	314
7	.334	13.8	.979	789	.216	16.1	.915	1846
8	.209	19.6	.949	343	.198	3.47	.956	434
9	.327	25.0	.941	159	.192	9.58	.979	1503
10	.287	17.2	.929	631	.231	4.70	.973	1231
11	.340	9.94	.951	411	.257	4.48	.987	817
mean	.273	14.6	.932		.237	7.06	.937	
s	.036	5.86	.046		.042	4.99	.045	

θ_w, maximum reference soil water content; *a*, parameter of Eq. (5.5); C_{eff}, Nash-Sutcliffe coefficient; *n*, number of data used; *s*, standard deviation.

The coefficient of efficiency ranged from 0.85 to 0.98, with an average value of near 0.93 for both the IR and UC areas. The reference soil water content, θ_w, ranged from 0.21 to 0.34 m^3m^{-3}, and from 0.19 to 0.36 m^3 m^{-3} at IR and UC locations, respectively. The average θ_w of 0.27 m^3 m^{-3}at IR and 0.24 m^3 m^{-3} at UC locations were not significantly different (p=0.08). The parameter *a* was on average significantly different (p=0.004) between IR and UC locations. The average value was 14.6 and 7.1 $cm^{-1}min^{1/2}$ at IR and UC locations, respectively. Fig. 5.3 illustrates the different shape of the $\eta(\theta)$ relationship at the IR and UC areas of location 2 and the adequacy of Eq. (5.5). Observed differences are a result of different soil conditions at IR and UC locations, leading to higher water contents at IR locations and faster drying rates of the soil at UC ones.

Comparison of this 2-parameter equation with other expressions for the $\eta(\theta)$ relationship yielded similar results. Despite two additional parameters, the equation proposed by Evangelides et al. (2010)

$$\theta = -\theta_d - \alpha_E \tan^{-1}\left(\beta_E + \gamma_E \eta\right), \qquad \text{Eq. (5.9)}$$

where θ_d, α_E, β_E, and γ_E are parameters, yielded average coefficients of efficiency of 0.94 and 0.90 at the IR and UC locations, respectively, similar to those found for Eq. (5.5). Fig. 5.3 also exhibits the fit for this equation for data from location 2.

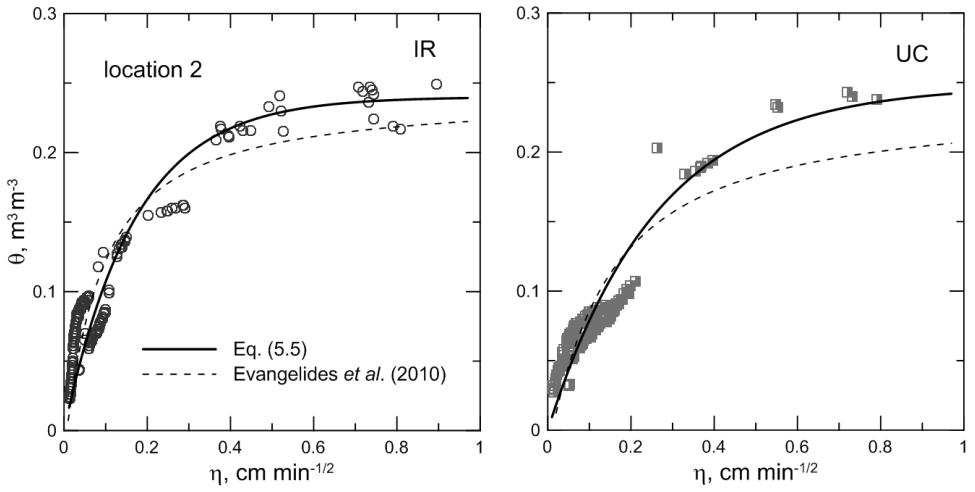

Fig. 5.3. Transformed profiles of soil water content, θ, as a function of the Boltzmann variable, η, at location 2 for the inter-row area (IR) and under the canopy (UC). Fitting lines are Eq. (5.5) and the equation proposed by Evangelides et al. (2010).

The McBride and Horton (1985) equation was not compared since its results were very similar to those obtained by Evangelides et al. (2010), as can be appreciated in the latter work. The Philip (1960) equations were simpler but less adequate for the specific conditions of the present work.

Fig. 5.4 shows the relationship between the normalized water content, θ/θ_w, and the product of the Boltzmann variable and parameter *a* from Eq.(5.5) for IR and UC areas at all locations. Data from different locations merge reasonably well into a single relationship, indicating the adequacy of the Boltzmann transform at both IR and UC locations.

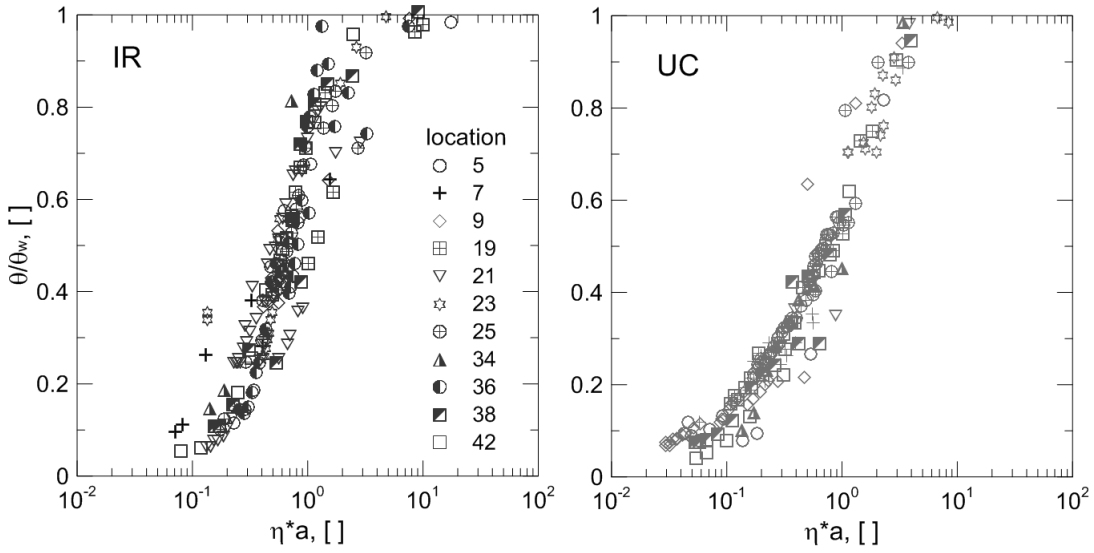

Fig. 5.4. Relationship between the normalized water content, θ/θ_w, and the product of the Boltzmann variable and parameter *a* from Eq. (5.5) for inter-row (IR) and under canopy (UC) areas at all locations.

5.4.2. Estimation of diffusivity and hydraulic conductivity.

Soil water diffusivity $D(\theta)$ was estimated using Eqs. (5.5) – (5.7) for UC and IR areas at all measurement locations. Fig. 5.5 shows the diffusivity function for UC and IR areas at location 2. A similar shape was observed at the other measurement locations. Diffusivity was larger at UC locations as compared to IR ones. The difference in $D(\theta)$ between IR and UC was largest at intermediate water contents, roughly between 0.1 and 0.2 m^3m^{-3},as a result of the smaller bulk density observed at the UC locations, and possibly a larger organic matter content due to the presence of dead leaves and roots and

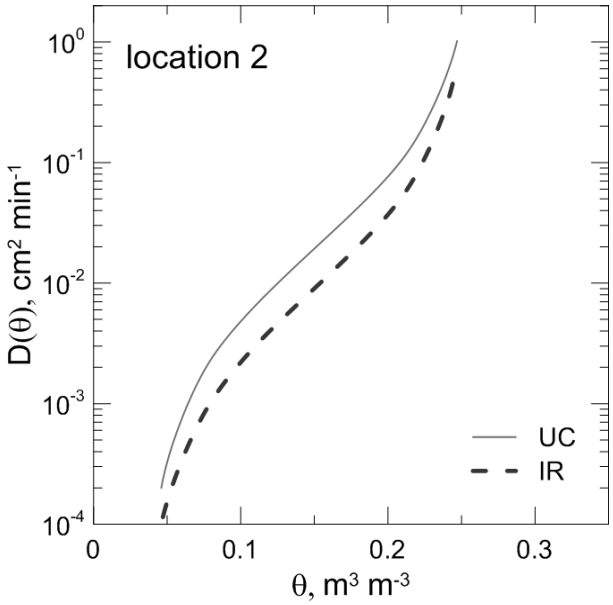

Fig. 5.5. Estimated hydraulic conductivity function k(θ) at inter-row areas (IR) and under the tree canopy (UC) at location 2.

the protective role of the canopy retarding organic matter decay.The beneficial effect of soil organic matter on structure favors higher soil water transmission rates. The soil at IR areas was more compacted than the UC soil as a result of intense heavy machinery traffic during olive harvesting. In addition, the UC soil was more protected by the canopy from natural consolidation than the IR soil. Fig. 5.6 shows the relationship between the fitted *a* parameter and topsoil (0-0.2 m) bulk density at IR and UC areas for the 11 measurement locations. The correlation coefficient was 0.70.

The hydraulic conductivity function $k(\theta)$ was estimated using Eq. (5.8) for UC and IR areas at the 11 measurement locations. Fig. 5.7 shows the hydraulic conductivity function for UC and IR areas at location 2. A similar shape was observed at the other measurement locations.The hydraulic conductivity was one to two orders of magnitude larger at UC areas as compared to IR. The difference increased for decreasing soil water contents. Also, Lebron et al. (2007) found lower hydraulic conductivity values at IR locations in a pinyon-juniper woodland in the South West of the US.

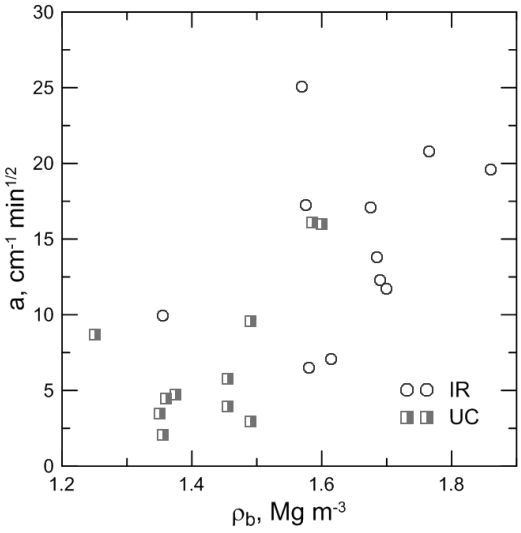

Fig. 5.6. Relationship between the fitted a parameter and topsoil (0–0.2 m) bulk density at inter-row (IR) areas and under the tree canopy (UC) for the 11 measurement locations.

5.4.3. Spatial variability of soil water dynamics.

The spatial variability in the fitted parameters of the water retention equation (Table 1) and the variability of the fitted parameters of Eq. (5.5) illustrate the spatial variability of the soil water dynamics across the experimental catchment and highlight the effect of the trees. Fig. 5.8 shows the spatial distribution of the fitted parameter *a* for the relationship between the Boltzmann variable and the water content at inter-row (IR) areas and under the tree canopy (UC).In both maps, the areas with the lowest values correspond to zones with shallow stony soil profiles, with protruding rock fragments.

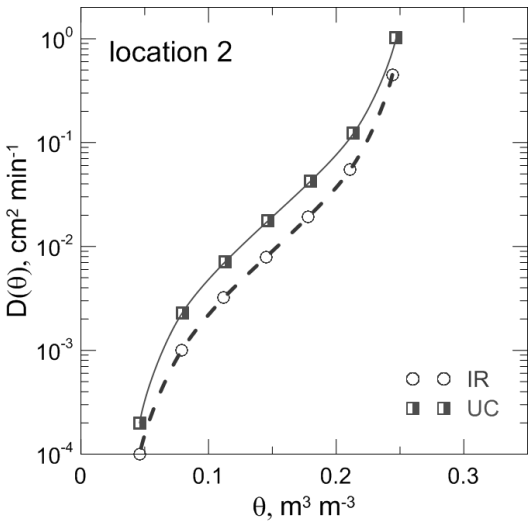

Fig. 5.7. Estimated hydraulic conductivity function k(θ) at inter-row areas (IR) and under the tree canopy (UC) at location 2.

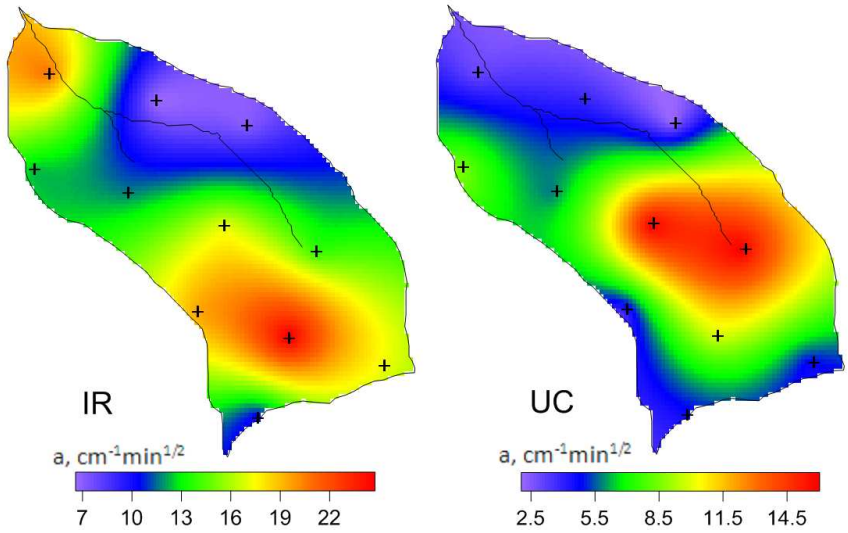

Fig. 5.8. Spatial distribution of the parameter *a* (Eq. 5.5) for inter-row (IR) areas and under the tree canopy (UC).

5.5. Conclusions.

The availability of frequent soil water measurements acquired using a sensor network in an olive cropped experimental watershed allowed a simple estimation of the soil water diffusivity functions using the Boltzmann transform. Only soil moisture data obtained during a drying period, for which desorption processes dominated, were employed. A simple exponential relationship between the Boltzmann coordinate and the soil water content fitted the measured soil water profile data well, with the parameters reflecting the main characteristics of the soils across the landscape. Using a continuous function for the water retention characteristic, the method can be further extended to provide the hydraulic conductivity function. The proposed method will be used for further research to analyze soil water processes throughout the year and the results obtained will be compared with laboratory measurements.The spatially distributed diffusivity functions were useful for describing the desorption processes that occurred during prolonged drying periods, and were relevant for soil and water management at the farm. The estimation of diffusivity during absorption as a result of infiltration processes requires other approaches such as the one proposed by Clothier and White (1981) or the inverse method of Sisson and van Genuchten (1991).

5.6. References.

Ahuja, L.R., and D. Swartzendruber. 1972. An improved form of soil-water diffusivity function. Soil Sci. Soc. Am. J. 36, 9-14.

Barry, D.A., J.Y. Parlange, C.L. Prevedello, J.M.T. Loyola, K. Reichardt, and D.R. Nielsen. 2010. Extension of a recent method for obtaining exact solutions of the Bruce and Klute Equation. Vadose Zone J. 9, 496-498.

Bruce, R.R., and A. Klute. 1956. The measurement of soil moisture diffusivity. Soil Sci. Soc. Am. J. 20, 458-462.

Brutsaert, W. 1979. Universal constants for scaling the exponential soil water diffusivity? WaterResour. Res. 15, 481-483.

Cassel, D.K., A.W. Warrick, D.R. Nielsen, and J.W. Biggar. 1968. Soil–water diffusivity values based upon time dependent soil-water content distributions. Soil Sci. Soc. Am. J. 32, 774–777.

Clothier, B.E., D.R. Scotter, and A.E. Green. 1983. Diffusivity and one dimensional absorption experiments. Soil Sci. Soc. Am. J. 47, 641-644.

Clothier, B.E., and I. White. 1981. Measurement of sorptivity and soil water diffusivity in the field. Soil Sci. Soc. Am. J. 45, 241-245.

Clothier, B.E., and R.A. Wooding. 1983. The soil water diffusivity near saturation. Soil Sci. Soc. Am. J. 47, 636-640.

Crank, J. 1956.The mathematics of diffusion. Oxford University Press, Oxford.

Evangelides, C., G. Arampatzis, and C. Tzimopoulos. 2010. Estimation of soil moisture profile and diffusivity using simple laboratory procedures. Soil Sci. 175, 118-127.

Evangelides, C., C. Tzimopoulos, and G. Arampatzis. 2005. Flux-saturation relationship for unsaturated horizontal flow. Soil Sci. 170, 671-679.

Gardner, W.R., and M.S. Mayhugh. 1958. Solutions and tests of the diffusion equation for the movement of water in soils. Soil Sci. Soc. Am. J. 22, 197-201,

Gardner, W.R. 1970. Field measurement of soil water diffusivity. Soil Sci. Soc. Am J. 34, 832-833.

Lebron, I., M.D. Madsen, D.G. Chandler, D.A. Robinson, O. Wendroth, and J. Belnap. 2007. Ecohydrological controls on soil moisture and hydraulic conductivity within a pinyon-juniper Woodland. Water Resour. Res. 43, doi: 10.1029/2006WR005398.

Ma, D., M. Shao, J. Zhang, and Q. Wang. 2010. Validation of an analytical method for determining soil hydraulic properties of stony soils using experimental data. Geoderma 159, 262-269.

Ma, D., Q. Wang, and M. Shao. 2009. Analytical method for estimating soil hydraulic parameters from horizontal absorption. Soil Sci. Soc. Am J. 73, 727-736.

Martinez, G., Y.A. Pachepsky, and H. Vereecken. 2013. Temporal stability of soil water content as affected by climate and soil hydraulic properties: a simulation study. Hydrol. Proc., doi: 10.1002/hyp.9737.

McBride, J.F., and R. Horton. 1985. An empirical function to describe measured water distributions from horizontal infiltration experiments. Water Resour. Res. 21, 1539-1544.

Miller, R.D., and E. Bresler, 1977. A quick method for estimating soil-water diffusivity functions. Soil Sci. Soc. Am. J. 41, 1020-1022.

Nash, J.E., and J.V. Sutcliffe. 1970. River flow forecasting through conceptual models, part I: A discussion of principles. J. Hydrol. 10, 282-290.

Press, W.H., S.A. Teukolsky, W.T. Vetterling, and B.P. Flannery. 1992. Numerical Recipes, 2nd ed. Cambridge Univ. Press. Cambridge, UK.

Prevedello, C.L., J.M.T. Loyola, K. Reichardt, and D.R. Nielsen. 2008. New analytic solution of Boltzmann transform for horizontal water infiltration into sand. Vadose Zone J. 7, 1170–1177.

Philip, J.R. 1960. General method of exact solution of the concentration-dependent diffusion equation. Aust. J. Phys. 13, 1-12.

Selim, H.M., D. Kirkham, and M. Amemiya. 1970. A comparison of two methods for determining soil water diffusivity. Soil Sci. Soc. Am. J. 34, 14-18.

Shao, M., and R. Horton. 1996. Soil water diffusivity determination by general similarity theory. Soil Sci. 161, 727-734.

Shao, M., and R. Horton. 1998. Integral method for estimating soil hydraulic properties. Soil Sci. Soc. Am. J. 62, 585-592.

Sisson, J.B., and M.Th. Van Genuchten. 1991. An improved analysis of gravity drainage experiments for estimating the unsaturated soil hydraulic functions. Water Resour. Res. 27, 569-575.

Soil Survey Staff. 1999. Soil Taxonomy. 2nd. ed. USDA Agr. Hdbk. 436. NRCS. Washington.

Taguas E.V., J.L. Ayuso, A. Peña, Y. Yuan, and R. Pérez. 2009. Evaluating and modelling the hydrological and erosive behaviour of an olive orchard microcatchment under no-tillage with bare soil in Spain. Earth Surf. Process. Landf. 34, 738–751.

Turner, N.C., and J.Y. Parlange. 1975. Two-Dimensional Similarity Solution: Theory and Application to the Determination of Soil-Water Diffusivity. Soil Sci. Soc. Am. J. 39, 387-390.

Vereecken, H., J.A. Huisman, H. Bogena, J. Vanderborght, J.A. Vrugt, and J.W. Hopmans. 2008. On the value of soil moisture measurements in vadose zone hydrology: A review. Water Resour. Res., 44: W00D06, doi: 10.1029/2008WR006829.

van Genuchten, M.Th. 1980. A closed-form equation for predicting the hydraulic conductivity of unsaturated soil. Soil Sci. Soc. Am. J. 44, 892-898.

Wang, Q., R. Horton, and M. Shao. 2002. Horizontal infiltration method for determining Brooks-Corey model parameters. Soil Sci. Soc. Am. J. 66, 1733-1739.

Wang, Q., M. Shao, and R. Horton. 2004. A simple method for estimating water diffusivity of unsaturated soils. Soil Sci. Soc. Am. J. 68, 713-718.

Warrick, A.W. 2003. Soil water dynamics. Oxford Univ. Press. Oxford. U.K.

Whisler, F.D., A. Klute, and D.B. Peters. 1968. Soil water diffusivity from horizontal infiltration. Soil Sci. Soc. Amer. J. 32, 6-11

Chapter 6

Soil moisture modelling to identify spatial and temporal hydrological patterns[1]

[1]Modified from: Espejo, A.J., L. Brocca, K. Vanderlinden, T. Moramarco, and J.V. Giráldez. Soil moisture modelling in an olive-tree -planted catchment in Spain to identify spatial and temporal hydrological patterns. Unpublished, submitted to Geoderma on June 2014, 6.

6.1. Abstract.

Information on soil moisture dynamics is essential for improving land use and soil management in catchments. In this work soil moisture content was measured using a sensor network placed across eleven locations within a rainfed catchment cropped with olive trees in south-western Spain. The sensors were installed under the olive tree canopy (UC) and between tree rows (IR) to explore the influence of the vegetation on soil water dynamics. The information gathered after two years of observations has been used to evaluate the performance of the soil water balance model (SWBM) of Brocca et al. (2008), by considering the calibration of a single parameter, saturated hydraulic conductivity, Ks. The spatial variability of soil hydraulic properties and rainfall canopy interception, was analysed.

Results indicated that the model successfully captured hourly soil moisture dynamics with a Nash-Sutcliffe efficiency index above 0.90 for UC and IR locations by using, for both locations, the spatially averaged and point soil moisture data. Moreover, for UC sites, a closer representation of soil moisture dynamics was found by adopting a simple interception formulation in the original model scheme. The simple interception component indicated an average fraction of 10% of the rainfall during the two-year period. The spatial mean hydraulic conductivity, Ks, estimated was 6.5 mm h^{-1} and 23.7 mm h^{-1} for IR and UC, respectively. The spatial distribution of the Ks showed a

clear influence of bulk density. Therefore, the proposed model is a useful tool for the interpretation of the hydrology of this catchment.

6.2. Introduction.

Cachment management requires a precise understanding of soil water dynamics in agriculture (Martínez et al. 2010), flood washing (Brocca et al. 2011a; Camici et al. 2011) and climate change forecasting (Mittelbach et al. 2011). However, the high spatio-temporal variability of soil moisture represents a barrier that precludes a closer characterization of catchment properties (Vanderlinden et al. 2012; Vereecken et al. 2008).

Moisture controls the energy and mass exchange between soil-plant interface and the atmosphere, (*e.g*. Koster et al. 2009). Evaporation determines plant growth and agricultural productivity (Viola et al. 2012; Rodriguez-Iturbe et al. 1999) and depends on soil moisture (Brutsaert, 2014; Betts, 2004). Furthermore, vegetation regulates soil moisture dynamics (Guswa, 2012), while soil moisture also governs carbon fluxes between the soil and the atmosphere (Williams and Albertson, 2004).

Despite some exceptions (Robock et al. 2000; Hollinger and Isard, 1994) and recent efforts (Dorigo et al. 2013), historical series of soil moisture measurements are not generally available, in contrast to rainfall or other meteorological data (Palecki and Bell, 2013). Nowadays, due to technological advances, it is possible to measure soil moisture frequently and simultaneously in multiple sites. Remote sensing provides quite accurate soil moisture information (Brocca et al. 2011b) although its spatial and temporal resolution is often insufficient for small-scale applications (<1 km²) or for precise analyses of the mutual influence between the vegetation and the soil moisture content. These limitations can be overcome through moisture sensor networks for monitoring soil moisture at intermediate scales, ~1 km², and higher temporal resolutions, *e.g*. hourly (Fares et al. 2013; Robinson et al. 2008).

In situ measurements are essential for evaluating soil moisture dynamics, but this information must be integrated into large space and time scales (Beven, 2000). Several

models have been developed for the description of the spatio-temporal evolution of moisture (Brocca et al. 2013a; Baudena et al. 2012; Albertson and Kiely, 2001; Famiglietti and Wood, 1994). The large number of parameters of many of these models, which are not always available, restrict their usefulness. Brocca et al. (2008) developed a simple conceptual model to represent the temporal evolution of soil moisture in an experimental catchment. Its main advantage is that, in spite of its simplicity, it yields accurate estimations of measured soil data.

Soil hydraulic conductivity is one essential parameter of hydrological models. Nevertheless, it is not easily estimated through direct measurements in the field. Inverse methods are usually adopted for this purpose (Schelle et al. 2011), which can be carried out with the help of soil moisture data (Espejo et al. 2014; Pan et al. 2012).

Many Mediterranean catchments are covered with olive orchards. However, few studies have evaluated their influence on soil moisture dynamics.

The main objective of this work was to explore soil moisture evolution using a simple model to identify spatial and temporal hydrological patterns. The tree´s role in the hydrology of the catchment will be analysed.

6.3. Material and methods.

6.3.1. Data sources.

The work was performed in the experimental catchment of Setenil. Section 2.5 describes the experimental catchment and the field data acquisition. In this chapter, data collected during two years, from June 1, 2011 to May 31, 2013 were used. Measurements of soil water content recorded by the 10HS sensor at 0.05 and 0.15 m depths were averaged, thus representing the top 0.2 m of the soil.

6.3.2. Soil moisture modelling.

The soil water balance model (SWBM) of Brocca et al. (2008) was used in this work. The model is described in Fig. 6.1. The model has been exhaustively tested in other applications, providing excellent results under different conditions, sites and scenarios (*e.g.* Gumuzzio et al. 2013; Brocca et al. 2013, 2011b, 2008; Lacava et al. 2012). The model can be downloaded free at http://hydrology.irpi.cnr.it/people/l.brocca. The inputs of model are air temperature and rainfall data. The model parameters are the maximum moisture storage of the soil layer, W_{max}, the saturated soil hydraulic conductivity, K_s, the pore size distribution index, λ, the air entry pressure head, ψ_b, and the crop coefficient, K_c. Readers interested are referred to Brocca et al. (2013a) for a full description of the model equations and parameterization.

6.3.3. Interception modelling.

Preceding studies (Espejo et al. 2014) indicated an important influence of the olive trees on the temporal evolution of soil moisture due to rainfall interception and transpiration. Therefore, the SWBM model was modified (SWBMI) to account for canopy interception at UC locations. A schematic diagram of the SWBMI model is shown in Fig. 6.1.

Interception, I, was modelled based on the scheme of Rutter et al. (1971). Stemflow was assumed to be negligible because the canopies were small and the UC sites were located far from the trunk (Lebron et al., 2007) outside the stemflow infiltration area (Gómez et al. 2002). The net rainfall infiltrating into the soil, r_n, was computed as

$$r_n(t) = \begin{cases} 0, & R(t) < S_{\max} \\ R(t) - S_{\max}, & otherwise \end{cases} \qquad \text{Eq. (6.1)}$$

where $R(t)$ is the total amount of rainfall from the beginning of a rainfall event until time t, and S_{max} is the total capacity of the canopy interception storage. A minimum of 6 hours without rainfall was assumed in order to separate two consecutive rainfall events (Hershfield, 1963).

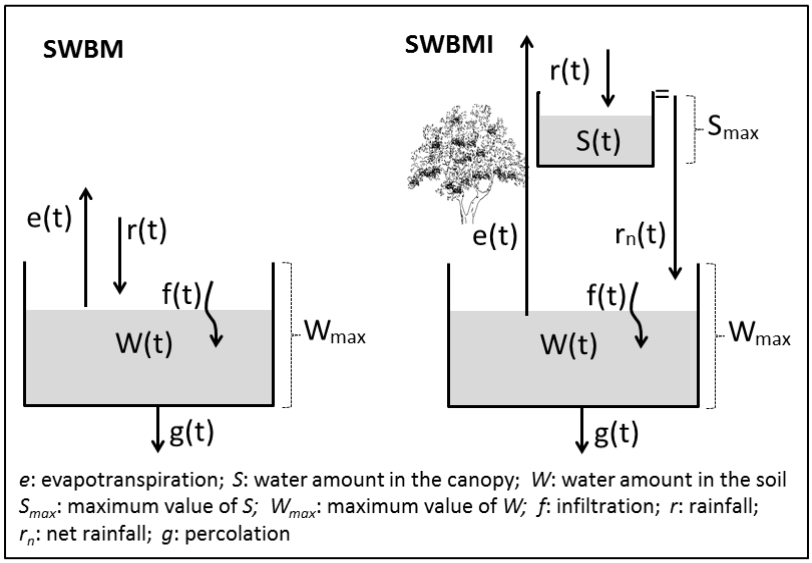

Fig. 6.1. Schematic diagram of the Soil Water Balance Model (SWBM) and of that model with the addition of the canopy interception storage (SWBMI).

6.3.4. Model calibration and validation.

For both the SWBM and the SWBMI models, the values of the parameters were estimated through a gradient-based optimization algorithm. The maximization of the Nash-Sutcliffe (1970) efficiency index between observed and simulated moisture data was taken as an objective function. The Root Mean Square Error, RMSE, and the coefficient of determination, R^2, were also used for evaluating the models performance.

The reduced parameterization scheme proposed by Brocca et al. (2013a, 2013b) was employed to improve the identification of the model parameters. This scheme reduces the number of parameters to be estimated with the optimization procedure from 5 to one, *i.e.*, K_s, which is often found as the main driving parameter for soil moisture dynamics (Martinez et al. 2014; Morbidelli et al. 2012). The λ and ψ_b values were derived as a function of K_s fitting the values reported for Rawls et al. (1982), while K_c was fixed in accordance with the probe-error runs of the models, varying all the parameters freely, and literature (Villalobos et al. 2000). For W_{max} the same procedure was followed and the values obtained were compared with those calculated using the minimum and maximum moisture observations and the soil layer depth. Note that, for

the SWBMI model, two parameters were optimized, *i.e.*, K_s and S_{max}. For the calibration of both models the K_s value was constrained to vary between 0.01 and 50 mm h^{-1}. At the UC areas, a feasible range of S_{max} values ranging between 0.01 and 2.60 mm was adopted from those given by Gómez et al. (2001), who also developed an empirical relationship between the leaf area index and S_{max}.

Spatially averaged moisture values for UC and IR locations were used to analyse the model capacity to simulate hourly moisture time series and its robustness. Following Brocca et al. (2013a), five configurations for calibration and validation of models were tested. The calibration periods were: year 1, year 2, the dry period of year 1 (from June to October), the wet period of year 1 (from November to March), the dry-wet transition period of year 1 (from February to June), and the wet-dry transition period of year 1 (from December to April). Except for the second configuration, the second year was always used for model validation. This procedure allowed us to evaluate the performance of the models in reproducing spatial mean soil moisture measurements, to select the best configuration for model calibration and validation, and to compare the temporal evolution at IR and UC, respectively.

Once the configuration for their calibration and validation was selected, the models were applied individually to each of the 11 monitoring sites. The SWBM model was applied to the IR locations. For UC, the SWBMI model was applied, except points 10 and 11, where the SWBM model was used because the trees were young with a small canopy (see southeast area in Fig.1). This procedure allowed us to determine the spatial distribution of the soil hydraulic properties across the catchment, especially the saturated hydraulic conductivity, K_s, and to evaluate the rainfall interception by the adult trees.

6.4. Results and discussion.

6.4.1. Soil moisture measurements.

The temporal evolution of mean spatial moisture (0-0.2 m horizon) showed a seasonal pattern in response to weather conditions, with long drying periods reaching values near

0.03, and 0.04 m^3 m^{-3} at IR and UC locations, respectively, (Fig. 6.2). Note also that, in the first year of available data, the rainfall was very sparse (357 mm yr^{-1}) as compared to the average annual rainfall of 650 mm yr^{-1} in the area, while in the second year the rainfall was abundant (1108 mm yr^{-1}).

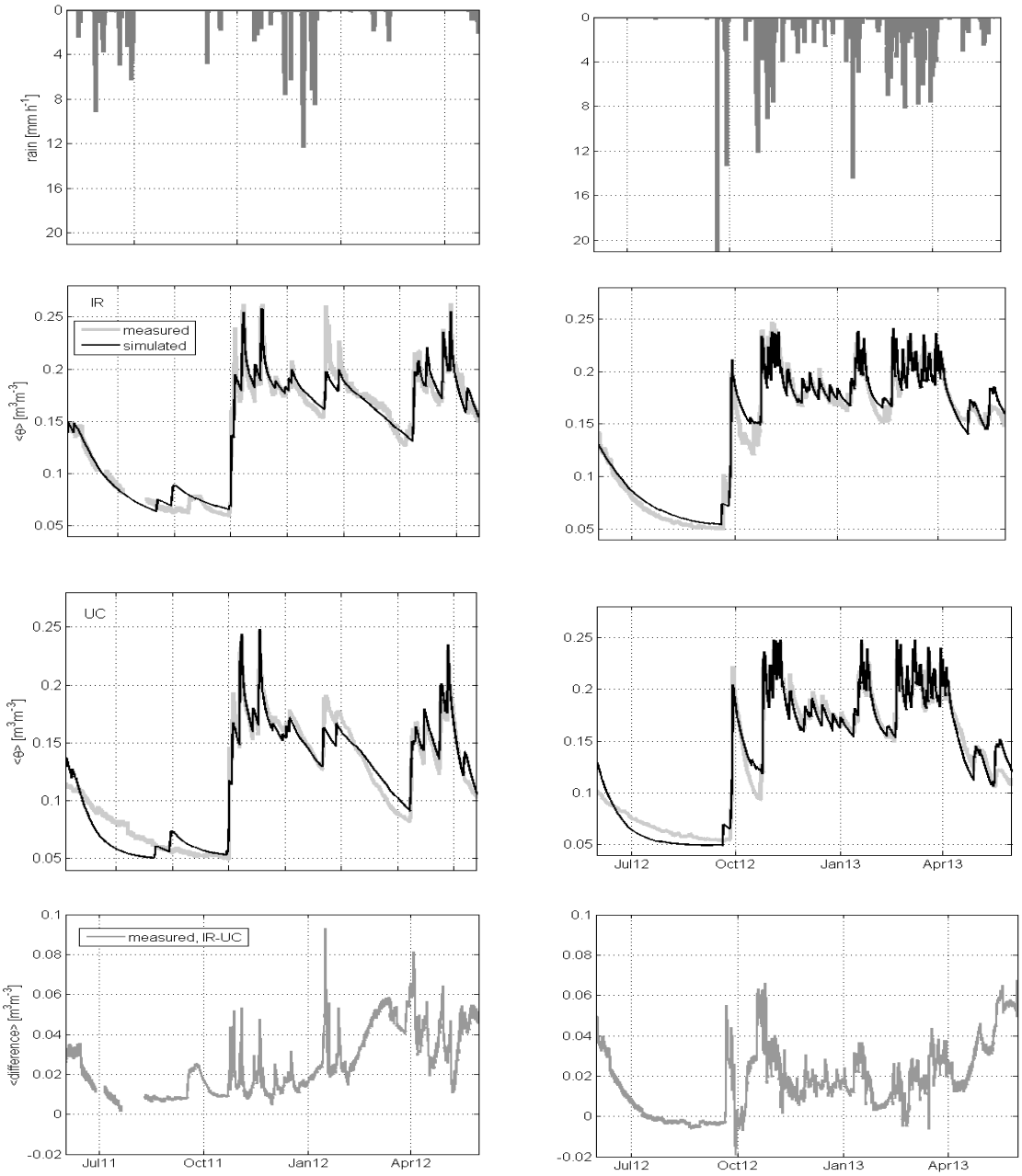

year 1 year 2

Fig. 6.2. Hourly evolution of spatial mean measured (‹θ_{obs}›) and SWBM simulated (‹θ_{sim}›) soil moisture at inter-row, IR, locations and under canopy, UC, for year 1 for calibration (left) and year 2 for validation (right). At the top, the rainfall is shown and at the bottom, the differences between spatial mean moisture measured at IR minus those of the UC location are displayed.

The data evidenced that for most of the year soil moisture at IR locations was higher than at UC locations. This is in contrast with the observations of some authors for other tree species with larger canopies (*e.g*. Liang et al. 2011), but agrees with the observations of Gómez et al. (2002) in olive orchards in Andalusia. The largest differences were observed after low intensity rainfall, for which canopy interception was significant, and during periods without rainfall as a result of transpiration (see also Espejo et al. 2014).

6.4.2. Modelling spatially averaged soil moisture.

As a preliminary step, the W_{max} and K_c model parameters were fixed. The results of the different model runs for several calibration/validation configurations yielded for W_{max} an average value of 70 mm. This value was similar to that of the corresponding data for a 0.3 m thick layer according to the differences between the maximum and minimum observed moisture values observed. The latter were 0.27 and 0.03 m^3 m^{-3} at IR locations, and 0.25 and 0.04 m^3 m^{-3} at UC, respectively. For $K_{c,}$ model runs gave values in the range of 0.30-0.51 at IR, and 0.64-0.82 for UC sites, respectively. These values were in accordance with the values suggested in the literature (Villalobos et al., 2000; Orgáz and Fereres, 1997). Thus K_c was fixed at 0.45 for IR and 0.70 for UC, and W_{max} at 70 mm for both locations.

The models performance for the different calibration and validation configurations selected is summarised in Table 6.1 for IR location. The best result was found using year 1 for model calibration and year 2 for validation. For the calibration, the Nash and Sutcliffe efficiency index ranged from 0.54 using the dry period of year 1 to 0.96 using complete year 1 and complete year 2. Validation efficiencies ranged from 0.84 to 0.97 using the wet period of year 1 and complete year 2, respectively. As expected, the worst values were obtained when short periods of time were used for model calibration (*e.g.*

dry period of year 1 and wet period of year 1), while the best results were obtained if periods characterized by a wet-dry or dry-wet transition were considered.

Table 6.1. Summary of the model performance and parameters obtained for inter-row (IR) locations using the SWBM model to simulate spatial mean soil moisture for different calibration/validation (cal/val) configurations, see Fig. 3 or section 2.5.

IR	model parameters			model performance (cal / val)		
cal/val period	K_s (mm h^{-1})	$-\psi_b$ (mm)	λ	NS	R^2	RMSE (m^3 m^{-3}) x10^{-2}
year1/year2	2.95	264.6	0.249	0.96 / 0.97	0.96 / 0.97	1.00 / 1.17
year2/year1	2.60	271.8	0.238	0.96 / 0.96	0.96 / 0.96	1.20 / 1.10
dry year1/year 2	3.56	254.4	0.265	0.54 / 0.89	0.56 / 0.91	1.38 / 2.00
wet year1/year 2	3.10	261.9	0.254	0.63 / 0.84	0.655 / 0.85	1.23 / 0.84
dry-wet year1/year 2	3.48	255.7	0.263	0.84 / 0.92	0.901 / 0.94	0.90 / 1.14
wet-dry year1/year 2	2.78	267.9	0.244	0.82 / 0.93	0.852 / 0.94	0.93 / 1.65

K_c: crop coefficient, (0.45 for IR and 0.70 for UC), K_s: saturated soil hydraulic conductivity, ψ_b: air entry head, λ: pore size distribution index, *NS*: Nash-Sutcliffe efficiency index. ψ_b and λ were estimated as a function of K_s according to Brocca et al., (2013a).

The K_s values obtained at IR locations were in the range of those found in the literature for sandy loam soils (Rawls et al. 1982). Only small differences were observed for the different calibration/validation configurations. This further demonstrates the robustness of the model for representing temporal moisture variability, as claimed by Brocca et al. (2008 and 2013a). The average K_s value for the different calibration/validation periods was 3 mm h^{-1}, resulting in values of 263 mm and 0.25 for ψ_b and λ, respectively, using the expressions fitting the data given by Rawls et al. (1982).

Overall, the models performance at UC locations improved when taking into account canopy interception. The results for the different calibration/validation periods are shown in Table 6.2 applying the SWBM and SWBMI models. The SWBMI model performed better in all the calibration cases, and it was found to be superior in four out of six validation cases. The monthly pattern of model errors indicated that the largest improvements in the SWBMI performance with respect to the SWBM performance

were found in Spring (calibration and validation), when the effect of canopy interception is expected to be more significant because of shorter rain events of a low intensity (Rutter, 1975). Using the SWBMI model average, Nash and Sutcliffe and RMSE values for calibration were 0.82 and 9.8×10^{-3} m^3 m^{-3}, respectively. For the validation, the values of these model performance indexes were 0.92 and 14.8×10^{-3} m^3 m^{-3}, respectively.

Table 6.2. As in Table 6.1 but for under-canopy (UC) locations and by using the SWBM and SWBMI models. The first line of each configuration represents the results applying SWBM while those of the second line applying SWBMI.

UC	model parameters				model performance (cal / val)		
cal/val period	S_{max} (mm)	K_s (mm h^{-1})	$-\psi_b$ (mm)	λ	NS	R^2	RMSE (m^3 m^{-3}) x10^{-2}
year1/year2		4.03	247.7	0.276	0.93 / 0.95	0.93 / 0.95	1.26 / 1.25
	1.56	4.06	248.1	0.277	0.93 / 0.95	0.93 / 0.96	1.26 / 1.22
year2/year1		3.34	257.8	0.260	0.95 / 0.91	0.96 / 0.92	1.24 / 1.35
	2.57	3.19	260.4	0.256	0.97 / 0.87	0.97 / 0.88	0.96 / 1.76
dry year1/year 2		2.53	273.1	0.236	0.21 / 0.94	0.30 / 0.96	1.24 / 1.31
	2.58	3.20	260.4	0.256	0.36 / 0.96	0.51 / 0.97	1.11 / 1.13
wet year1/year 2		3.13	261.5	0.254	0.75 / 0.92	0.75 / 0.93	1.00 / 1.56
	1.64	2.84	266.7	0.246	0.83 / 0.93	0.83 / 0.93	0.82 / 1.47
dry-wet year1/year 2		6.34	222.8	0.314	0.95 / 0.90	0.94 / 0.94	0.73 / 1.74
	2.48	5.16	234.1	0.297	0.95 / 0.91	0.95 / 0.96	0.70 / 1.63
wet-dry year1/year 2		4.27	244.5	0.281	0.86 / 0.92	0.95 / 0.92	1.08 / 1.53
	0.01	4.49	241.8	0.285	0.87 / 0.91	0.96 / 0.91	1.02 / 1.65

The S_{max} was on average 1.8 mm, and ranged from 0.01 (wet-dry period for calibration) to 2.58 mm (dry period). These ratios were in agreement with the values given by Gómez et al. (2001). For the SWBMI, the average K_s value, for the different calibration/validation periods, was 3.8 mm h^{-1}, resulting in ψ_b = 252 mm and λ = 0.27.

The observed and modelled mean moisture data for IR (top) and UC (bottom) locations, and the difference between moisture values for IR and UC, are compared in Fig. 6.2, for model calibration using year 1 and model validation using year 2, respectively. The figures highlight the good results obtained with the use of moisture models. The greatest differences between observed and modelled values were observed in January 2012,

especially for IR locations, but this might be attributed to an underestimation of the rainfall observed.

6.4.3. Spatial distribution of K_s.

In the second part, the SWBM and SWBMI were applied to each monitoring location for IR and UC areas, respectively, according to what is described in section 6.3.4. The models' performance in terms of R^2 and the parameter estimated for each location are displayed in Table 6.3. In addition to W_{max}, the table also shows minimum and maximum moisture values measured at each location.

The accuracy of the soil moisture models decreased slightly when compared to their application to the spatially averaged data. Their average values ranged from 0.86 to 0.89 at UC and IR locations, respectively, for calibration, and between 0.81 and 0.89 for validation. The saturated hydraulic conductivity varied significantly across the catchment and was on average significantly higher ($p=0.09$) at UC locations as compared to IR. A lower variation was also found at UC compared to IR as a consequence of the transit of machinery, with variation coefficient values of 0.7 and 1.0, respectively. The mean of the estimated K_s-values was 6.5 and 23.7 mm h^{-1} at IR and UC locations, respectively. Only at points 4 and 10, UC locations show a lower K_s-value. The greater soil depth at IR with respect to UC at location 4, and an accumulation of manure and frequent tilling operations in this part of the catchment at the IR area of location 10 could explain these differences.

Table 6.3. Estimated soil hydraulic parameters for the eleven sample points at inter-row (IR) and under-canopy (UC) locations, applying the SWBM and SWBMI models at individual points, respectively, and year 1/year 2 configuration for calibration and validation. Note that for 10 and 11 UC locations the SWBM model was applied.

	θ_{min} ($m^3\,m^{-3}$)	θ_{max} ($m^3\,m^{-3}$)	W_{max} (mm)	K_s (mm h^{-1})	R^2	θ_{min} ($m^3\,m^{-3}$)	θ_{max} ($m^3\,m^{-3}$)	W_{max} (mm)	K_s (mm h^{-1})	S_{max} (mm)	R^2
location			IR						UC		
1	0.03	0.32	110	2.7	0.89 / 0.89	0.01	0.16	80	28.4	1.65	0.70 / 0.70
2	0.02	0.27	80	31.1	0.92 / 0.88	0.02	0.33	50	49.8	2.58	0.80 / 0.78
3	0.04	0.27	100	8.7	0.92 / 0.89	0.01	0.30	60	20.5	2.09	0.92 / 0.86
4	0.04	0.38	70	18.3	0.86 / 0.87	0.03	0.25	70	9.5	1.71	0.93 / 0.93
5	0.01	0.26	80	2.0	0.92 / 0.94	0.02	0.28	80	27.6	1.65	0.85 / 0.84
6	0.08	0.39	80	1.7	0.93 / 0.96	0.04	0.33	70	48.8	1.71	0.82 / 0.75
7	0.04	0.25	80	6.3	0.92 / 0.96	0.05	0.25	70	9.0	1.50	0.90 / 0.91
8	0.03	0.39	70	3.2	0.82 / 0.80	0.01	0.19	60	34.7	1.71	0.88 / 0.60
9	0.04	0.25	70	1.7	0.88 / 0.88	0.05	0.24	70	11.2	2.09	0.91 / 0.91
10	0.04	0.30	70	24.0	0.85 / 0.89	0.01	0.19	70	20.9	-	0.87 / 0.88
11	0.02	0.32	75	22.6	0.85 / 0.81	0.01	0.30	80	49.8	-	0.86 / 0.84
min	0.01	0.25	70	1.7	0.82 / 0.80	0.01	0.16	50	9.0	1.50	0.70 / 0.60
max	0.08	0.39	110	31.0	0.93 / 0.96	0.05	0.33	80	49.8	2.58	0.93 / 0.93
GM	0.03	0.30	80	6.5	0.89 / 0.89	0.02	0.25	68	23.7	1.83	0.86 / 0.81
CV	0.51	0.18	0	1.0	0.04 / 0.06	0.69	0.23	0	0.7	0.19	0.08 / 0.12
median	0.04	0.30	80	6.3	0.89 / 0.89	0.02	0.25	70	27.5	1.71	0.87 / 0.84

θ_{min} minimum value observed for soil moisture, θ_{max}: maximum value, W_{max}: maximum soil moisture storage, K_s: saturated soil hydraulic conductivity, *GM*: geometric mean, *CV*: coefficient of variation.

The spatial distribution of K_s was consistent with laboratory analyses aimed at determining the water retention curves for the first 0.02 m depth of the soil at these monitoring locations (Espejo et al. 2004). These analyses indicated a lower porosity at IR locations, which can be accounted for by the lower bulk density. Tilling operations and the transit of machinery between trees increases the spatial variability of soil properties, and, consequently, modifies the hydrological patterns of the catchment compared to natural conditions (*e.g.* by modifying the K_s value, Gómez et al. 1999). Plant canopies protect the surface layer preventing the soil surface from sealing, and usually concentrate soil microorganisms, which improve the water infiltration into the soil compared to bare soil (Thompson and Katul, 2012).

The scatter plot between the estimated K_s value for the eleven sample points, for IR and UC locations separately, versus the measured topsoil (0-0.2 m) bulk density, ρ_b, is shown in Fig. 6.3. In general, IR bulk density values were higher than those in UC for the same location, and the value measured at point 8 for IR location was particularly high, 1.86 Mg m^{-3}. At this location, the maximum soil depth for IR was 0.20 m. The trend of the data indicated a clear decrease in soil water transmission with the increase in ρ_b, although the correlation coefficient was 0.51. The relationship was more consistent at the IR location. The influence of ρ_b on important soil hydraulic properties such as K_s agrees with the results previously found by Espejo et al. (2014) for the same sample points by using an independent methodology. They determined the soil diffusivity, *D*, by using moisture measurements during soil drying periods and the Boltzmann transform for space and time coordinates, and identified that ρ_b also had an important effect on this property.

6.4.4. Canopy interception.

Even though the proposed interception model was very simple (section 6.3.3), results were encouraging. A total of 89 rain events were considered in this analysis using the SWBMI at the 9 individual monitoring UC locations (only points with adult trees, Fig. 2.3, positions from 1 to 9). The average accumulated rainfall depth per event was 16.2 and 14.8 mm for year 1 and year 2, respectively.

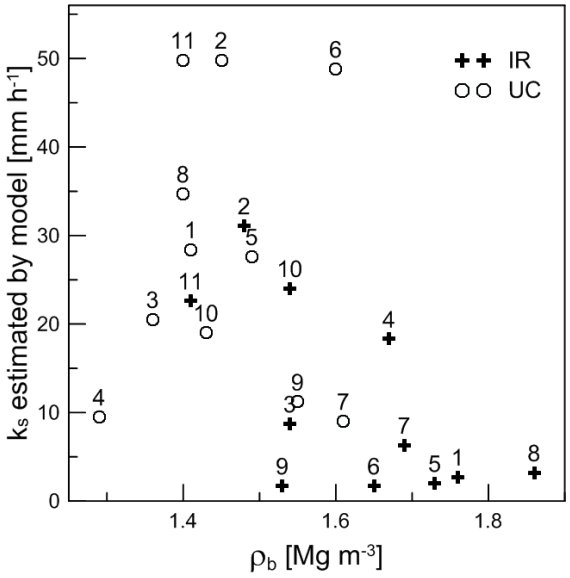

Fig. 6.3. Relationship between the measured bulk density, ρ_b, for 0-0.2 m, and estimated saturated hydraulic conductivity, K_s, for the individual monitoring locations at inter-row, IR, and under canopy, UC**.**

Exponential relationships were found between rain events and the canopy interception ratio using the SWBMI with year 1 for calibration and year 2 for validation, for the different UC locations (Fig. 6.4). The figure represents the interception value for each monitoring point and event. An exponential fit for the UC locations was proposed, with a determination coefficient, R^2= 0.77. For comparison, the general relationship proposed by Gómez et al. (2001) obtained by observations at five typical olive trees with a different leaf area index during successive events, was also plotted. A similar pattern was found for rainfall depths lower than 7 mm with interception values reaching 90%. Estimated canopy interception for rainfall depths of over 7 mm was significantly lower than that observed by Gómez et al (2001), because the S_{max} ratios measured by these authors were higher. However, the tree named E by these authors had a value of S_{max} equal to 1.51 mm, similar to that found by us (1.83 mm). Thus, the exponential fit proposed by us was fitted to adapted data from the authors at this tree. A fit score, R^2= 0.56, was obtained, and the pattern was similar to the one proposed in this work.

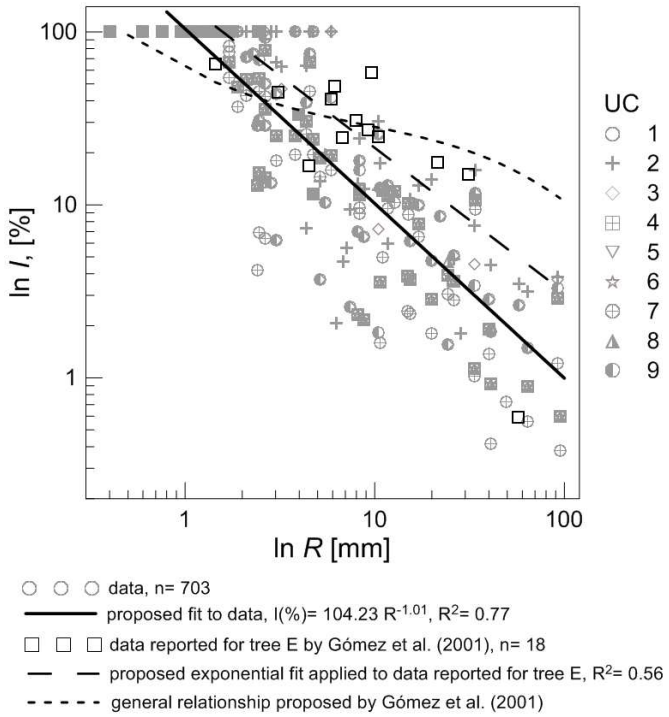

Fig. 6.4. Relationship between the estimated rainfall canopy interception, *I*, and measured rainfall, *R*, at each UC monitoring location, and fit proposed, in a solid line. Added to this was the relationship suggested by Gómez et al. (2001) from observations at five typical olive trees with different leaf area indexes, and reported data for a single tree, named tree E. Tree E had a similar maximum canopy interception storage, S_{max}, to that obtained by us, and thus our proposed fit was applied.

A mean spatio-temporal interception ratio of approximately 0.10 was estimated considering the average event rainfall depth of the two year period, 15.0 mm. This ratio is a low one compared to other plant species under Mediterranean conditions, as summarized by Llorens and Domingo (2007), but it was in the range reported by Gómez et al. (2001), *i.e.*, 7-25%. This can be explained by the small size of the olive leaf, which limits its ability to store water, and by the structure of their canopies.

However, this value ranged from 17.3 to 48.3% for year 1 and year 2 when averaging temporal and spatially the interception ratios obtained in the individual rainfall events in the 9 locations. Comparable ratios of 29.2% and 35.8% for year 1 and year 2, respectively, were found on averaging the interception values estimated by applying the relationship proposed by Gómez et al. (2001) to the rainfall collected. The highest

interception ratios were obtained in the Spring months, and although the canopy interception model proposed here does not consider the effect of rainfall intensity over the canopy saturation process, lower rainfall intensities could explain this interception increase (Ramirez and Senarath, 2000). Equally, the higher interception values for the second year were attributed to a greater occurrence of small and low intensity rain events (Rutter, 1975).

6.5. Conclusions.

The soil water balance models employed in this study (Brocca et al. 2008) were found to be successful in reproducing the hourly soil moisture temporal evolution in an olive tree-planted catchment in south-western Spain. Moreover, the models were able to highlight the differences between the process at inter row and under canopy areas. By using spatial mean soil moisture and records of individual sample locations, the performance score values in terms of the determination coefficient, R^2, and Nash and Sutcliffe efficiency indices were found to be over 0.90, while the RMSE was very low and always below 0.02 $m^3\ m^{-3}$.

The procedure allowed the estimation of relevant soil hydraulic parameter values at a small catchment scale. Specifically, the average value of K_s was equal to 6.5 mm h^{-1} at inter row areas and lower than the value obtained at under canopy locations (23.7 mm h^{-1}). These results showed a lower capacity of soil moisture transmission at inter row location, and agreed with the previous results obtained by Espejo et al. (2014).

Moreover, the rainfall canopy interception process was investigated by means of the model. The average value of the maximum capacity of canopy water retention was equal to 1.83 mm. A simple relationship between the rainfall canopy interception and rainfall depth was also proposed, indicating an average canopy interception ratio of around 0.10 for the period analysed.

Overall, this work shows the usefulness of measuring soil moisture intensively by using a sensor network to improve the calibration of models and to identify spatial and temporal hydrological patterns. The hydrological processes at inter row and under

canopy locations have been compared. Future works will be addressed to analyze the runoff process of this catchment and the effect of antecedent soil moisture by using the soil water balance model as an exploration tool.

6.6. References.

Albertson, J.D., and G. Kiely. 2001. On the structure of soil moisture time series in the context of land surface models. J. Hydrol. 243, 101-119.

Baudena, M., I. Bevilacqua, D. Canone, S. Ferraris, M. Previati, and A. Provenzale. 2012. Soil water dynamics at a mid-latitude test site: Field measurements and box modeling approaches. J. Hydrol. 414-415, 329-340.

Betts, A.K. 2004. Understanding hydrometeorology using global models. Bull. Am. Meteor. Soc. 85, 1673-1688.

Beven, K.J. 2000. Rainfall-runoff modelling, the primer. John Wiley, Chichester, UK.

Brocca, L., S. Camici, F. Melone, T. Moramarco, J. Martínez-Fernandez, J.F. Didon-Lescot, and R. Morbidelli. 2014. Improving the representation of soil moisture by using a semi-analytical infiltration model. Hydrol. Proc. 28, 2103-2115.

Brocca, L., G. Zucco, T. Moramarco, and R. Morbidelli. 2013. Developing and testing a long-term soil moisture dataset at the catchment scale. J. Hydrol. 490, 144-151.

Brocca, L., F. Melone, and T. Moramarco. 2011a. Distributed rainfall-runoff modelling for flood frequency estimation and flood forecasting. Hydrol. Proc. 25, 2801-2813.

Brocca, L., S. Hasenauer, T. Lacava, F. Melone, T. Moramarco, W. Wagner, W. Dorigo, P. Matgen, J. Martínez-Fernández, P. Llorens, J. Latron, C. Martin, and M. Bittelli. 2011b. Soil moisture estimation through ASCAT and AMSR-E sensors: an intercomparison and validation study across Europe. Rem. Sens. Environ. 115, 3390-3408.

Brocca, L., F. Melone, and T. Moramarco. 2008. On the estimation of antecedent wetness condition in rainfall-runoff modelling. Hydrol. Proc. 22, 629–642.

Brutsaert, W. 2014. Daily evaporation from drying soil: Universal parameterization with similarity.Water Resour. Res. 50, 3206-3215.

Camici, S., A. Tarpanelli, L. Brocca, F. Melone, and T. Moramarco. 2011. Design soil moisture estimation by comparing continuous and storm-based rainfall-runoff modelling. Water Resour. Res. 47, W05527, doi:10.1029/2010WR009298.

CAP, Consejería de Agricultura y Pesca de la Junta de Andalucía, 2013. Datos de la Red de Alerta e Informacion Fitosanitaria (RAIF). Available at: http://www.juntadeandalucia.es/agriculturaypesca/portal/servicios/estadisticas/servicio-de-informacion-agroclimatica/red-de-alerta-e-informacion/datos-de-las-estaciones-agroclimaticas.html, accessed on 06/05/2013.

Dorigo, W.A., A. Xaver, M. Vreugdenhil, A. Gruber, A. Hegyiová, A.D. Sanchis-Dufau, and M. Drusch. 2013. Global automated quality control of in situ soil moisture data from the International Soil Moisture Network. Vadose Zone J. 12, doi:10.2136/vzj2012.0097.

Espejo, A.J., J.V. Giráldez, K. Vanderlinden, E.V. Taguas, and A. Pedrera. 2014. A method for estimating soil water diffusivity from moisture profiles and its application across an experimental catchment. J. Hydrol. 516, 161-168.

Famiglietti, J.S., and E.F. Wood. 1994. Multiscale modeling of spatially variable water and energy balance processes. Water Resour. Res. 11, 3061-3078.

Fares, A., M. Temimi, K. Morgan, and T.J. Kelleners. 2013. In-situ and remote soil moisture sensing technologies for vadose zone hydrology. Vadose Zone J., doi:10.2136/vzj2013.03.0058.

García del Barrio, I., L. Malvárez, and J.I. González. 1971. Mapas provinciales de suelos, Cádiz, Ministerio de Agricultura, Madrid, Spain.

Gómez, J.A., K. Vanderlinden, J.V. Giráldez, J.V., and E. Fereres. 2002. Rainfall concentration under olive trees. Agric. Water Manag. 55, 53-70.

Gómez, J.A., J.V. Giráldez, and E. Fereres. 2001. Rainfall interception by olive trees in relation to leaf area. Agric. Water. Manag. 49, 65-76.

Gómez, J.A., J.V. Giráldez, M. Pastor, and E. Fereres. 1999. Effects of tillage method on soil physical properties, infiltration y yield in a olive orchard. Soil Till. Res. 52, 167-175.

Gumuzzio, A., L. Brocca, J. Martínez-Fernandez, F. Melone, and T. Moramarco. 2013. Large scale soil moisture modelling in Northwest of Spain. Proc. Int. Conf. 6th International Perspective on Water Resour. & the Environ. (IPWE 2013), 7-9 January 2013, Izmir, Turkey.

Guswa, A.J. 2012. Canopy versus roots: Production and destruction of variability in soil moisture and hydrologic fluxes. Vadose Zone J. 11, doi:10.2136/vzj2011.0159.

Hershfield, D.M. 1963. Rainfall frequency atlas of the United States for duration from 30 minutes to 24 hours and return periods from 1 to 100 years. US Weather Bureau Technical paper 40, Washington, DC, USA.

Hollinger, S.E., and S.A. Isard. 1994. A soil moisture climatology of Illinois. J. Clim. 7, 822–833.

Koster, R.D., Z. Guo, P.A. Dirmeyer, R. Yang, K. Mitchell, and M.J. Puma. 2009. On the nature of soil moisture in land surface models. J. Clim. 22, 4322-4335.

Lacava, T., P. Matgen, L. Brocca, M. Bittelli, and T. Moramarco. 2012. A first assessment of the SMOS soil moisture product with in situ and modelled data in Italy and Luxembourg. IEEE T. Geosci. Remote 50, 1612–1622.

Lebron, I., M.D. Madsen, D.G. Chandler, D.A. Robinson, O. Wendroth, and J. Belnap. 2007. Ecohydrological controls on soil moisture and hydraulic conductivity within a pinyon-juniper Woodland. Water Resour. Res. 43, doi:10.1029/2006WR005398.

Liang, W.L., K. Kosugi, and T. Mizuyama. 2011. Soil water dynamics around a tree on a hillslope with or without rainwater supplied by stemflow. Water Resour. Res. 47, W02541, doi:10.1029/2010WR009856.

Maetens, W., J. Poesen, and M. Vanmaercke. 2012. How effective are soil conservation techniques in reducing plot runoff and soil loss in Europe and the Mediterranean?. Earth Sci. Reviews 115, 21-36.

Martínez, G., Y.A. Pachepsky, and H. Vereecken. 2014. Temporal stability of soil water content as affected by climate and soil hydraulic properties: a simulation study. Hydrol. Proc. 28, 1899-1915.

Martínez, G., K. Vanderlinden, J.V. Giráldez, A.J. Espejo, and J.L. Muriel. 2010. Field-scale soil moisture pattern mapping using electromagnetic induction. Vadose Zone J. 9, 871-881.

Mittelbach, H., F. Casini, I. Lehner, A.J. Teuling, and S.I. Seneviratne. 2011. Soil moisture monitoring for climate research: Evaluation of a low cost sensor in the framework of the Swiss Soil Moisture Experiment (SwissSMEX) campaign. J. Geophys. Res. 116, D05111, doi:10.1029/2010JD014907.

Morbidelli, R., C. Corradini, C. Saltalippi, and L. Brocca. 2012. Initial soil water content as input to field-scale infiltration and surface runoff models. Water Resour. Manag. 26, 1793-1807.

Nash, J.E., and J.V. Sutcliffe. 1970. River flow forecasting through conceptual models, part I: A discussion of principles. J. Hydrol. 10, 282-290.

Orgaz, F., and E. Fereres. 1997. Riego, in: Barranco, D., R. Fernández-Escobar, and L. Rallo (Eds.), El cultivo del olivo. Mundi Prensa, Madrid, Spain, pp. 251–272.

Palecki, M.A., and J.E. Bell. 2013. U.S. Climate reference network soil moisture observations with triple redundancy: measurement variability. Vadose Zone J. 13, doi:10.2136/vzj2012.0158.

Pan, F., Y. Pachepsky, D. Jacques, A. Guber, A. Hill, and L. Robert. 2012. Data Assimilation with Soil Water Content Sensors and Pedotransfer Functions in Soil Water Flow Modelling. Soil Sci. Soc. Am. J. 276, 829-844.

Ramirez, J.A., and S.U.S, Senarath. 2000. A statistical–dynamical parameterization of interception and land surface–atmosphere interactions. J. Clim. 13, 4050-4063.

Rawls, W.J., D.L. Brakensiek, and K.E. Saxton. 1982. Estimation of soil water properties. Trans. ASAE 25, 1316-1320.

Robinson, D.A., C.S. Campbell, J.W. Hopmans, B.K. Hornbuckle, S.B. Jones, R. Knight, F. Ogden, J. Selker, and O. Wendroth. 2008. Soil moisture measurement for ecological and hydrological watershed-scale observatories: A review. Vadose Zone J. 7, 358-389.

Robock, A., K.Y. Vinnikov, G. Srinivasan, J.K. Entin, S.E. Hollinger, N.A. Speranskaya, S. Liu, and A. Namkhai. 2000. The Global Soil Moisture Data Bank. Bull. Am. Meteorol. Soc. 81, 1281-1299.

Rodríguez-Iturbe, I., P. D'odorico, A. Porporato, and L. Ridolfi. 1999. On the spatial and temporal links between vegetation, climate, and soil moisture. Water Resour. Res. 35, 3789-3805.

Rutter, A.J., K.A. Kershaw, P.C. Robins, and A.J. Morton. 1971. A predictive model of rainfall interception in forests. I. Derivation of the model from observations in a plantation of Corsican pine. Agric. Meteorol. 9, 367-384.

Rutter, A.J. 1975. The hydrological cycle in vegetation, in: Montheith, J.L. (Ed.), Vegetation and the Atmosphere, vol. 1. Academic Press, London, pp. 111-154.

Schelle, H., S.C. Iden, J. Fank, and W. Durner. 2012. Inverse estimation of soil hydraulic and root distribution parameters from lysimeter data. Vadose Zone J. 11, doi:10.2136/vzj2011.0169.

Soil Survey Staff. 1999. Soil Taxonomy. 2nd ed. USDA Agr. Hdbk. nº. 436. NRCS. Washington, USA.

Taguas E.V., J.L. Ayuso, A. Peña, Y. Yuan, and R. Pérez. 2009. Evaluating and modelling the hydrological and erosive behaviour of an olive orchard microcatchment under no-tillage with bare soil in Spain. Earth Surf. Process. Landf. 34, 738–751.

Thompson, S.E., and G.G. Katul. 2012. Hydraulic determinism as a constraint on the evolution of organisms and ecosystems, J. Hydraul. Res. 50, 547-557.

Vanderlinden K, H. Vereecken, H. Hardelauf, M. Herbs, G. Martínez, M.H. Cosh, and Y. Pachepsky. 2012. Temporal stability of soil water contents: a review of data and analyses. Vadose Zone J. 11, doi:10.2136/vzj2011.0178.

Vereecken, H., J.A. Huisman, H. Bogena, J. Vanderborght, J.A. Vrugt, and J.W. Hopmans. 2008. On the value of soil moisture measurements in vadose zone hydrology: A review. Water Resour. Res. 44, W00D06, doi:10.1029/2008WR006829.

Villalobos, F.J., F. Orgaz, L. Testi, and E. Fereres. 2000. Measurement and modelling of evapotranspiration of olive (Olea europaea L.) orchards. Eur. J. Agron., 13, 155-163.

Viola, F., L.V. Noto, M. Cannarozzo, G. La Loggia, and A. Porporato. 2012. Olive yield as a function of soil moisture dynamics. Ecohydrol. 5, 99-107.

Williams, C.A., and J.D. Albertson. 2004. Soil moisture controls on canopy-scale water and carbon fluxes in an African savanna. Water Resour. Res. 40, W09302, doi:10.1029/2004WR003208.

Chapter 7

Control of soil water and olive trees on measured and modelled rainfall-runoff relationships in a small Mediterranean catchment

7.1. Abstract.

Soil and water conservation is a necessary element of any catchment management system. A simple hydrological model, MISDc, developed by Brocca et al. (2011) has been applied to the rainfall runoff response of an instrumented catchment of south-western Spain. Runoff was measured by using a gauging station built at outlet of the catchment. Soil water content was measured across eleven locations within the catchment, and at each one the landscape was divided in to under canopy, UC, and inter-row areas, IR, of trees. The model reliability and robustness were evaluated in terms of runoff and soil water content simulation, with the objective to analyse the influence of vegetation and the antecedent soil water content on catchment behaviour.

Calibration-validation results showed that the model performance was consistent in reproducing the ten-minutes runoff hydrograph, with a Nash-Sutcliffe efficiency index of around 0.65, and 0.85 for the spatial mean soil water content, at IR and UC for both, respectively. No differences were found in the runoff generation between IR and UC, although differences on soil water dynamics were detected. A clear influence of antecedent soil water content with a minimum threshold around 0.60 was appreciated, and the annual average runoff ratio was 0.21. A simulation of 9 years showed that annual rainfall was concentrated during 4 months. Fifty percent of the events accumulated 28% of rainfall, of which only 10% caused runoff.

7.2. Introduction.

Catchment hydrological processes result from the simultaneous interaction of multiple factors (Graham and McDonnell, 2010; Detty and McGuire, 2010). To get a clear, although simpler characterization of those processes the rainfall-runoff relationship can be a useful tool to explore the influence of climate, soil properties and land use (Soulsby et al., 2008).

After an extended review of the scientific advances in the hydrology of ungauged catchments during the last decade, Hrachowitz et al. (2013) concluded that there is still a long way to go in terms of achieving more robust and reliable predictions. Nowadays a plethora of rainfall-runoff models exist, but the great number of parameters they demand precludes their accessibility. Simplified rainfall-runoff models can be more versatile for the description of hydrological processes with a few parameters (*e.g*. Brocca et al. 2011; Majone et al. 2010; Sivakumar, 2008). Assessing such models in terms of runoff simulation performance is insufficient. Internal validation is still required to assess their reliability and robustness.

Recently instrumented basins allow more precise interpretations of their behavior (Spence, 2010). Soil moisture is one of the relevant factors that control the hydrological response of catchments, (Zhang et al. 2011; Brocca et al. 2008; Fitzjohn et al. 1998). A sound hydrological knowledge of a basin is essential to implementing successfully soil and water conservation practices, particularly in sensitive areas such as the Mediterranean. Despite the representativeness of tree crops (*i.e.* olives) in the Mediterranean, few studies have evaluated soil water dynamics and runoff generation, including the influence of the trees in both processes, in catchments with this land use.

The temporal soil water pattern within this catchment has been discussed in chapter 6, focusing in the influence of the inter row and under canopy areas. The results showed a lower soil water content in the latter throughout the measurement period and an average canopy interception of 0.10. Espejo et al (2014) estimated the spatial distribution of the hydraulic conductivity within the catchment and found that the values were one to two orders of magnitude larger at under canopy areas as compared to inter row, and they identified the spatial distribution of the soil water dynamics across the catchment.

The objectives of this work are to evaluate rainfall-runoff relationships for the catchment by using a simple model, and to analyse the influence of vegetation and the antecedent soil water content on runoff generation. In addition, simulated long-term runoff was analysed.

7.3. Material and methods.

7.3.1. Data sources.

Data were collected in the Setenil experimental catchment, described in section 2.2. Soil moisture records, collected with the 10HS sensor model, and runoff, correspond to the period between September 1, 2011 to August 31, 2013. For rainfall 9 years of rainfall data were used for the period from September 1, 2004 to August 31, 2013, in order to calibrate the model and simulate the runoff discharge.

7.3.2. Runoff modelling.

A lumped version of the Modello Idrologico Semi-Distribuito in Continuo, MISDc model, developed by Brocca et al. (2011) was used in this study. The model was already tested for other applications providing satisfactory results in different conditions, sites and scenarios (*e.g.* Massari et al. 2013; Camici et al. 2011).

The model consists of the coupling of two main components: a soil water balance model (SWBM) to simulate the soil water temporal pattern, and a semi-distributed event-based rainfall runoff model (MISDc) for flood simulation. For the SWBM reader is referred to Brocca et al. (2008).

The MISDc model computes the rainfall excess by using the geomorphological instantaneous unit hydrograph (GIUH), and the soil conservation service-curve number method (SCS-CN) for estimation of losses (Kim and Lee, 2008). By using this method, the antecedent wetness condition for the rainfall events, S_{obs}, is calculated based on the

dimensionless CN, as function of soil group, land use and cumulated rainfall of 5 days before, representing the latter the wetness state of the catchment. According to Brocca et al. (2008, 2009) and Melone et al. (2001) in Mediterranean catchments the estimation of the wetness state of the catchment can be improved, and consequently the model uses an experimentally derived relationships to calculate S_{obs}:

$$S_{obs} = a \left(1 - \frac{W(t)}{W_{\max}}\right) \qquad \text{Eq. (7.1)}$$

where $W(t)/W_{max}$ is the normalized soil water content, or degree of saturation, and a is an empirical coefficient to estimate from field observations.

Finally, the discharge hydrograph is computed by the convolution of the rainfall excess and the GIUH following Gupta et al. (1980), where the lag time is given by the experimental relationship of Melone et al. (2002).

The inputs of the model are rainfall, air temperature, and catchment discharge for calibration of the model parameters. The model predictions are the direct runoff hydrograph at the lower part of the catchment, and the mean degree of saturation and soil water content.

The Nash-Sutcliffe (1970) efficiency index, NS, and the absolute value of the relative error on peak discharge, Q_p, were used as objective functions. Additionally the determination coefficient, R^2, the Root Mean Square Error, RMSE were also used for comparison purposes.

7.3.3. Application of the model and data analysis.

The MISDc model coupled to the Soil Water Balance model, SWBM, of Brocca et al. (2008) was used for the IR location. According to chapter 6, at UC areas a canopy interception component was included into the SWBM model, with a canopy interception threshold, *I*, of 1.86 mm.

For calibration and validation purposes of the MISDc model, twelve rainfall-runoff events were manually extracted from the weather data and soil moisture series (Table 7.1). Only events with a minimum total rainfall depth of 5 mm were retained. Inter-event periods lasted at least 6 hours and produced less than 2 mm rainfall. Seven of the events were used for calibration and five for validation. Once calibrated and validated the models, a dataset was simulated for the 2004-2013 period.

Although the model was calibrated with discrete rain events from 2011 to 2013, for comparison of spatial mean soil water modelled and observed, the soil water content was simulated continuously for this period. Performance scores were calculated using data of soil water obtained by models and the mean spatial observations for 0-0.10 m, and from 0-0.20 to 0-0.50 m, calculated as the integrations of the corresponding soil depth measurements.

7.4. Results and discussion.

7.4.1. MISDc model performance for runoff generation.

The annual rainfall for 2011-2012 and for 2012-2013 hydrological years was 331 and 1089 mm yr^{-1}, respectively, and the average event rainfall depth was 23 mm. The average observed runoff coefficient, RC, was 0.21, and the average time lag between the onset of the rain and the observed peak runoff was 9.4 h. Four events accounted for 31% of the total rainfall and produced 59% of the total runoff.

Table 7.1. Characteristics of the 12 selected rainfall-runoff events.

Date		Rainfall			Runoff					‹AWC›‡	
		R	I_{30}	Duration†	Q_p	Lag ††	Q_e	RC	Duration†	IR	UC
		mm	mm h^{-1}	hh:min	L s^{-1}	hh.min	mm	[ ]	hh.min	[ ]	[ ]
24 Oct 2011	1	12.6	6.61	7.30	12.09	6.50	0.40	.03	3.30	.10	.01
27 Oct 2011	2	19.7	12.18	17.20	26.12	16.20	1.41	.07	15.10	.49	.44
2-3 Nov 2011	3	29.3	18.56	8.50	217.15	8.00	6.00	.20	1.50	.58	.49
3-4 Nov 2011	4	28.1	8.46	9.00	115.11	7.40	6.86	.24	16.10	.78	.79
19 Nov 2011	5	16.9	8.09	10.50	82.12	2.40	3.34	.20	9.10	.62	.57
20 Nov 2011	6	28.8	5.51	19.40	58.29	17.10	9.73	.34	9.30	.83	.80
5 6 May 2012	7	27.8	9.21	17.10	70.78	6.10	3.49	.13	13.00	.69	.60
24 Jan 2013	8	20.1	4.40	15.20	49.40	9.40	5.40	.27	14.00	.74	.73
19-20 Mar 2013	9	36.2	12.2	22.20	242.4	21.50	14.10	.39	19.40	.78	.69
24 Mar 2013	10	16.7	9.20	11.30	78.42	9.50	3.70	.22	10.30	.81	.74
29-30 Mar 2013	11	25.9	8.50	8.50	140.8	6.20	7.10	.27	7.20	.77	.70
1 Apr 2013	12	14.3	7.40	5.00	62.03	2.00	2.30	.19	1.40	.74	.71
mean		23.0	9.19	12.60	96.22	9.36	5.32	.21	9.99	.66	.61
st.dev.		7.3	3.75	5.44	71.54	5.96	3.83	.10	5.83	.20	.22

†: duration of rainfall and runoff event, respectively.

††: lag time between onset of rainfall event and peak flow.

‡: observed mean spatial antecedent soil water content averaging at topsoil, 0-0.20 m depth, for inter row, IR, and under canopy, UC, of trees, expressed as relative soil water.

The histograms and hydrographs of observed and modelled runoff, at IR and UC areas are shown in Fig. 7.1. Both, observations and estimations showed similar trends in the catchment response. Generally the model underestimated runoff generation, with small differences between UC and IR areas. The runoff ratios for IC and UC were similar in nine cases, and lower for UC than for IR in 3 cases. Unless we know, no studies have investigated the effect of olive trees on runoff generation.

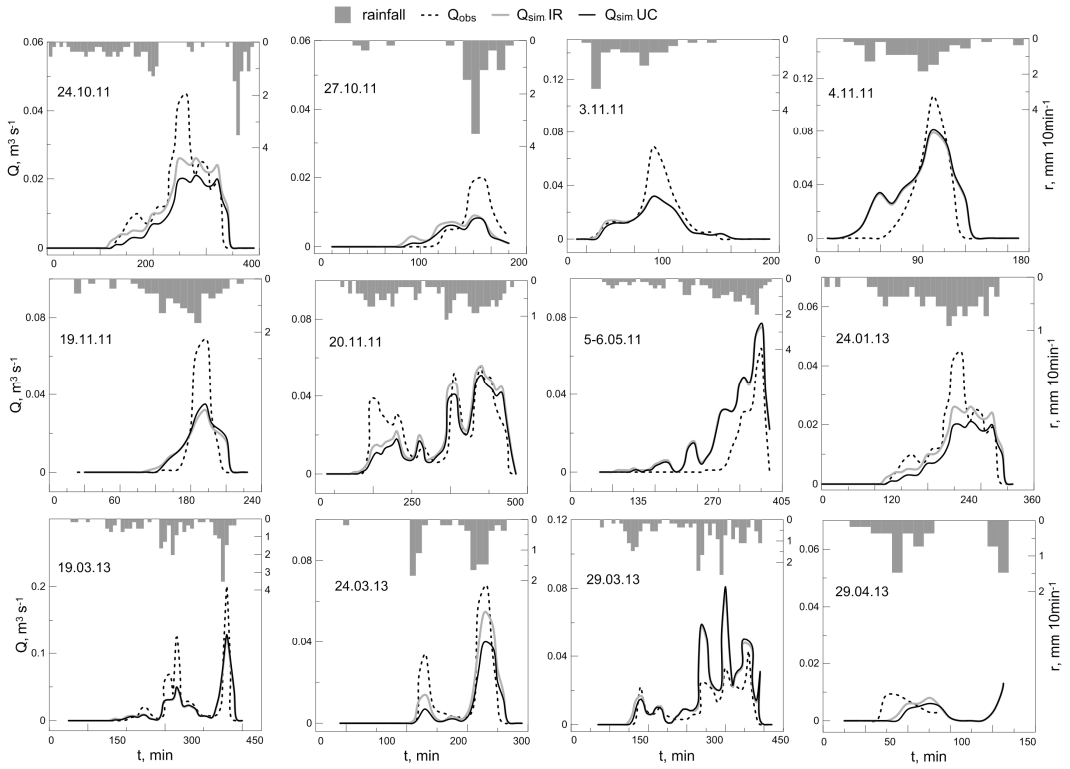

Fig. 7.1. Rainfall and observed (dashed black line) and modelled hydrographs at 10 min interval for the 12 selected flood events. Continuous grey line for inter row, IR, and in black under canopy, UC, areas.

The Nash-Sutcliffe efficiencies for reproducing runoff generation after calibration were 0.73 at IR and 0.64 at UC. Validation efficiencies were 0.64 at IR and 0.62 at UC. The model error, RMSE, estimating Q_e was 31 and 37% for IR and UC after calibration, and became 37 and 49%, respectively during validation. Q_p error ranged between 27% for calibration and 53% for validation at IR, and from 35 to 61% at UC, respectively.

7.4.2. Relationship between observed/modelled soil water content and initial conditions.

Table 7.2 shows the resulting values of parameter *a*, for IR and UC, when fitting Eq. (7.1) to estimated and observed water content at different depths using data for the 12 selected events. Fig. 7.2 shows the corresponding graphs for estimated and observed 0-0.5-m profile soil water content. Coefficients of determination were higher at UC and similar for profile estimations and observations. For each event S_{obs} was calculated by using the SCS-CN method with observed rainfall and direct runoff depth (*e.g.* Massari et al. 2013). It was assumed a value of 0.027 mm^{-1} for λ, derived from an analysis of the best-fit results on the model calibration period. The *a* parameter ranged from 150 to 250 mm^{-1}, and was higher at IR as compared to UC.

Table 7.2. Slope and coefficient of determination of the linear relationship between the wetness of the soil, $W(t)/W_{max}$, and the soil potential maximum retention, *S* (Eq. 7.1), for inter row, IR, and under canopy, UC, areas.

	IR		UC	
W/W_{max}	a mm^{-1}	R^2	a mm^{-1}	R^2
model	253.88	0.56	178.26	0.72
observed				
0-0.10m †	216.15	0.56	200.26	0.49
0-0.20m ‡	224.88	0.54	197.97	0.57
0-0.30m ‡	206.79	0.64	182.90	0.60
0-0.40m ‡	198.59	0.61	177.25	0.75
0-0.50m ‡	185.61	0.67	169.72	0.76

† I

‡ Integrated measurements

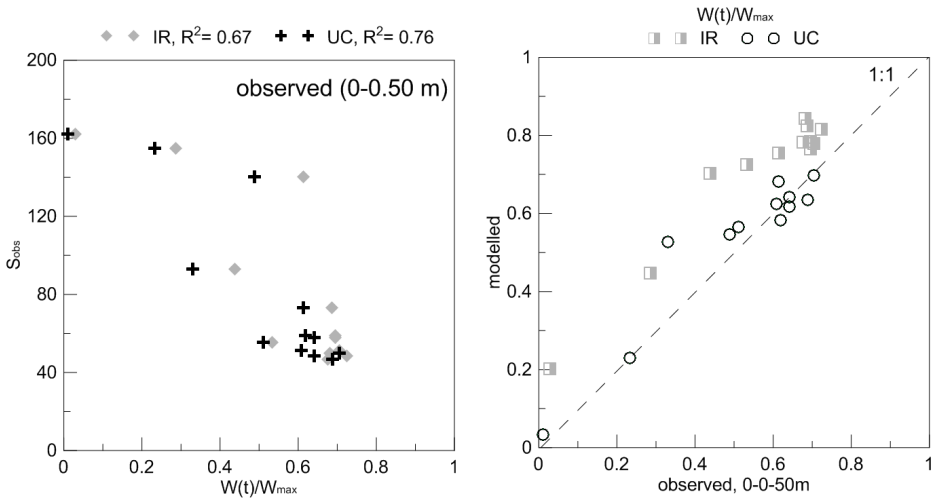

Fig. 7.2. Relationship between observed soil potential maximum retention, S_{obs}, and degree of saturation, estimated for each rainfall event with Eq. (7.1) using measured soil water content at inter row, IR, and at under canopy, UC areas. Figure in the left represents the relationship between the degree of saturation using observed and simulated values.

7.4.3. MISDc performance for soil water content simulation.

The model performance in reproducing measured soil water content at IR and UC after calibrating with discharge data is shown in Table 7.3. The model performed slightly worsed when calibrated with discharge data as compared to calibration with soil water content data (chapter 6), with R^2 above 0.90 and 0.82 at IR and UC. The best results were obtained for the 0-0.20-m layer at IR, and for the 0-0.10-m layer at UC. Overall model performance with respect to soil moisture estimation was better during wet periods as compared to dry periods.

Table 7.3. Comparison of the coefficient of determination, R^2, the root mean squared error, RMSE, and the Nash-Sutcliffe efficiency, NS, for simulated relative spatial mean soil water content at inter row, IR, and at under canopy, UC, areas and integrated at different soil horizons.

	IR			UC		
soil depth m	R^2	RMSE % †	NS	R^2	RMSE % †	NS
0-0.10	0.913	17.0	0.553	0.864	10.5	0.845
0-0.20	0.933	12.7	0.761	0.852	10.5	0.839
0-0.30	0.921	14.4	0.640	0.830	11.2	0.800
0-0.40	0.908	14.9	0.605	0.825	11.2	0.796
0-0.50	0.902	16.5	0.476	0.842	10.8	0.791

†: mean relative square error in estimating relative soil water content.

7.4.4. Influence of the antecedent soil water content (AWC) on runoff prediction.

An apparent exponential relationship between Q_e and AWC was found, as shown in Fig. 7.3. The model overestimated slightly AWC at IR as compared to UC. A minimum threshold of AWC reaching between 60% and 80% indicated a rapid increase for Q_e. As a result of rainfall canopy interception and lower soil moisture contents, a lower AWC threshold was found at UC as compared to IR.

The effect of soil depth on the AWC-Q_e relationship at UC and for one event is illustrated in Fig. 7.3. A more gradual increment of RC with AWC was found than for Qe. These results indicate that higher topsoil water contents are required, as compared at deeper soil layers, to produce similar Q_e and RCs, and that the highest Qe and RCs are found in situations where the entire soil profile has been uniformly wetted.

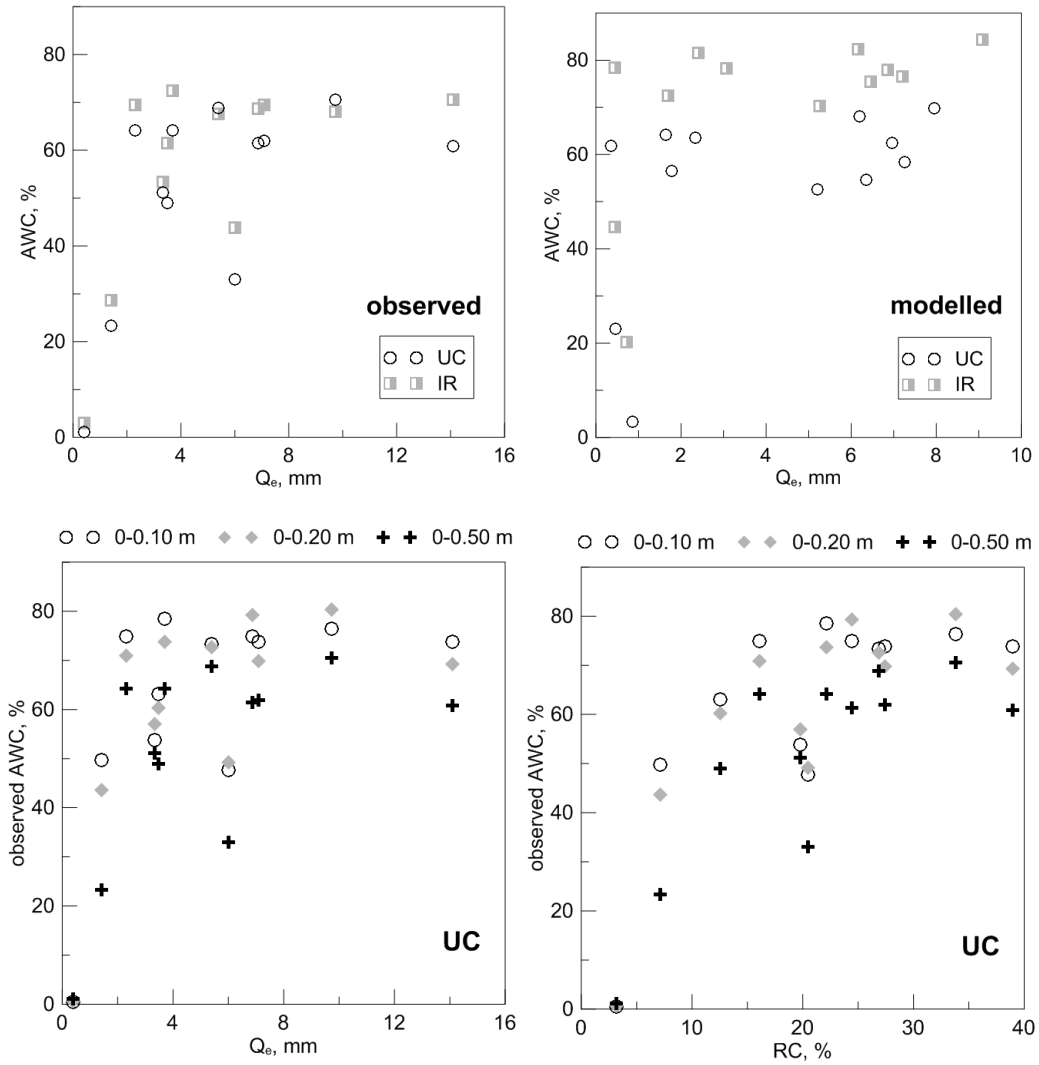

Fig. 7.3. Top: Relationship between relative antecedent soil water content, AWC, and accumulated runoff at inter row, IR, and at under canopy, UC, using observed data (left, 0-0.50 m for AWC) and e data (right), for the 12 selected events during the calibration-validation period. Bottom: relationship between observed AWC at different soil depths, observed discharge (left) and observed runoff coefficient, RC, (right) at UC location.

7.4.5. Simulation of runoff for a long-term period (2004-2013).

Since the MISDc model was found adequate for simulating both runoff and soil water content, the model was used to assess the the seasonal behaviour of the catchment by simulating a 9 year period with a total of 268 rainfall events. No significant differences in annual runoff ratios between IR and UC were found during the simulated period (Table 7.4). The average runoff coefficient was 0.20 and the cumulative runoff for the

Table 7.4. Observed annual rainfall, and runoff discharge and relative antecedent soil water content (AWC) simulated at inter row, IR, and at under canopy, UC, areas for the 2004-2013 simulation period.

year	site	R	n†	I‡	DOR	Q_e	$Q_{p.25††}$ x10^3	$Q_{p.75††}$ x10^3	RC_{25}	RC_{75}	AWC_{25}	AWC_{75}
		mm y^{-1}		mm h^{-1}	d	mm	m^3 s^{-1}	m^3 s^{-1}	%	%	%	%
04.05	IR	279	15	3.97	7	57	3.3	24.1	5.8	25.5	56.1	81.1
	UC					59	4.2	23.5	5.9	29.9	37.6	62.0
05.06	IR	435	24	4.40	8	61	6.6	21.9	10.8	18.5	56.7	80.5
	UC					64	6.5	25.5	11.8	21.1	41.6	65.1
06.07	IR	459	25	4.94	10	73	5.4	23.5	8.1	26.9	58.9	78.8
	UC					81	6.6	30.2	10.1	27.0	45.0	65.4
07.08	IR	300	20	5.32	7	47	2.5	14.6	4.5	21.4	47.1	80.4
	UC					52	3.7	16.1	5.8	21.0	32.9	65.4
08.09	IR	624	30	4.40	13	163	6.8	32.7	11.4	32.8	67.2	81.3
	UC					167	5.8	34.0	10.4	30.5	45.7	66.1
09.10	IR	986	52	5.24	25	337	7.2	25.5	12.4	33.7	74.7	85.0
	UC					323	7.1	35.2	12.5	31.8	58.3	70.8
10.11	IR	662	38	5.06	16	139	10.4	27.1	11.6	29.3	65.5	83.3
	UC					148	9.2	34.1	13.8	28.0	44.6	68.1
11.12	IR	333	18	5.49	7	104	4.5	21.3	9.0	23.3	54.8	75.2
	UC					101	5.4	26.1	7.5	24.9	37.5	55.7
12.13	IR	1089	46	4.87	45	405	7.7	47.0	13.6	44.4	69.7	83.8
	UC					420	7.1	51.9	12.3	43.7	53.3	69.5

†: annual number of events; ‡: annual mean intensity using the I_{max} during 1 hr; ††: 25^{th} and 75^{th} percentile respectively; DOR: accumulated annual time of rain expressed in days.

wettest year was 405 mm yr^{-1} at IR and 420 at UC, respectively. This runoff was six times higher than for the driest year, with runoff discharges of 57 and 59 mm yr^{-1} at IR and at UC.

The relative accumulated monthly rainfall and runoff at IR for the 9 years is plotted in Fig. 7.4. A similar pattern was found at UC. Years 2004-2005, 2007-2008 and 2011-2012 were moderately dry, with an annual rainfall below 400 mm yr^{-1}. Nevertheless year 2007-2008 was unusually dry during the autumn-winter period.

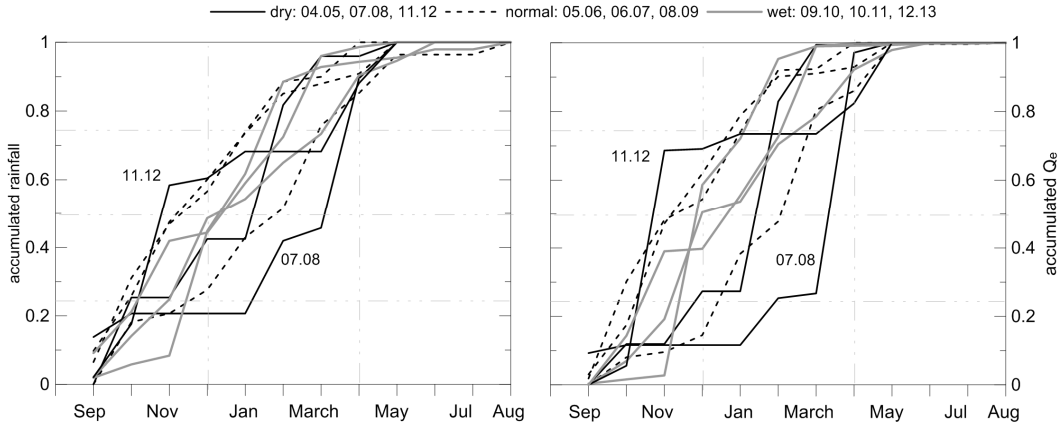

Fig. 7.4. Accumulated temporal pattern of annual rainfall and water loss, Q_e, for the long-term simulation, differencing years with low annual rainfall (continuous line in black colour), average (dashed black line) and years with high annual rainfall (continuous grey line), for inter row, IR.

The rain period was usually from October to April, and the runoff was concentrated only in a few of these events. December and February accumulated the major percentage of rainfall and runoff, with values of 30% and 35% respectively during the two months. This pattern was influenced by the characteristics and the temporal distribution of the rainfall during the year. While April 2008 (year 07.08) accumulated 44% of annual rainfall, the relative contribution to annual runoff was 70%. Similar trends were observed for December 2009, year 09.10 (rainfall, 36% and runoff, 56) and November 2011, year 11.12 (41 and 63%). This result indicates the higher erosion risk of these months.

The 268 rainfall events were decreasingly ordered according to the runoff coefficient. Fig. 7.5 compares the cumulative runoff and rainfall. The results showed that 30% of the events generated 54% of the total rainfall and 80% of runoff. Fifty percent of the events concentrated 28% of the rainfall and produced 10% of the total runoff.

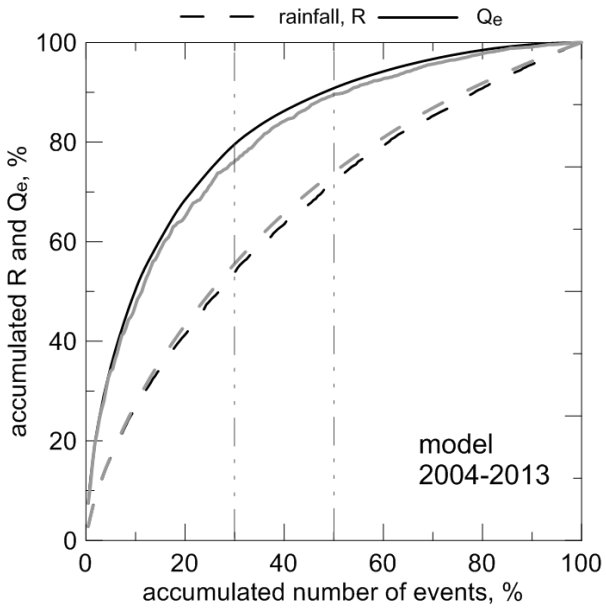

Fig. 7.5. Rank accumulated events decreasingly ordered according to their contribution to simulate runoff (black lines) and rainfall depth (grey lines) versus accumulated rainfall per event (dashed lines) and runoff (continuous lines) obtained for each event criteria ordering. Data used correspond to the 268 events simulated for 2004-2013 period, at inter row, IR, simulation.

The relationship between observed rainfall and runoff is explored in Fig. 7.6 using simulated data for the 2004-2013 period and observations for selected events of the 2011-2013 period. As we expected due to the method used, runoff curve number, a clear linear relationship was observed between observed rainfall and accumulated runoff for the 268 events simulated and for the observations used in the model calibration. The dependence was less precise in the case of rainfall-peak flow relationship. Both observed and estimated Qe and Qp showed that the rainfall threshold for producing surface runoff at the end of catchment was 10 mm, and events upper than 40 mm were unusual.

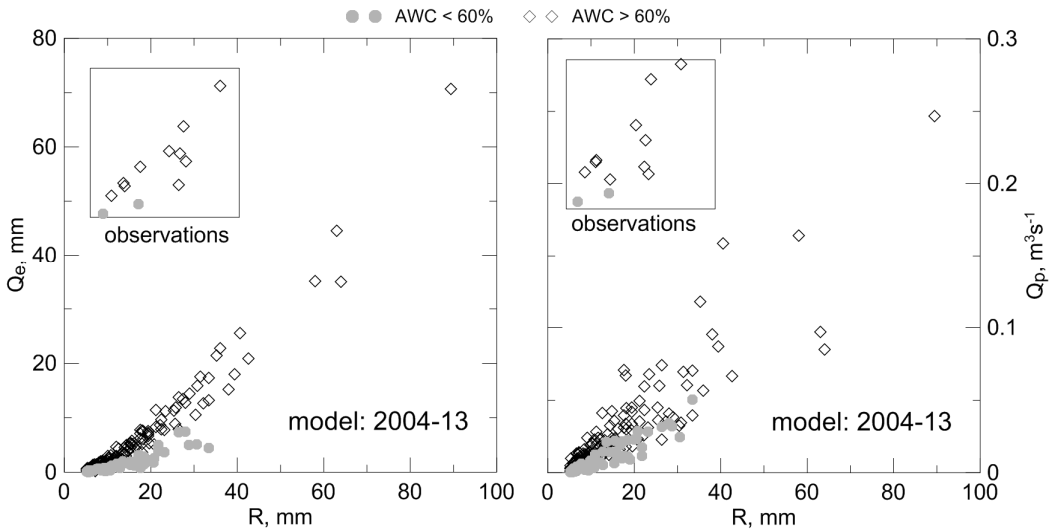

Fig. 7.6. Observed rainfall event versus estimate runoff discharge (left, accumulated, and right, peak flow) of 268 events modelled for 2004-2013 period (large figures), and 12 events observed during 2011-2013 (small figures inserted inside), differencing two levels of relative antecedent soil water content, AWC. Data correspond at inter row, IR, simulation.

Although the minimum threshold for producing runoff discharge depend of soil type, the value estimated was well below to others found in literature (*e.g.* 54 mm was found at Panola catchment, Tromp-van Meerveld and MCDonnell (2006); and between 16 to 27 mm at Maimai, Graham et al. (2010)), and similar to obtained by Detty and McGuire (2010). The slope of the relationship was influenced by the antecedent soil water content, reinforcing its role in RR relations, as highlighted Graham and MCDonnnell (2010) using synthetic data series with the model developed and calibrated at Maimai catchment (maimodel).

7.5. Conclusions.

The MISDc model was used to analyze the influence of tree canopies on the catchment rainfall-runoff relationship, and this reproduced ten minute catchment runoff response to rainfall events with a Nash and Sutcliffe efficiency near 0.70. The model performed generally better in reproducing accumulated runoff events, Q_e, than peak flow, Q_p. The model was successful in reproducing spatial mean soil water content with coefficients

of determination, R^2, ranging from 0.90 at IR to 0.85 at UC. No significant differences between IR and UC were found for runoff estimation.

The simulation and analysis of long-term rainfall-runoff data provided information on the inter-annual rainfall-runoff pattern and on the relative contribution of individual events, and a mean runoff ratio of 20% was observed, in agreement with the observations used for model calibration. Fifty percent of the events accumulated 28% of rainfall, of which only 10% caused runoff.

This work highlights the important control of soil water on rainfall runoff relations, and the influence of vegetation, which must be further addressed in future work. Overall the use of a simple model and data from instrumented catchments are useful tools to improve our knowledge about important hydrological processes at the catchment scale.

7.6. References.

Brocca, L., F. Melone, and T. Moramarco. 2011. Distributed rainfall-runoff modelling for flood frequency estimation and flood forecasting. Hydrol. Proc. 25, 2801-2813.

Brocca, L., F. Melone, T. Moramarco, and V.P. Singh. 2009. Assimilation of observed soil moisture data in storm rainfall-runoff modeling, J. Hydrol. Eng. ASCE 14, 153–165.

Brocca, L., F. Melone, and T. Moramarco. 2008. On the estimation of antecedent wetness condition in rainfall-runoff modelling. Hydrol. Proc. 22, 629–642.

Camici, S., A. Tarpanelli, L. Brocca, F. Melone, and T. Moramarco. 2011. Design soil moisture estimation by comparing continuous and storm-based rainfall-runoff modelling. Water Resour. Res. 47, W05527, doi:10.1029/2010WR009298.

Detty, J.M., and K.J. McGuire. 2010. Threshold changes in storm runoff generation at a till‐mantled headwater catchment. Water Resour. Res. 46, W07525, doi:10.1029/2009WR008102.

Espejo, A.J., J.V. Giráldez, K. Vanderlinden, E.V. Taguas, and A. Pedrera. 2014. A method for estimating soil water diffusivity from moisture profiles and its application across an experimental catchment. J. Hydrol., 516, 161-168.

Fitzjohn C., J.L. Ternan, and A.G. Williams. 1998. Soil moisture variability in a semi-arid gully catchment: implications for runoff and erosion control. Catena 32, 55-70.

Graham, C.B., J.J. McDonnell, and R. Woods. 2010. Hillslope threshold response to rainfall: (1) a field based forensic approach. J. Hydrol. 393, 65-76.

Graham, C.B., and J.J. McDonnell. 2010. Hillslope threshold response to rainfall: (2) Development and use of a macroscale model. J. Hydrol. 393, 77-93.

Gupta, V.K., E. Waymire, and C.T. Wang. 1980. A representation of an instantaneous unit hydrograph from geomorphology. Water Resour. Res. 16, 855–862.

Hrachowitz, M., H.H.G. Savenije, G. Blöschl, J.J. McDonnell, M. Sivapalan, J.W. Pomeroy, B. Arheimer, T. Blume, M.P. Clark, U. Ehret, F. Fenicia, J.E. Freer, A. Gelfan, H.V. Gupta, D.A. Hughes, R.W. Hut, A. Montanari, S. Pande, D. Tetzlaff, P.A. Troch, S. Uhlenbrook, T. Wagener, H.C. Winsemius, R.A. Woods, E. Zehe, and C. Cudennec. 2013. A decade of Predictions in Ungauged Basins (PUB)-a review. Hydrol. Sci. J. 58, 1198-1255.

Kim, N.W., and J. Lee. 2008. Temporally weighted average curve number method for daily runoff simulation. Hydrol. Proc. 22, 4936–4948.

Majone, B., A. Bertagnoli, and A. Bellin. 2010. A non-linear runoff generation model in small Alpine catchments. J. Hydrol. 385, 300-312.

Massari, C., L. Brocca, S. Barbetta, C. Papathanasiou, M. Mimikou, and T. Moramarco. 2013. Using globally available soil moisture indicators for flood modelling in Mediterranean catchments. Hydrol. Earth Syst. Sci. Disc. 10, 10997–11033.

Melone, F., C. Corradini, and V.P. Singh. 2002. Lag prediction in ungauged basins: An investigation through actual data of the upper Tiber River valley. Hydrol. Proc. 16, 1085–1094.

Melone, F., N. Neri, R. Morbidelli, and C. Saltalippi. 2001. A conceptual model for flood prediction in basins of moderate size. In: Applied simulation and modelling. Hamza, M.H. (Eds.). 25, 461–466, California: IASTED Acta Press, 2001.

Nash, J.E., and J.V. Sutcliffe. 1970. River flow forecasting through conceptual models, part I: A discussion of principles. J. Hydrol. 10, 282-290.

Sivakumar, B. 2008. The more things change, the more they stay the same: the state of hydrologic modelling. Hydrol. Proc. 22, 4333–4337.

Soulsby, C., C. Neal, H. Laudon, D.A. Burns, P. Merot, M. Bonell, S.M. Dunn, and D. Tetzlaff. 2008. Catchment data for process conceptualization: Simply not enough?, Hydrol. Proc. 22, 2057-2061.

Spence, C. 2010. A paradigm shift in hydrology: storage thresholds across scales influence catchment runoff generation. Geogr. Comp. 4, 819-833.

Tromp-van Meerveld, H.J., and J.J. McDonnell. 2006. Threshold relations in subsurface stormflow: 2. The fill and spill hypothesis. Water Resour. Res. 42, W02410, doi:10.1029/2004WR003778.

Zhang, Y., H. Wei, and M.A. Nearing. 2011. Effects of antecedent soil moisture on runoff modelling in small semiarid catchments of southeastern Arizona. Hydrol. Earth Syst. Sci. Disc. 8, 6227–6256.

Chapter 8

Detection of runoff flow patterns within an experimental catchment by using information of a soil water sensor network

8.1. Abstract.

Soil water movement across catchments plays an important role in agriculture and environmental systems. Therefore, runoff data measured at the outlet of instrumented agricultural catchments are becoming increasingly available. Nevertheless the surface flow within of them can often neither be measured, nor the influence of vegetation on it be detected. We might overcome this limitation by using high frequency measurementss from a soil water sensor network to estimate infiltration, and from it runoff through a water balance considering rainfall and evaporation. The aim of this work is to characterize the infiltration and runoff within a small catchment of olives.

Measurements were made in a 6.7-ha experimental catchment in SW Spain cropped with olives. Rainfall was recorded in an automatic weather station nearby while runoff was measured at the outlet. The water content at the soil profile was evaluated at eleven locations, with two sites each, one under the canopy, UC, an other in the alley between tree lines, IR, distributed in the catchment by using capacitance techniques at 10 minutes temporal resolution.

Soil water content during the year was greater at inter-row areas than under the tree canopy. However the estimated event water storage increment was lower at inter-row than under canopy. The spatial pattern of soil recharge during rain pulses at the two locations, inter row and under canopy, was similar, with an increasing event water

storage increment trend at downslope areas, close to the gully channel. Estimated runoff was greater at inter-row sites than under canopy, although the differences were not statistically significant at all locations. No consistent pattern was found for runoff at UC, and was observed a negative correlation with clay content and maximum water storage capacity. At IR a clearer pattern for estimated runoff was found and was negatively correlated with the wetness topographic index, indicating that upper areas of catchment produced higher runoff volumes. These locations were place at the south-easthern part of catchment, where the slope was longer. Although the method has limitations in space, it can be used to understand the catchment hydrology.

8.2. Introduction.

The frequent dry periods in semiarid areas, interspersed with irregular rain bursts, make effective water control difficult in Agricultural and urban settings, and complicate landscape planning. The rainfall-runoff response of a catchment depends on the soil water dynamics (Hrachowitz et al. 2013). In some cases (Camici et al. 2011) a simple probabilistic model can be adopted to generate soil water content data. In other cases soil water can be estimated through remote sensing (Massari et al. 2013). Abrahams et al. (2003), Bhark and Small (2003), and Ludwig et al. (2005), among others, described the interaction of vegetation with runoff and erosion, originating oases of soil water content under the canopy as a consequence of a higher infiltration rate. The influence of the antecedent soil water content on runoff generation in this catchment has been discussed in Chapter 6.

The objective of this chapter is to compare water infiltration under the canopy and at inter row areas, to detect spatial runoff patterns within the catchment.

8.3. Materials and methods.

8.3.1. Study site and data acquisition.

Data were collected in the Setenil experimental catchment, described in section 2.2. In addition to this information, relevant topographic indices like the Topographic Wetness Index, TWI, of Beven and Kirkby (1979) were calculated (Table 8.1). Locations 6 and 7 show the highest TWI values of the catchment. The northern part of the catchment showed steeper slopes, although with a shorter slope length than in the southern part. Differences in relative elevation between adjacent IR and UC locations were due to small mounds surrounding the olive trees (Fig. 2.5), mostly notable at locations 1, 5, 6 and 7, in the vicinity of the outlet of the gully. The average maximum estimated soil water storage was similar at IR and UC, with a mean value of 117 mm (see section 3.2). Despite apparently similar soil depths (Table 2.3), differences between maximum water storage at IR and UR were prominent, 72 at location 1 and 47 mm at location 7, respectively.

Table 8.1. Summary of the topographic indices and maximum water storage, S_{max}, for inter row, IR, and under canopy, UC, of olive trees. Slope, average slope of grid cells around the measurement location; TWI, topographic wetness index; h, relative elevation with respect to the catchment outlet.

			IR	UC	IR	UC
	slope	TWI	h		S_{max}	
location	[%]	[ ]	m		mm	
1	8.3	5.5	4.7	5.4	182	110
2	7.3	5.4	15.5	15.2	70	76
3	7.0	4.3	22.3	21.9	132	106
4	5.7	4.9	13.7	14.2	78	97
5	7.7	6.4	19.1	19.9	163	129
6	6.5	7.5	25.8	26.5	145	167
7	6.0	7.1	29.3	30.2	185	138
8	6.7	3.7	35.4	35.6	51	90
9	3.7	6.4	36.4	36.6	96	126
10	2.4	3.2	39.0	38.8	88	121
11	1.8	3.0	41.2	41.1	88	131
average	5.7	5.2	25.7	26.0	116	117

8.3.2. Selection of rainfall event.

Only events with a minimum total rainfall depth of 5 mm were retained. Inter-event periods lasted at least 6 hours (Hershfield, 1963) and produced less than 2 mm rainfall. The used data corresponds to the period from September 1, 2011 to May 31, 2013. A wet period from December 2010 to January 2013 was chosen for a detailed analysis of

the runoff process. During the selected period rainfall depth ranged from 5.0 to 56.4 mm, with an average of 17.4 mm. Event rainfall intensity ranged from 1.3 to 4.5 mm h^{-1}, with an average of 1.5 mm h^{-1}.

8.3.3. Soil water budget.

A simple soil water balance was adopted,

$$Q = R - \Delta S - ET \qquad \text{Eq. (8.1)}$$

where Q represents runoff, R rainfall, ΔS event soil water storage increment (estimated infiltration), and ET evapotranspiration per event. Reference ET was computed by using the Penman-Monteith method, and actual evapotranspiration was estimated introducing a crop coefficient of 0.45 and 0.70 at IR and UC, respectively, according to chapter 6. Event soil water storage increment was estimated as the difference between the soil water storage after and before of the event.

To estimate the soil water storage, ΔS, at each sample point, measured soil water profiles were interpolated using natural cubic splines (*e.g.* Press et al. 2007, section 3.3). At locations where the soil profile was deeper than 0.50 m, the soil water content below 0.50 m was assumed equal to the value measured at 0.40-0.50 m. Hence the soil water storage was estimated for complete horizons at for different soil depths intervals to avoid the effect of differences in maximum soil depth between IR and UC in the same measurement location (*i.e.* 0-0.20, 0-0.30 and 0-0.30 m).

8.3.4. Statistical analysis.

A one-way ANOVA was used to evaluate the influence of location (IR and UC) on the event water storage increment process. Means for different soil horizons and complete profile at IR and at UC for each measurement location were compared using the least significant difference.

Principal components, PCs, were calculated from the estimated runoff at each location across the collected rainfall events determining the common spatial pattern (Davis, 2002). The Pearson product-moment correlation coefficient was used to evaluate the influence of soil properties on runoff generation across the calculated PC_s.

8.4. Results and discussion.

8.4.1. Temporal evolution of soil water content during the year.

Measured soil water content was higher at IR than at UC for most of the two-year monitoring period. The soil remains generally dry throughout the year due to a pronounced drought period from June to September, extending to December during some years. A typical temporal soil water content evolution at IR and UC during a rainfall event is shown in Fig. 8.1. Similar trends were observed at all locations. In general, differences in soil water content between UC and IR are most significant after the rainfall event, during the drying period.

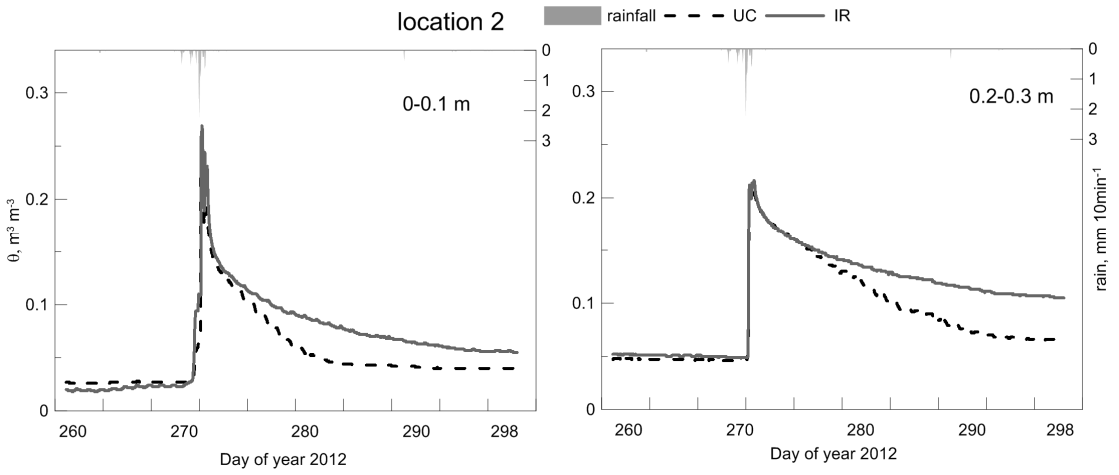

Fig. 8.1. Temporal evolution of measured soil water content at depths of 0-0.1 and 0.20-0.30 m in the inter-row area, IR, and under the olive tree canopy, UC, at location 2.

According to Espejo et al. (2014) the faster drying of the soil at UC as compared to IR can be explain by the lower soil water retention at UC. Similar results were found by Joffre and Rambal (1993) under Mediterranean evergreen oak trees located not far from

this catchment. They attributed these differences to the higher suction and evaporative losses beneath canopies. Also Moran et al. (2010) observed that soil water content was lower at UC as compared to IR in scrubland. However, under similar conditions for the same plant species Bhark and Small (2003) reported that under canopies of grassland and shrubs frequently a higher soil water content was found as result of higher infiltration. Potts et al. (2010) found greater soil water beneath canopies of a mesquite canopy than at adjacent areas, and the differences increased with soil depth.

8.4.2. Event water storage increment at IR and at UC.

The results of the ANOVA to detect differences in event water storage increment between IR and UC at the eleven locations and for different soil horizons are displayed in Table 8.2. In 31 out of 66 occasions event water storage increment was higher at IR as compared to UC. Only for 4 cases was the event water storage increment at IR significantly larger ($p=0.05$). The event water storage increment at IR was lower than at UC in 28 cases, of which 22 were significant ($p<0.05$). The analysis for all locations indicated a greater event water storage increment at UC compared to IR for all soil depths. The most notable differences between event water storage increment at IR and UC areas were observed at 0.10-0.20 m interval. The soil bulk density was generally higher at IR at this depth as a result of soil compaction due to intensive tillage (*e.g.* Ordóñez-Fernández et al. 2007).

Locations 1, 2, 3, 6 and 7, near the gully channel, presented a greater event water storage increment at IR as compared to UC. The remaining locations showed the opposite. At location 9 differences between intervals was found in the comparisons. This locations was near a path to access the olive field, with compacted soil surface layers. Locations 10 and 11 within the frequently tilled are with young trees in the southeastern part of the catchment (Fig. 2.3).

Table 8.2. ANOVA α-values for the comparison of estimated event water storage increment at inter row, IR, and at under canopy, UC, of olive trees, for the eleven locations, using different representative depth intervals for 33 selected rainfall events. Bold faces remark the statically significant ($p<0.05$) differences. Positive values between parentheses indicate greater event water storage increment at IR compared to UC site, while negative values stand for the opposite.

location	entire soil profile	0-0.10 m	0.10-0.20 m	0.20-0.30 m	0-0.20 m	0-0.30 m
1	-	.858 (+)	.162 (+)	.332 (+)	.646 (+)	.636 (+)
2	.119 (+)	**.012 (+)**	.526 (+)	.584 (+)	.064 (+)	.119 (+)
3	.097 (+)	.073 (+)	.050 (+)	.655 (+)	.064 (+)	.151 (+)
4	.526 (-)	**.000 (-)**	.544 (-)	**.000 (+)**	**.005 (-)**	.527 (+)
5	**.036 (-)**	**.000 (-)**	**.034 (-)**	**.000 (-)**	**.000 (-)**	**.000 (-)**
6	-	-	.524 (+)	.938 (+)	-	-
7	.069 (+)	**.014 (+)**	.516 (+)	.637 (+)	.065 (+)	.134 (+)
8	**.004 (-)**	.803 (-)	**.000 (-)**	-	.087 (-)	-
9	.261 (+)	**.005 (+)**	**.015 (-)**	.095 (+)	.946 (-)	.527 (+)
10	**.000 (-)**	**.000 (-)**	**.001 (-)**	.364 (-)	**.000 (-)**	**.002 (-)**
11	**.000 (-)**	**.000 (-)**	**.000 (-)**	**.000 (-)**	**.000 (-)**	**.000 (-)**
all locations	.053 (-)	.303 (-)	**.000 (-)**	.538 (-)	**.004 (-)**	.092 (-)

The relationship between event water storage increment in the 0-0.20 m interval and rainfall depth at IR and UC is presented in Fig. 8.2. Except for the largest rainfall depths, event water storage increment appeared to reach a maximum near 16 mm at both IR and UC, corresponding to a threshold rainfall depth near 17 mm, beyond which event water storage increment does not further increase with increasing rainfall. Locations farther away from the gully, showed clearly higher event water storage increment at UC as compared to IR, especially for rainfall depth larger than 17 mm.

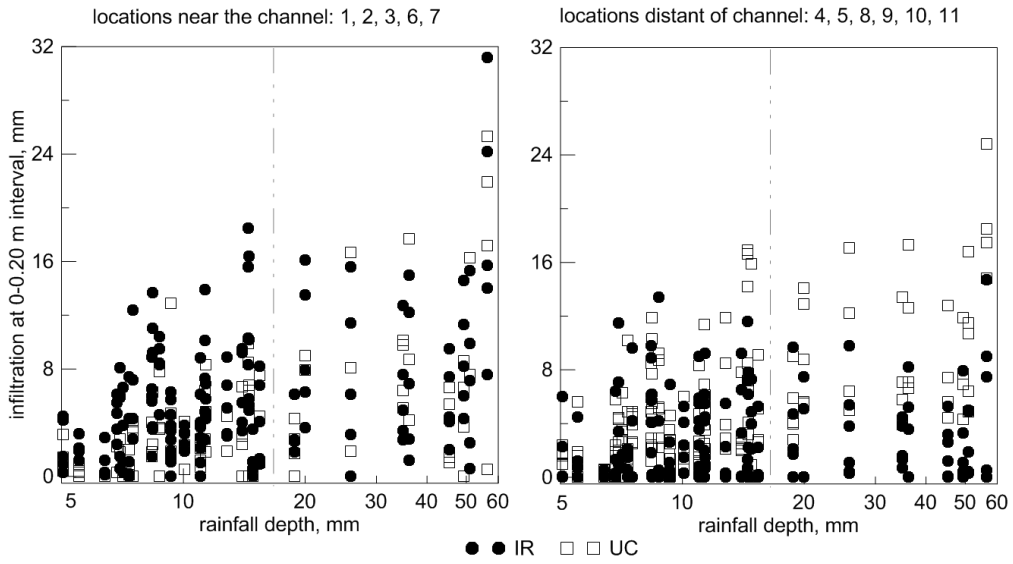

Fig. 8.2. Relationship between event water storage increment and rainfall depth at inter row areas, IR, and under the tree canopies, UC, for locations nearby and further away from the central gully.

These results agree with findings of Gómez et al. (1999) for an olive orchard under different soil managements, with greater infiltration beneath the canopy than at IR areas. They also found that infiltration at UC was not greater than at IR when rainfall was limited. Moran et al. (2010) also compared infiltration at IR and UC in shrub and found that root zone (0-0.30 m) infiltration was not significantly different. In addition, they found that the ratio of infiltration UC:IR was not related with rainfall depth or intensity, as also was observed by Bhark and Small (2003). The stems of grasses and shrubs channel part of the intercepted water towards the central roots. This pattern is not as evident in olive trees with different vertices pointing downwards within their canopies.

The rainfall event collected on March 19, 2013, is shown in Fig. 8.3. The total rainfall depth was 36.2 mm, and the runoff depth was 19.2 mm. The runoff ratio was 0.53, which was more elevated than annual average ratio, 0.20. The peak flow corresponded in time with the maximum rainfall pulse, and occurred at about 500 minutes after the rain began

A detailed analysis of the water storage increment during a short time during a characteristic event is represented in Fig. 8.4 for locations 2 and 4, which are nearby and further away from the gully, respectively. In a short time the rainfall depth increased by

1.5 mm, and the increment of soil water in the first 0.20 m was higher than rainfall at location 2, near at the channel, with values of 7.8 mm at IR and 4.6 mm at UC. However, the values of event water storage increment estimated at location 4 were lower than rain, with values of 0.6 and 0.0 mm at IR and at UC, respectively.

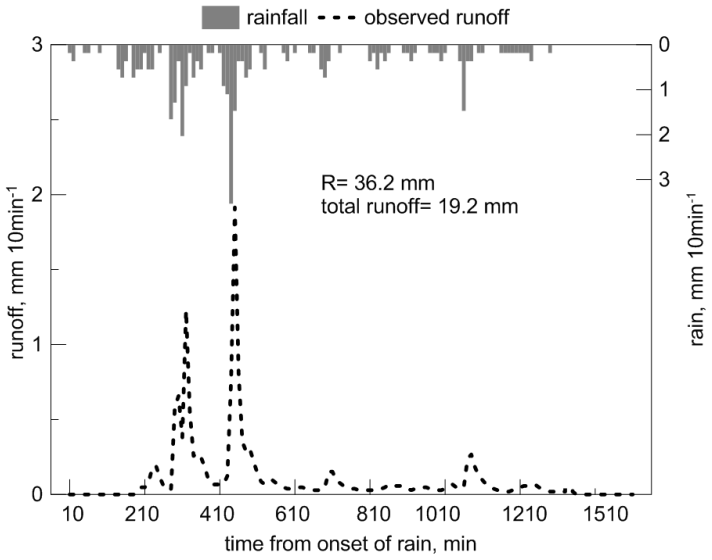

Fig. 8.3. Hyetograph and hydrograph for the flood event of March 19, 2013.

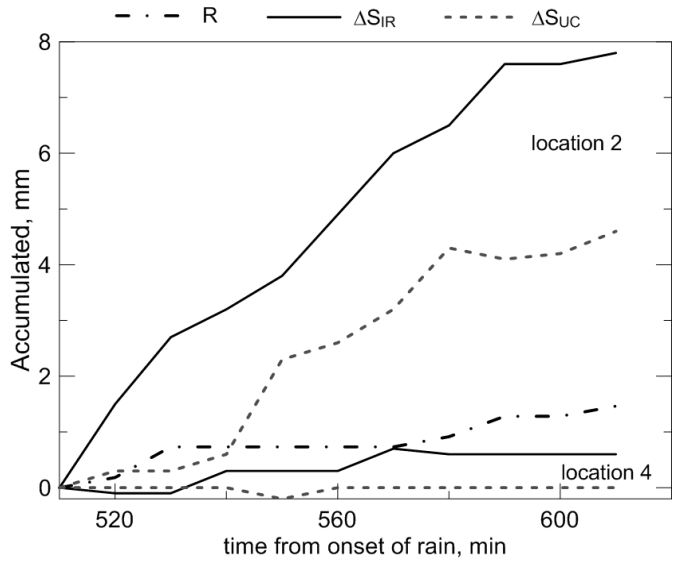

Fig. 8.4. Cumulative rainfall, R, and water storage increment, ΔS, in the 0-0.20 m horizon at locations 2 and 4 during the rainfall event shown in Fig. 8.3, at inter row, IR, areas and under the canopy, UC.

8.4.3. Spatial patterns of water storage increment and runoff.

A similar spatial water storage increment pattern was observed within the catchment at IR and at UC, during the different rain events The temporal evolution of water storage at the 11 locations for the event described in previous section is shown in Fig. 8.5, separately for IR and UC. Locations 1, 5, 6 and 7 had the maximum water storage rate with values ranging from 100 to 160 mm at both locations. The ratio between the water storage and the maximum water storage, S/S_{max}, indicates that soil was near saturation, with an average value of 0.84 at IR and 0.68 at UC, respectively. Location 2, 4 and 9, with low values of S_{max}, showed the lowest antecedent soil water content at both, IR and UC. In general the antecedent soil water content was lower at UC in comparison to IR, and can be explained by the higher capacity of soil water transmissibility and by the tree transpiration at UC area (Espejo et al. 2014).

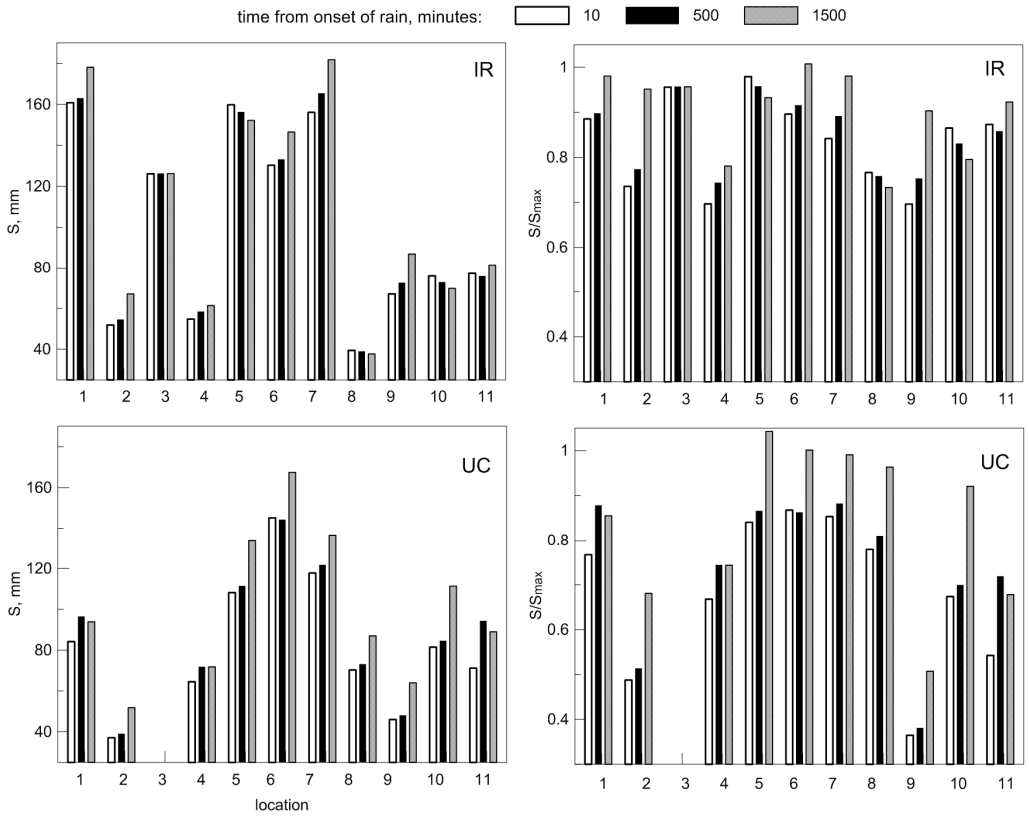

Fig. 8.5. Temporal evolution of profile water storage, S, (left) and the S/S_{max} ratio (right) for the rainfall event shown in Fig. 8.3, at the 11 measurement locations, for both inter row, IR, and under canopy, UC, areas.

The water storage increment with time is shown in Fig. 8.6 (left) for IR and UC. Both figures indicate that soil response to intense rain pulses is fast, as seen for the 500-750 min interval. Cumulative rainfall of event was 23.7 mm after 500 min, and only 3.7 mm between 500 and 750 minutes.

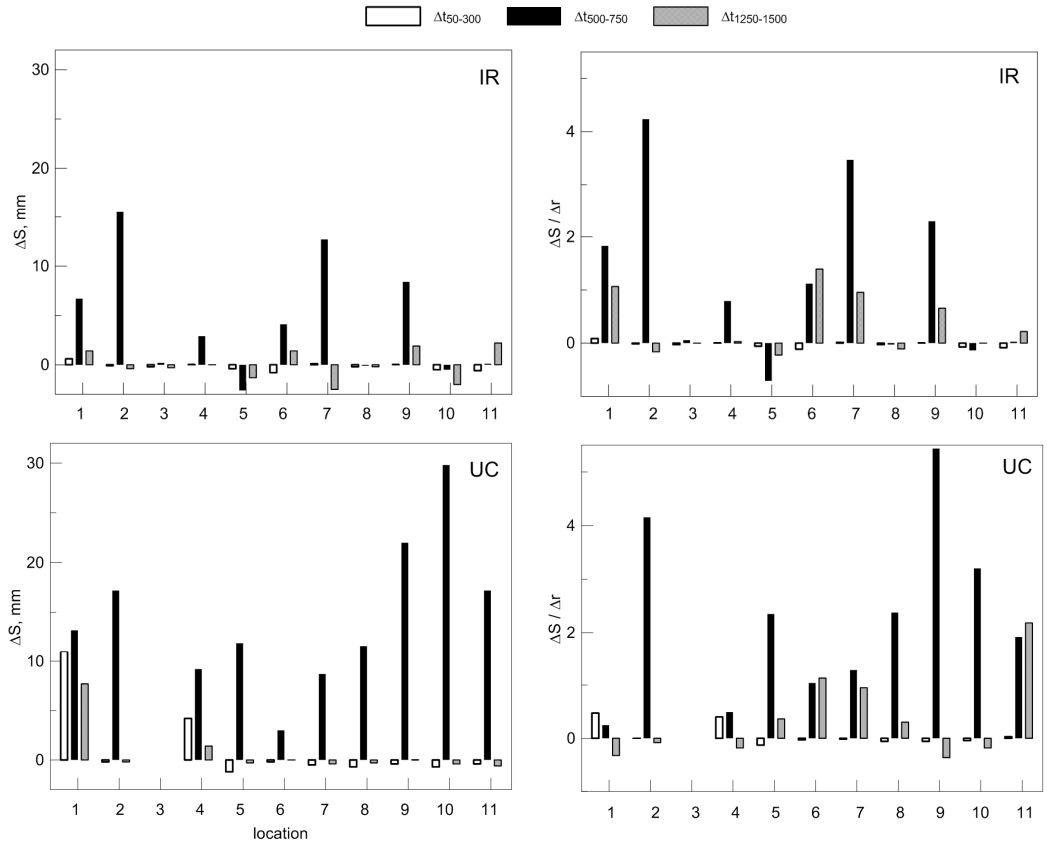

Fig. 8.6. Temporal evolution of profile water storage increments (left), ΔS, and ratio between ΔS and the rainfall increment, Δr (right) for the 11 locations at inter row, IR, areas and under the canopy, UC, for the event shown in Fig. 8.3.

In general the increments were greater at UC in comparison with IR. The increment was more pronounced for IR at locations 2, 7, 9 and 1, close to the gully channel. Increments at UC were higher than at IR at locations 10, 9, 2 and 11. Figures on the right show the ratio between the soil water and rain increments. Locations 2 and 7 at IR, and locations 9, 2 and 10, at UC, had a ratio greater than one. In general these locations were located in lower areas, indicating that they received water from upslope areas. Dunne et al. (1991) suggested that on longer hillslopes, in the absence of spatial trends affecting infiltration, ΔS/Δr increases downslope due to the presence of microtopographic depressions that induce hydraulic conductivity increases (*e.g.* Aryal et al. 2002). Also

the hydrologic active bedrock hypothesis reported by Sayama et al. (2011) indicated a saturated area near the drainage channel after rainfall as a result of run-on from upslope areas when the catchment soil was near saturation.

The common spatial pattern of runoff within the catchment was determined by calculating the PCs from the estimated runoff at each event at the eleven locations. The analysis was performed separately at IR and at UC. The variance of the first two PCA axes accounted for 85 and 7% for the first and second PC respectively at IR (Table 8.3). At UC the PC1 and PC2 explained 82 and 14% respectively. The contribution of the soil variables to each component extracted is summarised in Table 8.3. At IR the most consistent relationship was found with the topographic wetness index, TWI, showing a negative dependence with a value of 0.59 ($p<0.1$) for the correlation coefficient. A positive correlation was observed with the bulk density (0.59, $p<0.1$). In case of UC the analysis showed that PC1 had a negative correlation with the clay content, 0.90 ($p<0.05$), and with the maximum water storage, 0.82 ($p<0.1$); and a positive relationship was found ($p<0.1$) with slope gradient and relative elevation, with a value of 0.82 for both.

Table 8.3. Correlation coefficients between the principal component, PC, 1 and 2, calculated for the estimated runoff at each sample location, and average soil properties of the profile (see table 2.3), for inter rows, IR, and under canopy, UC, areas. In parenthesis is the total variance explained. h, relative elevation respect the lower sample point; TWI, topographic wetness index; Slope, average slope value for a grid cells around the sample point; S_{max}, maximum water storage; stone, percentage of stone.

		h	TWI	slope	S_{max}	θ_{sat}	clay	sand	ρ_b	stone	k_s
IR	PC1 (.85)	.18	-.59*	-.11	-.34	-.26	-.25	.33	.59*	.11	.47
	PC2 (.07)	-.04	.34	-.04	.10	.15	.29	.46	.16	.13	-.65*
UC	PC1 (.82)	.82*	.37	.82*	-.82*	.09	-.90**	.85*	.29	-.60	.04
	PC2 (.14)	.24	-.38	.24	-.38	.70	.04	-.23	-.30	-.29	-.41

* Significant at the 0.1 probability level.

** Significant at the 0.05 probability level.

The spatial distribution of PC1 values for the measurement locations is represented in Fig. 8.7. At IR, higher values of PC1 were observed in the south and south-eastern areas of the catchment. No consistent spatial pattern was found at UC for estimated runoff

because of the asymmetry between trees. The lower runoff yield at location 11 can be explained because there was a small depression near the tree stem. Moreover UC locations were downslope from the trunk northern of the gully channel, and upslope southern in the southern part. This asymmetry can affect the results because the relative position can increase the runoff flow at downslope areas and reduce it in upslope areas (Liang et al. 2011). However IR relative position from the trunk is always at upslope direction from the trunk, especifically in central part of preferential direction of runoff.

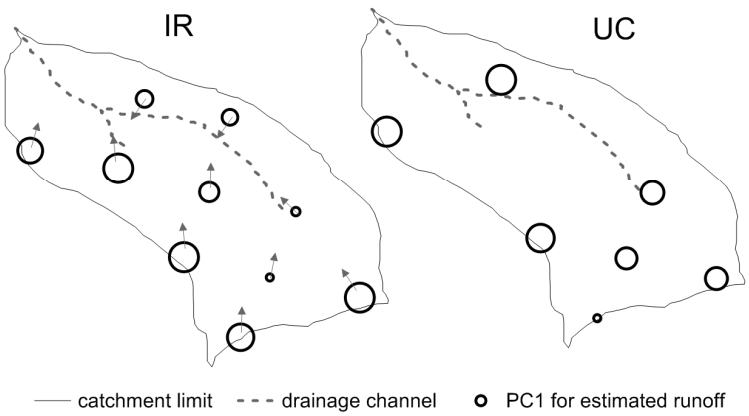

Fig. 8.7. Map of principal component 1 (PC1) at inter row, IR, and at under canopy, UC, locations, calculated from estimated runoff for events. The diameter of the circles is proportional to PC1 value and arrows indicate the runoff direction.

In general the total estimated runoff was lower at UC as compared to IR, Fig. 8.8, although the differences were not statistically significant at the 0.05 level. These results agree with the obtained by Castro et al. (2006) comparing the ratios between infiltration under olive canopies and at inter-row areas. For the event represented in Fig. 8.3, the estimated value was 17.4 ± 6.8 mm at UC and 27.6 ± 11.3 mm at IR, comparable with the runoff of 19.2 mm measured at the catchment outlet.

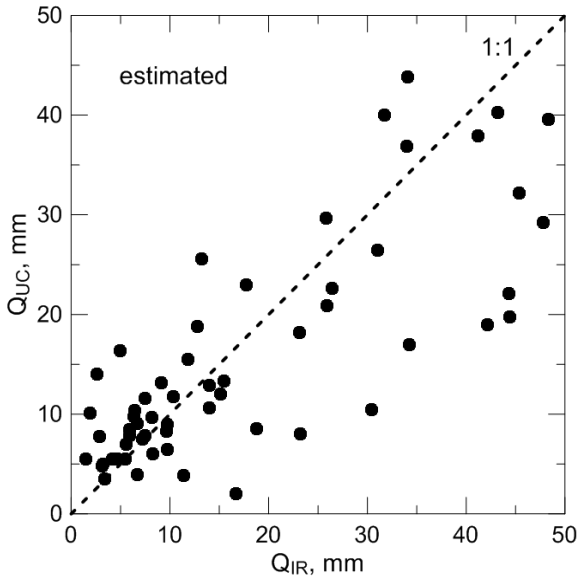

Fig. 8.8. Relationship between estimated runoff at inter row, IR, areas and under the canopy, UC.

8.5. Conclusions.

Intensive soil water observations allowed an estimation of the event water storage increment and runoff generation of several parts of a catchment planted with olives, and so investigate the runoff patterns within the catchment and the influence of trees. Soil water observations showed greater contents at inter-row areas compared than under the tree canopies. However the event water storage at inter-row was lower, although the differences were not significant in all sample locations. Hence, the estimated runoff was greater at inter row as compared to under canopy. The spatial pattern of event water storage increment during rain events at inter row and at under canopy of trees was similar, showing greater event water storage increments in areas close the gully channel. No consistent spatial pattern was found at under canopy for estimated runoff because of the asymmetry between trees. In general the runoff production was greater at the south-easthern part of catchment, where the slope was longer. These results illustrate that data provided by a soil water sensor network can be used to assess water flow at smaller scale than catchment.

8.6. References.

Abrahams, A.D., A.J. Parsons, and J. Wainwright. 2003. Disposition of rainwater under creosotebush. Hydrol. Proc. 17, 2555-2566.

Aryal, S., E. O'Loughlin, and R. Mein. 2002. A similarity approach to predict landscape saturation in catchments, Water Resour. Res. 38, 1208, doi:10.1029/2001WR000864.

Bhark, E.W., and E.E. Small. 2003. Association between plant canopies and the spatial patterns of infiltration in shrubland and grassland of the Chihuahuan desert, New Mexico. Ecosyst. 6, 185-196.

Camici, S., A. Tarpanelli, L. Brocca, F. Melone, and T. Moramarco. 2011. Design soil moisture estimation by comparing continuous and storm-based rainfall-runoff modelling. Water Resour. Res. 47, W05527, doi:10.1029/2010WR009298.

Castro, G., P. Romero, J.A. Gómez, and E. Fereres. 2006. Rainfall redistribution beneath an olive orchard. Agric. Water Manag. 86, 249-258.

Davis, J.C. 2002. Statistical and data analysis in Geology. 3rd ed. John Wiley Chichester, UK.

Dunne, T., W. Zhang, and B.F. Aubry. 1991. Effects of rainfall, vegetation, and microtopography on infiltration and runoff. Water Resour. Res. 27, 2271–2285.

Espejo, A.J., J.V. Giráldez, K. Vanderlinden, E.V. Taguas, and A. Pedrera. 2014. A method for estimating soil water diffusivity from moisture profiles and its application across an experimental catchment. J. Hydrol. 516, 161-168.

Gómez, J.A., J.V. Giráldez, M. Pastor, and E. Fereres. 1999. Effects of tillage method on soil physical properties, infiltration and yield in an olive orchard. Soil Till. Res. 52, 167-175.

Hershfield, D.M. 1963. Rainfall frequency atlas of the United States for duration from 30 minutes to 24 hours and return periods from 1 to 100 years. US Weather Bureau Techn. Pap. no.º 40, Washington, DC, USA.

Hrachowitz, M., H.H.G. Savenije, G. Blöschl, J.J. McDonnell, M. Sivapalan, J.W. Pomeroy, B. Arheimer, T. Blume, M.P. Clark, U. Ehret, F. Fenicia, J.E. Freer, A. Gelfan, H.V. Gupta, D.A. Hughes, R.W. Hut, A. Montanari, S. Pande, D. Tetzlaff, P.A. Troch, S. Uhlenbrook, T. Wagener, H.C. Winsemius, R.A. Woods, E. Zehe & C. Cudennec. 2013. A decade of Predictions in Ungauged Basins (PUB) - A review, Hydrol.l Sci. J.l 58, 1198-1255.

Joffre, R, Rambal, S. 1993. How tree cover influences the water balance of mediterranean rangelands. Ecol. 74:570-582.

Liang, W.L., K. Kosugi, and T. Mizuyama. 2011. Soil water dynamics around a tree on a hillslope with or without rainwater supplied by stemflow, Water Resour. Res. 47, W02541, doi:10.1029/2010WR009856.

Ludwig, J.A., B.P. Wilcox, D.D. Breshears, D.J. Tongway, and A.C. Imeson. 2005. Vegetation patches and runoff-erosion as interacting ecohydrological processes in semiarid landscapes. Ecol. 86:288-297.

Massari, C., L. Brocca, S. Barbetta, C. Papathanasiou, M. Mimikou, and T. Moramarco. 2013. Using globally available soil moisture indicators for flood modelling in Mediterranean catchments. Hydrol. Earth Syst. Sci. Disc. 10, 10997–11033.

Moran, M.S., E.P. Hamerlynck, R.L. Scott, J.J. Stone, C.D. Holifield Collins, T.O. Keefer, R. Bryant, L. DeYoung, G.S. Nearing, Z. Sugg, and D.C. Hymer. 2010. Hydrologic response to precipitation pulses under and between shrubs in the Chihuahuan Desert, Arizona. Water Resour. Res. 46, W10509, doi:10.1029/2009WR008842.

Ordóñez-Fernández, R., P. González-Fernández, J.V. Giráldez, and F. Perea. 2007. Soil properties and crop yields after 21 years of direct drilling trials in southern Spain. Soil Till. Res. 94, 47-54.

Potts, D.L., R.L. Scott, S. Bayram, and J. Carbonara. 2010. Woody plants modulate the temporal dynamics of soil moisture in a semi-arid mesquite savanna. Ecohydrol. 3, 20-27.

Press, W.H., S.A. Teukolsky, W.T. Vetterling, and B.P. Flannery. 2007. Numerical Recipes. 3rd ed. Cambridge Univ. Press. Cambridge, UK.

Sayama, T., J.J. McDonnell, A. Dhakal, and K. Sullivan. 2011. How much water can a watershed store? Hydrol. Proc. 25, 3899-3908.

Chapter 9

General conclusions and future research

9.1. General conclusions.

The general conclusions are outlined as answers to the research questions formulated in Chapter 1:

1) Is it possible to reduce soil and water loss to tolerable levels with a better soil management?

Yes.

Cover crops diminished soil losses on average by 76% with respect to conventional tillage in all the experimental plots. Water loss was also reduced on average by 22% with respect to conventional tillage in 6 out of 8 fields. The results showed also the large impact of the fraction of the soil surface covered on the observed reductions in soil loss and sediment yield. The positive effects of the runoff reduction on water storage can however be counteracted by the water consumption of the cover vegetation if not managed properly.

2) Can the erosive processes be expressed in a simple probabilistic form?

Yes.

A simple probabilistic framework is proposed to describe runoff and sediment yield in olive orchards in Mediterranean environments under cover crop and conventional tillage management systems. Using specific probability density functions for rain depth, slope, and fraction of the soil surface covered by vegetation, runoff and sediment yield can be simulated to extend the experimental results obtained with the microplots

3) Is it possible to make field estimations of soil hydraulic properties using high frequency *data series of soil water content?*

Yes, for a soil drying period.

A simple exponential relationship between the Boltzmann coordinate and the soil water content fitted the measured soil water profile data well, with the parameters reflecting the main characteristics of the soils across the catchment. Using a continuous function for the water retention characteristic, the method can be further extended to provide the hydraulic conductivity function. The method has been evaluated using soil water profile data observed at inter-row and under canopy locations across a rainfed olive orchard. A significantly different effective diffusivity relationship was found across the catchment between areas under the tree canopies and inter-row areas, reflecting the effect of trees on soil physical properties and water dynamics across olive orchards.

4) Can intensive soil water monitoring in combination with modelling be successfully used to characterize soil water dynamics in agricultural catchments?

Yes, the model performance depends on the field data accuracy.

Soil water modelling in combination with intensively monitored soil water content records allowed successful representation of the soil moisture dynamics at catchment scale and at specific locations at inter-row areas and under the tree canopies, with Nash-Sutcliffe efficiency indexes above 0.90. A better representation of soil moisture dynamics under the tree canopies was obtained by adding a simple expression for canopy interception to the model. A simple relationship between canopy interception and rainfall was found, with an average canopy interception ratio near 0.10 for the olives. Also the spatial distribution of the saturated hydraulic conductivity was inferred, with smaller values at inter-row areas as compared to areas beneath the canopies.

5) Which factors influence most catchment runoff?

A simple rainfall-runoff model reproduced the ten-minute runoff hydrograph measured at the catchment outlet and the spatial soil water dynamics well. Runoff was similar under the canopies as compared to the inter-row areas, although differences on soil water dynamics were detected. A clear influence of antecedent soil water content on catchment runoff was found, with a minimum threshold for soil moisture near 0.60. The annual average runoff ratio was 0.21, and 50% of the annual runoff was generated during a few storms, from December to March.

6) Is it possible to determine runoff flow patterns within catchments using intensive soil water observations?

Yes.

The proposed methods allowed evaluating infiltration and runoff generation below the olive tree canopies and at inter-row areas. The spatial recharge pattern during rain pulses was similar for both locations, with increasing event water storage increment towards downslope areas, nearby the gully. Event water storage increment was usually larger, and estimated runoff smaller, under the canopy as compared to inter-row areas, although soil water content was on average higher at the latter. The estimated spatial runoff pattern was influenced by the position within the catchment, generally with larger runoff at upslope locations.

This thesis remarks the usefulness of intensive field monitoring efforts, complemented with simple modelling approaches, to improve our knowledge of hydrological processes, including their main controls, and to assess possible soil management strategies. Chapters 3-4 show how soil protection using cover crops can help to reduce the severity of soil erosion in olive orchards, and how the involved processes can be represented in a simple probabilistic framework. Chapters 5-8 highlights the influence of olive trees on soil hydraulic properties controlling the soil water dynamics and how rainfall is split-up into runoff and infiltration.

9.2. Future research.

Further research should be conducted to integrate available runoff and sediment yield information, collected across different scales, into the proposed probabilistic framework, with the aim of reducing the uncertainty in their estimations. Extending this idea the soil moisture probability density function should be included, given that it is a key control for runoff generation and vegetation growth.

Currently, the sensor network is still operative and has been extended to monitor soil water content in different soil managements. In doing so, soil moisture records are becoming available under the tree canopies and at inter-row areas, for bare soil and

cover crop management. This will allow us to evaluate the influence of cover crops at both, under canopy and inter-row locations, on soil water dynamics and compare these results with those obtained for bare soil management, in order to adopt adequate crop cover management decisions.

Curriculum Vitae

Antonio Jesús Espejo Pérez

ajespejo@gmail.com
Soil scientist/ hydrologist
Ph. D. in Soil Science (en course)
Department of Agronomy, University of Cordoba (Spain).
Ctra Madrid km 396, 14071. Phone (+34) 957212241

EDUCATION

2011. M. Sci. in Environmental Hydraulics. Department of Agronomy, University of Cordoba (Spain). Topic: determination of hydrological and erosion patterns in agricultural watersheds.

2004. Bachelor degree in agricultural engineering. Higher Technical School of Agricultural Engineering, University of Cordoba (Spain). Topic Msc thesis: analysis of erosion and runoff in watersheds of olive orchard.

PROFESSIONAL EXPERIENCE

2010 - present. Ph. D. student at the Department of Agronomy of University of Cordoba, Spain.

2007 - 2009. Researcher at the Natural resources and Agroecology Department of the Andalusian Institute of Research and Training in Agriculture and Fishing, IFAPA. Seville, Spain.

2003 - 2007. Researcher at the Spanish Association of Soil Conservation and Living Soils, AEAC/SV. Cordoba, Spain.

RESEARCH INTERESTS

- Evaluation of in-situ soil moisture sensors.
- Soil moisture data assimilation techniques (Ensamble Kalman filter).
- Spatio-temporal variability of soil moisture in South Spain.
- Soil and water erosion process modelling.
- Soil and water conservation.

SCI - PUBLICATIONS

2014

Espejo, A.J., L. Brocca, K. Vanderlinden, T. Moramarco, and J.V. Giráldez. Soil moisture modelling in an olive-tree -planted catchment in Spain to identify spatial and temporal hydrological patterns. Unpublished, submitted to Geoderma on June 2014, 6.

Espejo, A.J., J.V. Giráldez, K. Vanderlinden, E.V. Taguas, and A. Pedrera. 2014. A method for estimating soil water diffusivity from moisture profiles and its application across an experimental catchment. J. Hydrol., 516: 161-168.

2013

A.J. Espejo-Pérez; A. Rodríguez-Lizana; R. Ordóñez; and J.V. Giráldez. Reduction of soil losses and runoff in olive-tree dry-farming with cover crops. Soil Sci. Soc. Am. J., 77: 2140–2148

2012

G. Martinez; K. Vanderlinden; Y.A. Pachepsky; J.V. Giraldez; and **A.J. Espejo**. 2012. Estimating topsoil water content of clay soils with data from time-lapse electrical conductivity surveys. Soil Sci., 177: 369-376.

2010

G. Martinez; K. Vanderlinden; J.V.Giraldez; **A.J. Espejo**; and J.L. Muriel. 2010. Field-scale soil moisture pattern mapping using electromagnetic induction. Vadose Zone J., 9: 871-881.

2008

A. Rodríguez-Lizana; **A.J. Espejo-Pérez**; P. González-Fernández; and R. Ordóñez-Fernández. 2008. Pruning Residues as an Alternative to Traditional Tillage to Reduce Erosion and Pollutant Dispersion in Olive Groves. Water, Air, & Soil Pollution, 193: 165-173.

2007

R. Ordóñez; A. Rodríguez-Lizana; **A.J. Espejo-Pérez**; P. González-Fernández; and M.M. Saavedra. 2007. Soil and available phosphorus losses in ecological olive groves. European J. Agron., 27: 144-153.

A. Rodríguez-Lizana; R. Ordóñez; **A.J. Espejo-Pérez**; and P. González. 2007. Plant Cover and Control of Diffuse Pollution from P in Olive Groves. Water, Air & Soil Pollution, 181: 17-34.

RELEVANT NON-SCI PUBLICATIONS

2009

Espejo, A.J.; Vanderlinden, K.; Muriel, J.L.; Durán, V.H.; García, I.; Martínez, G. y Perea, F. 2009. Evolution of soil moisture during wetting-drying cycles in upland crops under two soil managements. AEAC, 13: 18-24.

García Tejero, I.; **Espejo Pérez, A.J.**; Martínez, G.; Vanderlinden, K.; Durán, V.H.; Muriel Fernández, J.L. 2009. Effects of tillage on the water retention curve of a soil under different soil managements. Vida rural, 297: 32-37.

Espejo Pérez, A.J.; Vanderlinden, K.; Infante, J.M.;Muriel Fernández, J.L. 2009. Use of capacitance probes to characterize the dynamics of water flow in irrigated strawberry. Vida rural, 295: 62-67.

2008

Márquez, F.; Giráldez, J.V.; Repullo, M.A.; Ordóñez, R.; **Espejo-Pérez, A.J.**; and Rodríguez, A. 2008. Efficiency of applying a crop cover system as a method of conserving soil and water in olive orchard. In: López-Geta; Rubio-Campos, J.C. and Martín-Machuca, M. (Eds.). Water and Culture of Water in Andalusia, Volume II: 631-641.

2007

Espejo-Pérez, A.J. 2007. A correct moment time of mowing the cover crops in dry-farming olive orchard. AEAC, 6: 22-24.

2006

Márquez, F.; Rodríguez-Lizana, A.; Giráldez, J.V.; and **Espejo-Pérez, A.J**. 2006. Evolution of soil moisture content in dry-farming olive orchard. Vida Rural, 236: 30-33.

Espejo-Pérez, A.J.; Márquez, F.; and Rodríguez-Lizana, A. 2006. Increasing of soil biodiversity in olive orchard using a conservationist soil management. Vida Rural, 236: 46-48 (2006)

PRESENTATIONS

- Analysis of the response of soil moisture content during a dry period pronounced. 2013. Congress of the unsaturated zone soil, ZNS'13. Lugo, Spain. Submitted for oral presentation (unconfirmed).
- Below-canopy versus inter-row soil water content dynamics across a rainfed olive orchard in SW Spain. 2013. EGU, Vienna. Submitted for oral presentation (unconfirmed).
- Methods for assessing soil moisture at plot and basin scales. 2012. Symposium of Water Resources in Andalusia, SIAGA'12.
- Management and soil conservation practices: application of conservation agriculture techniques. 2012. University of Cordoba, Spain.
- A probabilistic water erosion model for Mediterranean olive orchards with changing cover factor. 2012. EGU, Vienna.
- Application in Spain area of Common Agricultural Policy. 2010. University of Seville, Spain.
- Runoff and erosion processes in the olive groves of Andalusia. 2008. University of Cordoba, Spain.
- Comparison of different ways to express runoff and sediment yield measured in micro-plots. 2007. Congress of the unsaturated zone soil, ZNS'07. Cordoba, Spain.

- Assessing the degree of soil protection against erosion processes with cover crops in olive orchard. 2007. European Conference on Agriculture and Environment. Seville, Spain.

POSTERS

- 2014. A virtual lab environment for improving students' understanding of infiltration and runoff processes. HIC 2014, New York City, USA
- 2014. Use of electromagnetic induction surveys to delimit zones of contrasting tree development in an irrigated olive orchard in Southern Spain. European Geosciences Union, EGU. Vienna.
- 2014. Influence of Soil Management on Water Retention from Saturation to Oven Dryness and Dominant Soil Water States in a Vertisol under Crop Rotation. European Geosciences Union, EGU. Vienna.
- 2014. Detection of subsurface runoff flow with soil water sensor network in an experimental catchment. European Geosciences Union, EGU. Vienna.
- 2014. Geophysical surveys combined with laboratory soil column experiments to identify and explore risk areas for soil and water pollution in feedlots. European Geosciences Union, EGU. Vienna.
- 2013. Soil WATER modelling in a rainfed olive orchard catchment of Spain to identify spatial and temporal hydrological patterns. Florisa Melone Memorial Conference, Italy.
- 2013. Soil water diffusivity estimation from distributed water content observations across a rainfed olive orchard. ASA-CSSA-SSSA Technical Sessions., USA.
- 2010. Spatial and temporal organization of soil moisture at the field scale as affected by soil management. European Geosciences Union, EGU. Vienna.
- 2009. Spatio-temporal variability of moisture in different soil management systems. Congress of the unsaturated zone soil, ZNS'09. Barcelona, Spain.
- 2008. Use of capacitance soil water sensors to evaluate irrigation scheduling and irrigation distribution uniformity in field crops. EUROSOIL, Vienna.
- 2008. Influence of Soil Management on the Spatio-temporal Organization of Soil Moisture at the Field Scale. ASA-CSSA-SSSA Technical Sessions., USA.
- 2005. Nitrate pollution of runoff waters in ecological olive groves under different soil management systems. International Congress on Conservation Agriculture. Cordoba, Spain.

RELEVANT BOOK CHAPTERS (in Spanish)

Espejo-Pérez, A.J.; Giráldez-Cervera, J.V.; Rodríguez-Lizana, A.; and Ordóñez, R. 2007. Influence of vegetation cover live in water and soil loss in olive orchards. In: Rodríguez-Lizana; A.; Ordóñez-Fernández, R.; and Gil-Ribes, J. Use of cover crop in olive orchard. pp. 133-145.

Rodríguez-Lizana, A; **Espejo-Pérez, A.J**.; González-E; Ordóñez, R.; and González, P. 2007. Impact of using cover crops on the processes of nitrate pollution and runoff phosphorus in organic and conventional plots. In: Rodríguez-Lizana; A.; Ordóñez-Fernández, R.; and Gil-Ribes, J. Use of cover crop in olive orchard. pp. 170-184.

Studies of wheat and sunflower crop in conservation agriculture in Andalusia region. Years 2003-2006. Monographs published by the government of Andalusia, Spain.

RESEARCH STAYS

- 2014. Agricultural Engineering and Land Use Department of the Faculty of Agriculture, University of Buenos Aires. (Duration: 2 weeks).
- 2013. Research Institute for Hydrogeological Protection, National Research Council of Italy, city of Perugia. (Duration: 3 months).
- 2011. Agricultural Engineering and Land Use Department of the Faculty of Agriculture, University of Buenos Aires. (Duration: 1 month).
- 2010. Agricultural Engineering and Land Use Department of the Faculty of Agriculture, University of Buenos Aires. (Duration: 2 months).

REFERENCES OF THE RESEARCH TEAM AND TUTORS

- **Vanderlinden, Karl**. Senior Researcher in the Natural resources and Agroecology Department of the Andalusian Institute of Research and Training in Agriculture and Fishing, IFAPA. Seville, Spain.
- **Giráldez-Cervera, J.V.** Professor in the Department of Agronomy of University of Cordoba, and Senior Researcher in the Institute of Sustainable Agriculture, CSIC. Cordoba, Spain.